Molecular studies on *MYD88* alternative splicing in oncogenesis and Toll-like receptor 2 recognition of fungal chitin

Dissertation

der Mathematisch-Naturwissenschaftlichen Fakultät

der Eberhard Karls Universität Tübingen

zur Erlangung des Grades eines

Doktors der Naturwissenschaften

(Dr. rer. nat.)

vorgelegt von

MSc. Yamel I. Cardona Gloria

aus Jalisco, Mexiko

Tübingen

2018

Gedruckt mit Genehmigung der Mathematisch-Naturwissenschaftlichen Fakultät der Eberhard Karls Universität Tübingen.

Tag der mündlichen Qualifikation:	13.Juli.2018
Dekan:	Prof. Dr. Wolfgang Rosenstiel
1. Berichterstatter:	Prof. Dr. Alexander N.R. Weber
2. Berichterstatter:	Prof. Dr. Hans-Georg Rammensee

Summary

Toll-like receptors (TLRs) play critical roles in human innate and adaptive immune responses and although they are well characterized, there remain gaps in our understanding of the early events upon TLR activation. In this thesis I assessed two different topics: first the regulation and function of *MYD88* alternative splicing in B cell lymphomas and second, the role of the receptor TLR2 in the recognition of the very abundant natural agonist chitin.

First topic: MyD88, a pivotal signaling protein for almost all TLRs, has been determined as an oncogenic driver in numerous cancers especially in Non-Hodgkin B cell lymphomas (B-NHL). Already in the 90's, it has been found that the *MYD88* gene undergoes alternative splicing. Alternative splicing is a mechanism used by eukaryotic cells to increase the complexity of gene expression by generating multiple proteins from a single gene. To date, five MyD88 isoforms were found in transcriptional analyses, but little is known about their natural occurrence and abundance in specific cell types. Furthermore, alternative splicing is often aberrant in cancers, resulting in novel protein isoforms which could originate or aid oncogenesis. In this study, I evaluated the hypothesis that MyD88 alternatively spliced isoforms could be more highly expressed in B-NHL and might contribute to the well-studied oncogenic effect of MyD88. First, I tested whether the five known MyD88 isoforms could activate the pro-inflammatory and pro-survival transcription factor NF-κB (nuclear factor kappa-light-chain-enhancer of activated B cells). Using a reporter assay in HEK 293T cells, I found that three out of the five were able to induce NF-κB activity. Furthermore, I confirmed expression of all isoforms by quantification of MyD88 transcripts from healthy and lymphoma B cells performing qPCR and RNAseq data analysis. Finally, deeper analysis of RNAseq data revealed the existence of two novel isoforms and demonstrated that *MYD88* alternative splicing seems to be suppressed in B cell lymphomas. Thus, although results neglected the hypothesis that MyD88 alternative isoforms contribute to oncogenic signals in B-NHL, this study opens the possibility to attribute different roles to the isoforms especially in healthy conditions; for example, supporting the highly dynamic early events in MyD88-signaling.

Second topic: Chitin is the second most abundant polysaccharide in nature and has been linked to fungal infection and allergic asthma. To date, several different receptors have been proposed to recognize chitin and evoke an inflammatory response. However, literature presents contradictory results and the physical binding of immune receptors to chitin has not been shown. Colleagues and I speculated that the discrepancies might be due to chitin's highly polymeric nature and the use of crude extracts from crustaceans or fungi with variable purity as chitin preparations. Thus, here we proposed to use defined chitin (N-acetyl-glucosamine) oligomers comprising 4 to 15 subunits to overcome these limitations. We identified chitin made up of 6 subunits as the smallest immunologically

active chitin motif and a mixture of 10 to 15 chitin subunits showed the highest activity in innate immune cells. Using this mixture to stimulate bone marrow derived macrophages from different knockout mice enabled us to identify TLR2 as a specific chitin-receptor. Furthermore, we supported this finding by showing that mutations within the TLR2 ligand-binding pocket impaired TLR2 responses to chitin. Additionally, we could block the chitin induced response with the known TLR2 antagonist, staphylococcal superantigen-like protein 3 (SSL3). At last, we looked for the TLR2 co-receptor responsible to support chitin recognition. Based on data we suggest TLR1 and TLR6 as co-receptor candidates. Thus, this study found that chitin is recognized by TLR2 in mammals and proposes the chitin-TLR2 interaction as an attractive therapeutic target in chitin-related pathologies and fungal diseases.

Overall, this doctoral thesis contributes new insights into MyD88 and its previous uncharacterized alternative splicing in B cells and describes the molecular details of TLR2 recognition of chitin.

Zusammenfassung

Toll-like-Rezeptoren (TLRs) spielen eine wichtige Rolle in der humanen angeborenen und adaptiven Immunität. Obwohl TLRs gut charakterisiert sind, bleiben Lücken in unserem Verständnis der frühen Ereignisse nach TLR-Aktivierung. In dieser Arbeit untersuchte ich zwei Aspekte: Die Regulation und Funktion von alternativen Spleißvarianten des TLR Adapterproteins MyD88 in B-Zell-Lymphomen sowie die Rolle des Rezeptors TLR2 bei der Erkennung des Agonisten Chitin, einem in der Natur sehr häufig vorkommenden Polysaccharid.

Erstes Projekt: MyD88, ein wichtiges Adapterprotein, das Signale von fast allen aktivierten TLRs weiterleitet, ist häufig in verschiedenen B-Zellen Non-Hodgkin-Lymphomen (B-NHL) mutiert und trägt dadurch maßgebend zur Krebsentstehung bei. In den 90er Jahren wurde bereits herausgefunden, dass MyD88 alternative Spleißvarianten aufweist. Alternatives Spleißen ist ein Mechanismus, der von eukaryotischen Zellen verwendet wird. Dabei werden mehrere Proteine aus einem einzelnen Gen erzeugt, um die Komplexität der Genexpression zu erhöhen. Bislang wurden 5 MyD88-Isoformen in Transkriptom-Analysen gefunden, aber es ist wenig über das natürliche Vorkommen und die Häufigkeit von alternativen MyD88-Isoformen in spezifischen Zelltypen bekannt. Daher untersuchte ich hier alternatives Spleißen von MyD88 in humanen B-Zellen und B-NHL.
Meine Hypothese war, dass die alternativen Isoformen in Lymphomen stärker exprimiert würden und dadurch zu der onkogenen Wirkung von MyD88 beitragen könnten. Zunächst testete ich, ob die 5 bekannten MyD88-Isoformen den Transkriptionsfaktor NF-κB (*nuclear factor kappa-light-chain-enhancer of activated B cells*) aktivieren konnten. Mithilfe eines Reporter-Assays in HEK 293T-Zellen fand ich heraus, dass 3 von 5 Isoformen NF-κB-Aktivität induzieren konnten. Danach habe ich die Expression der Isoformen durch Quantifizierung von MyD88-mRNA-Molekülen aus gesunden und lymphomen B-Zellen durch qPCR- und RNAseq-Datenanalyse nachgewiesen. Zusätzlich deckte eine tiefere Analyse der RNAseq-Daten die Existenz von zwei neuen Isoformen auf und zeigte, dass alternatives Spleißen von MyD88 in B-Zell-Lymphomen unterdrückt zu sein scheint. Obwohl alternative MyD88-Isoformen nicht zur MyD88-Onkogenese beitragen, ermöglicht diese Studie MyD88 Isoformen unterschiedliche Rollen zuzuordnen. Beispielsweise als wichtiger Unterstützer bei der Entstehung des MyD88 Komplexes oder bei neuen Protein Interaktionen.

Zweites Projekt: Chitin ist das zweithäufigste in der Natur vorkommende Polysaccharid und wurde mit Pilzinfektionen und allergischem Asthma in Verbindung gebracht. Bis heute wurden mehrere verschiedene Rezeptoren vorgeschlagen, um Chitin zu erkennen und eine entzündliche Reaktion auszulösen. Dennoch zeigt die Literatur widersprüchliche Ergebnisse und die physikalische Bindung von Immunrezeptoren an Chitin wurde nicht

gezeigt. Meine Kollegen und ich haben vermutet, dass die Diskrepanzen auf Chitins hochpolymerer Natur und die Verwendung von Rohextrakten aus Krustentieren oder Pilzen mit variabler Reinheit als Chitinpräparate zurückzuführen sein könnten. Meine Kollegen und ich haben vermutet, dass diese Diskrepanzen auf die chemische Heterogenität von verwendeten Chitin-Präparaten zurückzuführen sind, welche häufig als Rohextrakte aus Krustentieren oder Pilzen mit variabler Reinheit gewonnen werden. Um diese Ungenauigkeiten auszuschließen, verwendeten wir definierte Chitin Oligomere aus 4 bis 15 N-Acetylglucosamin Untereinheiten. Wir identifizierten, dass mindestens sechs dieser Untereinheiten für eine immunologische Reaktion nötig sind. Eine Mischung von Chitin Oligomeren bestehend aus 10 bis 15 N-Acetylglucosaminen zeigte dabei die höchste inflammatorische Reaktion in angeborenen Immunzellen. Anhand von Versuchen mit Makrophagen aus dem Knochenmark von verschiedenen Knockout Mausstämmen, konnten wir TLR2 als spezifischen Rezeptor für oligomeres Chitin identifizieren. Darüber hinaus konnten wir zeigen, dass Mutationen in der TLR2 Ligandenbindungstasche die Aktivierung von Chitin reduzierten. Außerdem konnten wir die durch Chitin hervorgerufene Immunaktivierung mit dem TLR2-Antagonisten *Staphylococcus Superantigen-like Protein 3* (SSL3) blockieren. Weiterhin suchten wir nach einem Co-Rezeptor für TLR2, der die Chitin Erkennung sowie Signalübertragung unterstützen könnte. Ausgehend von unseren Untersuchungen schlagen wir TLR1 und TLR6 als Unterstützer vor.
Diese Studie zeigt, dass Chitin, sowohl im Menschen als auch bei Mäusen, durch TLR2 erkannt wird. Daher schlagen wir die Chitin-TLR2-Interaktion als therapeutischen Angriffspunkt gegen Chitin-assoziierten Pathologien und Pilzkrankheiten vor.

Insgesamt stellt diese Doktorarbeit neue Erkenntnisse zu MyD88 und seinen bisher nicht charakterisierten alternativen Isoformen in B-Zellen vor und beschreibt die molekularen Details der Erkennung von Chitin durch den Rezeptor TLR2.

Acknowledgments

I would like to express my deep gratitude to Prof. Alexander Weber for his excellent guidance through these projects and the critical review of this thesis. Furthermore, I thank him for the fastest acceptance ever and his trust in my work.

My grateful thanks to Dr. Oliver Wolz for being my Lab-angel in all possible aspects.
I would also like to extend my thanks to all actual and former members of the Weber group for technical support, great work-environment and fun social events.

Special acknowledge to Prof. Hans-Georg Rammensee for his supervision and consent to take part of the Integrated Research Training Group (IRTG) "Immunotherapy and be funded by the SFB685.

Here I would also like to thank all my former supervisors from all the labs I have visited during my studies for giving me the tools, knowledge and self-confidence to successfully achieve my doctoral degree. Special thanks to A. Stutz and D. Bertheloot for the critical review.

Many thanks to the Trzaska family for completing my family and for giving me the last push to start this PhD-adventure; to ***my mom and sister,*** whose love and care cross the world and to ***my father,*** who would had been the only person happier than me at this moment.

Finally, I infinitely thank ***my husband*** for his unconditional support until the completion of my long-lasting studies and beyond (*We did it!*). Furthermore, ***this work is specially dedicated to him and my lovely goddaughters Romina and Luciana***.

I hope this work inspires to realize that the world can be our playground.

And thanks to you for your attention.

Table of contents

List of figures

List of supplementary figures

List of tables

List of supplementary tables

List of abbreviations

AA:	Amino acids
Ab:	Antibody
ABC DLBCL:	Active B cell type Diffuse Large B cell Lymphoma
AML:	Acute myeloid leukemia
bp:	base pair(s)
BCR:	B cell receptor
BMDMs:	Bone marrow derived macrophages
B-NHL:	B cell non-Hodgkin-Lymphoma
BSA:	Bovine serum albumin
CDS:	Coding sequence
CLL:	Chronic lymphocytic leukemia
CTR:	C-terminal region
C10-15:	Chitin 10-15 oligomers
DAMPs:	Damage-associated molecular patterns
DD:	Death domain
DLA:	Dual luciferase assay
eGFP:	enhanced green fluorescent protein
FCS:	Fetal calf serum
FL:	Follicular lymphoma
GC-B:	Germinal center B cells
GCB DLBCL:	Germinal center B cell type Diffuse Large B cell Lymphoma
GOI:	gene of interest
h:	hour, hours
IL-1:	Interleukin-1
INT:	Intermediate domain
IRAK:	IL-1 receptor-associated kinase
LDS:	Lithium dodecyl sulphate sample loading buffer
LPS:	Lipopolysaccharide
MAMPs:	Microbe-associated molecular patterns

MAPKs:	Mitogen-activated protein kinases
MDS:	Myelodysplastic syndrome
min:	minutes
NF-κB:	nuclear factor 'kappa-light-chain-enhancer' of activated B cells
nt:	nucleotides
Pam2:	PAM2CSK4
Pam3:	PAM3CSK4
PRRs:	Pattern recognition receptors
TIR:	Toll-Interleukin receptor domain
TLR:	Toll-like receptor

Chapter 1: General Introduction

1.1 Innate and Adaptive immune system

The immune system is the second most complex system of eleven in the human body, which has been exhaustibly studied at distinct levels of structural organizations from organisms to molecules, but still not fully understood. The function of the immune system is to maintain homeostasis of the host by inducing defense mechanisms in the presence of microbes or danger signals resulting from e.g. tissue damage. In mammals, there are three levels of host defense: 1) physiologic barriers, 2) innate immunity and 3) adaptive immunity (Turvey and Broide 2010, Iwasaki and Medzhitov 2010), and here I focus on the last two.

After an intruder was able to overtake the physiologic barriers as e.g. the skin, the innate immunity defense mechanisms play crucial roles in the earliest phases of infection and may succeed in eradicating the pathogen. Innate immune protection is a task performed by cellular processes done by hematopoietic and nonhematopoietic cells, and humoral components. On one hand cellular processes start with the recognition of the pathogen by pattern recognition receptors, the induction of pro-inflammatory signaling pathways and end with the awakening of elimination mechanisms, e.g. phagocytosis (Turvey and Broide 2010). In brief, phagocytosis is the cellular uptake of particles/pathogens below 5 µm initiated by receptor-ligand interactions. Once the pathogen is internalized, the phagosome fuses to lysosomes, vesicles which contain hydrolytic enzymes and maintain an acidic environment (pH 4.5). Thus, the fusion of these two types of organelles, phagosome and lysosome, results in progressive acidification and digestion or the cargo (Gordon 2016, Pauwels et al. 2017). On the other hand, humoral components such as complement proteins, Lipopolysaccharide (LPS) binding proteins, antimicrobial peptides, among others (Turvey and Broide 2010), are able to opsonize and lyse cells, and have potent inflammatory activity. As example of together work of cellular processes and humoral components is the function of complement proteins to opsonize pathogens to facilitate phagocytosis (Frank 2010).

Pathogens, however, developed strategies that allow them to overcome these mechanisms. In these circumstances, the innate immune system is able to induce an adaptive immune response which takes several days to build up the tools needed to eliminate the pathogen (Iwasaki and Medzhitov 2015, Turvey and Broide 2010). It requires clonal differentiation and expansion of naïve lymphocytes into antibody-secreting B cells and effector T cells. Then, the adaptive immunity performs an efficient antigen-specific protection through highly specific antigen receptors, namely B-cell and T-cell receptors and immunoglobulins. These receptors are assembled through somatic recombination and therefore provide immense diversity to recognize antigens, while they

have also passed selection processes to avoid self-recognition. The long lasting and effective protection by the adaptive immunity is achieved also by its capacity for memory, which allows a greater and more rapid response against recurrently invading microorganisms (Gregersen and Behrens 2006, Janeway 2001). In contrast, innate immunity is considered as pattern-specific protection responding to evolutionary conserved structures of microbes through germline-encoded receptors known as pattern recognition receptors (PRRs). The engagement of PRRs with their specific molecular pattern (referred to also as ligand) activates intracellular signaling cascades that lead to the production of pro-inflammatory or anti-inflammatory cytokines and chemokines, which regulate processes such as activation, migration and differentiation of immune cells to develop an effective and pathogen-specific adaptive immune response (Murray and Wynn 2011, Rivera et al. 2016).

The high complexity of the immune system is also attributed to the cross-talk between innate and adaptive immunity. Communication between the two systems requires cell-cell interaction or external soluble signals such as cytokines and immunoglobulins (Zhang and An 2007). Antigen presentation is one example in which the innate system activates the adaptive system by cell-cell interaction. Upon activation via PRRs, a professional antigen presenting cell, e.g. a dendritic cell, presents an antigen from an engulfed microbe to a T cell together with co-stimulatory signals. Then, the T cell recognizing the presented antigen will expand efficiently and develop an effector function (den Haan, Arens, and van Zelm 2014). On the other hand, activated T cells can produce cytokines to recruit and stimulate phagocytic innate immune cells such as macrophages, who engulf pathogens or support healing processes (Kawakami et al. 1995, Gordon 2016, Smigiel and Parks 2018).

A system as complex as the immune system needs sophisticated regulatory mechanisms. Failure in its regulation can lead to a large number of diseases, such as inflammatory diseases due to an exaggerated response (e.g. allergy, asthma, Crohn's disease), autoimmune diseases due to unwarranted reactions against self-molecules (e.g. systemic lupus erythematosus, type 1 diabetes, rheumatoid arthritis), or cancer (Coussens and Werb 2001, Gregersen and Behrens 2006). However, a weak immune system, e.g. due to genetic diseases or other factors (e.g. HIV, drug use), often leads to recurring and life-threatening infections (Maarschalk-Ellerbroek et al. 2012).

1.2 Pattern recognition receptors and pathogen sensing

Pattern recognition receptors are germline-encoded receptors broadly expressed on the cell surface, internal membranes or within the cytoplasm of multiple cell types including blood cells, epithelial cells, nerve cells and others. Innate immune cells express the highest levels of PRRs. These receptors are important players in the innate immunity

since they are the first ones to recognize and classify the type of intruder or malignancy (e.g. cancer) that appears within a mammalian organism (Tan et al. 2014, Janeway 2001). Receptors recognize microbe-associated molecular pattern (MAMP) coming from e.g. bacteria, virus and fungi or a danger-associated molecular pattern (DAMP) appearing after tissue damage. Depending on which receptor is engaged and whether a MAMP or a DAMP has been recognized, the receptor signaling initiates an exclusive type of immune response against the specific microbe or danger signal (Newman et al. 2013, Rivera et al. 2016).

PRRs are classified in five families: 1) Toll like receptors (TLRs), 2) C-type lectin receptors (CLRs), 3) Retinoic acid-inducible gene-I-like receptors (RLRs), 4) NOD-like receptors (NLRs) together with absent in melanoma 2 (AIM2)-like receptors (ALRs) and 5) cytosolic DNA receptors. All families are specialist, but not exclusive, in recognizing certain microbes. For example RLRs mainly recognize molecular patterns of RNA viruses, cytosolic DNA receptors sense DNA and RNA viruses, CLRs detect MAMPs of fungi and NLRs identify mostly bacterial dipeptides (reviewed in (Brubaker et al. 2015, Takeuchi and Akira 2010, Gay et al. 2014, Ma and Damania 2016)). On the other hand, TLRs cover ligands from all type of microbes.

1.3 Toll-like receptors

1.3.1 Toll-like receptors and their corresponding ligands

The TLR family of PRRs senses MAMPs derived from bacteria, fungi, viruses and protozoa. Additionally, they can also recognize endogenous DAMPs from distressed, injured or necrotic cells (for a detailed list of TLR-ligands, see Table 1) (Braza et al. 2016, Gay et al. 2014). Besides being highly expressed in innate immune cells, such as macrophages or dendritic cells, TLRs are also expressed at lower levels in epithelial and endothelial cells, adipocytes, cardiac myocytes and some other cell types (Akira, Takeda, and Kaisho 2001). To date, 10 Toll-like receptors in humans (TLR1-10) have been identified, 13 in mouse (TLR1-13) and other fish-specific like TLR18 and TLR22 in *Cyprinus carpio L*. carp fish (Shan et al. 2017, Li et al. 2017, O'Neill, Golenbock, and Bowie 2013).

TLRs are type I transmembrane receptors and their characteristic domain architecture comprises a leucine-rich repeat ectodomain that mediates the recognition of the molecular patterns, a transmembrane domain and an intracellular Toll-interleukin 1 receptor (TIR) domain, which initiates downstream signal transduction. Based on their subcellular localization, TLRs can be divided into two groups: 1) TLR1, TLR2 and TLR6 are expressed in the plasma membrane and recognize lipopeptides; TLR4 recognizes LPS; TLR5 binds flagellin; and TLR11 and TLR12 bind MAMPs from uropathogenic bacteria. The TLR10 ligand remains to be elucidated. 2) The nucleic acid receptors TLR3, TLR7 and TLR8,

TLR9 and TLR13are expressed in endosomes and recognize dsRNA, ssRNA, CpG motifs derived from bacterial and viral DNA, and ribosomal RNA respectively (Akira, Takeda, and Kaisho 2001, O'Neill, Golenbock, and Bowie 2013).

In the inactive state most TLRs are monomeric and require dimerization to induce downstream signaling, with the exceptions of TLR7, 8 and 9 which exist as preformed dimers and their ectodomains need to be cleaved by endoproteases within acidified endolysosomes to start the signal transduction (Ewald et al. 2008, Gay et al. 2014). Another special TLR is TLR2, which increases the variety of ligands by forming heterodimers with TLR1, TLR6 and possibly TLR10 (Gay et al. 2014, Oosting et al. 2014).

An additional example is the heterodimer of mouse TLR11 and TLR12 to recognize the protein profilin from *Toxoplasma gondii* (Koblansky et al. 2013). Amongst the TLRs, TLR4 is unique because in addition to homodimerization its activation also requires the co-receptor myeloid differentiation factor 2 (MD2) (Lu, Yeh, and Ohashi 2008).

Table 1. List of known TLR-ligands

TLRs	Type of ligand	Ligands
TLR2	Bacterial	Bacterial lipopeptides, peptidoglycan, lipoteichoic acid (LTA), Porin B Lipopolyssacharide (LPS), lipopeptides from Mycoplasma and Spirochetes. Lipoarabinomannan, mannosylated phosphatidylinositol from Mycobacteria.
	Fungal	Chitin and Zymosan
	Parasitic	Glycophosphatidylinositol-anchored proteins
	Endogenous	Cardiac myosin
TLR2 with TLR1	Bacterial	Triacylated lipopeptides, peptidoglycan, LTA.
	Synthetic	Pam3CSK4
TLR2 with TLR6	Bacterial	Diacylated lipopeptides, peptidoglycan, LTA.
	Endogenous	Necrotic cell content from any cell type.
	Synthetic	Pam2CSK4, FSL-1, MALP-2 [Invivogen].
TLR3	Viral	double-stranded RNA
	Endogenous	RNA sequences, HMGB1*
	Synthetic	Polyinosinic:polycytidylic acid, known as Poly(I:C)
TLR4 with MD2	Bacterial	LPS, lipid A. Live *Mycobacteria tuberculosis* and *Treponema brennaborense* glycolipids.
	Viral	Respiratory syncytial virus protein F
	Endogenous	Heat shock protein 60*,70*,90*, fibrinogen 6, Defensin 2.
	Plant	Taxol
TLR5	Bacterial	Flagellin
TLR7	Viral	single- stranded viral RNA
	Endogenous	Host nucleic acids like uridine-rich RNAs
	Synthetic	Synthetic chemical imiquimod, Azoquinolines, R-848.
TLR8	Viral	Single-stranded viral RNA
	Endogenous	Host nucleic acids, cardiac myosin.
	Synthetic	Azoquinolines, R-848.
TLR9	Bacterial	CpG rich hypomethylated DNA motifs
	Viral	Herpesvirus DNA, MCMV in IPCs
	Endogenous	CpG in autoantibody complexes, HMGB1*
	Synthetic	Azoquinolines
TLR10 (human)	Bacterial	Viable *Listeria monocytogenes*
	Synthetic	anti-TLR10 antibody (cross-linker)
TLR11 (mouse)	Bacterial	Component of uropathogenic bacteria, profilin-like molecules
TLR11 with TLR12 (mouse)	Parasitic	*Toxoplasma gondii* profilin protein
TLR13 (mouse)	Bacterial	Ribosomal RNA

Table modified and completed from O'Neill, 2013. *controversial findings due to possible contaminated samples. List of references were summarized in Table S1.

1.3.2 Molecular steps in Toll-like receptor signaling

Ligand-induced dimerization and conformational changes in TLRs initiate downstream signaling cascades. TLR activation induces several signaling cascades. TLRs trigger activation of canonical nuclear factor kappa-light-chain enhancer of activated B cells (NF-κB), mitogen-activated protein kinase (MAPK) and Interferon regulatory factor 5 (IRF-5) pathways leading to expression of pro-inflammatory cytokines and chemokines, and they activate the Phosphoinositide 3-kinase (PI3K) pathway promoting cell survival. Some TLRs can also trigger transcription of antiviral type I IFN (interferon) via IRF3 and IRF7 (Gay et al. 2014, Stack et al. 2014) (See Fig.1).

Upon ligand engagement, the intracellular TIR domains of the TLRs come together, forming a platform that recruits one or two out of six TIR domain-containing adaptor proteins, such as MyD88 (myeloid differentiation primary response protein 88), MAL (MyD88 adaptor-like protein), TRIF (TIR domain-containing adaptor protein inducing IFNβ), TRAM (TRIF-related adaptor molecule), SARM (Sterile alpha and armadillo motif-containing protein) and BCAP (B-cell adaptor for Phosphoinositide 3-kinase) (Bernard and O'Neill 2013, O'Neill et al. 2003). This section only describes the MyD88/MAL and TRIF/TRAM-signaling pathways.

Activation of the MyD88-pathway requires the formation of the big signaling complex called Myddosome, whose assembly is detailed described in Section 1.4.1. This complex induces the activation of several transcription factors through distinct signaling-pathways. NF-κB activation is induced by the recruitment and activation of the E3 ubiquitin ligase, TNFR-associated factor 6 (TRAF6) to the Myddosome complex. Once activated, TRAF6 is released into the cytosol where it triggers the degradation of the IκBα (inhibitor of NF-κBα) leading to activation and nuclear translocation of NF-κB. In parallel, TRAF6 also activates IRF5 and prompt the MAP kinase pathway to activate AP-1 and CREB (Gay et al. 2014) (Fig.1). Through the activation of the transcription factors NF-κB, AP-1, CREB and IRF-5 an array of genes are expressed, which mediate the production of pro-inflammatory cytokines such as TNF-α, IL-12, IL-6, IL-8 and IL-1β, the anti-inflammatory cytokine IL-10 and chemokines like CCL2, CCL3, CCL5 and CXCL10 (Gurtler et al. 2014).

The TRIF-dependent pathway leads to phosphorylation and activation of transcription factor IRF3, when the N-terminal domain of TRIF interacts with TRAF3 (TNF receptor-associated factor 3), TBK1 (TRAF family member-associated NF-kappa-B activator binding protein 1) and the members of the inhibitor of NF-κB kinase family: IKKi and IKKε. TRIF-dependent activation of IRF7 requires IRAK1 instead of TBK1. Moreover, this pathway can initiate apoptosis via receptor interacting protein 1 (RIP1) and caspase-8, and NF-κB activation via TRAF6. TRIF's TIR domain mediates interaction with the TLRs and TRAM. These TRIF-pathways lead to the expression of the antiviral type I interferon, such as IFN-β. In unstimulated cells, the N-terminal and the TIR domains allow self-association,

thereby blocking interaction with the downstream signaling molecules and making TRIF a negative regulator of its own pathway (Gay et al. 2014, Ullah et al. 2016). It is important to mention that there is an extensive crosstalk between the IRF and NF-κB pathways, making it very complex to determine the signaling pathway engaged by a specific ligand (Iwanaszko and Kimmel 2015).

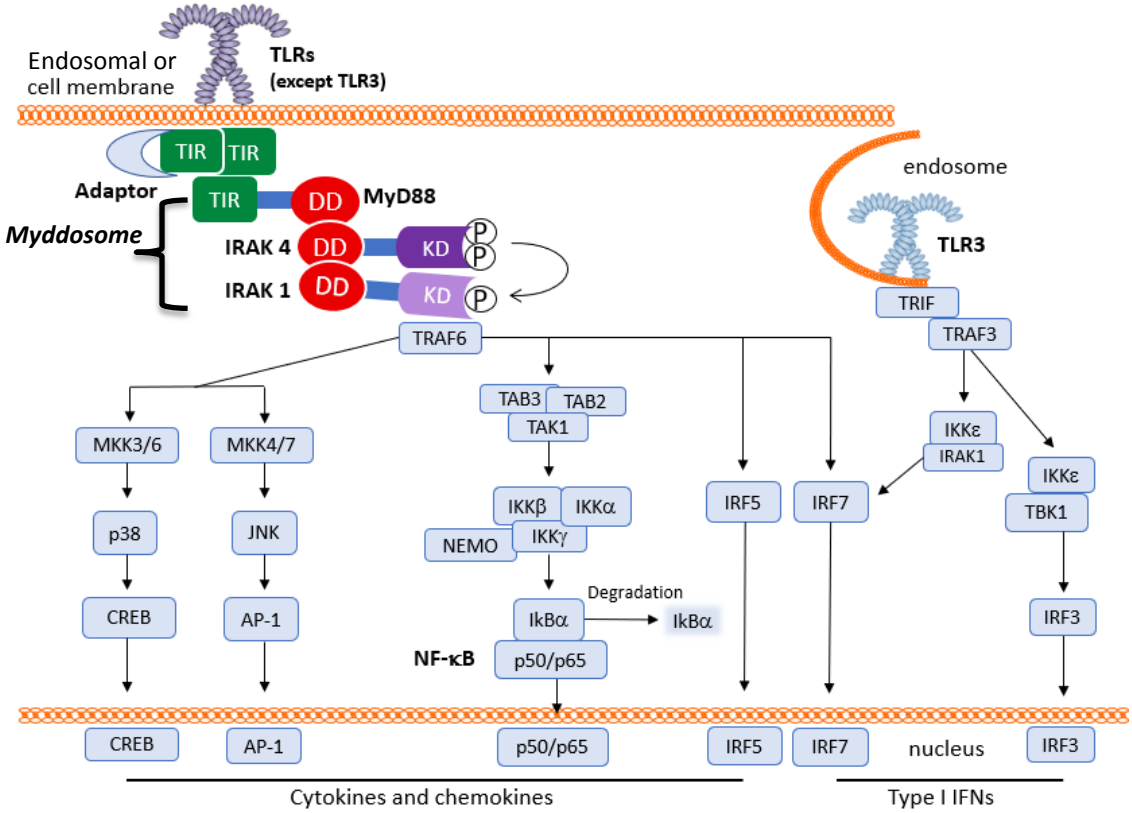

Figure 1. MyD88 and TRIF signaling steps until the activation of transcription factors. Adapted from Gay, et al. IRAK, interleukin-1 receptor-associated kinase; TRAF, tumor necrosis factor receptor-associated factor; TAK1, TGFβ-activated kinase 1; TAB, TAK1-binding protein; IKK, inhibitor of NF-κB kinase; IκBα, inhibitor of NF-κBα; MKK, mitogen activated protein kinase kinase; JNK, JUN N-terminal kinase; AP-1, activator protein 1; CREB, cAMP-responsive element-binding protein; TBK1, TANK-binding kinase 1; IRF, Interferon regulatory factor.

1.3.3 Toll-like receptor signaling in Disease

TLR signaling is essential for a functional immune system. Nevertheless, uncontrolled activation of the pathway or sustained exposure to agonists results in excessive inflammation and tissue damage giving rise to 1) inflammatory diseases such as bowel inflammation and asthma, and 2) autoimmune diseases as multiple sclerosis, systemic lupus erythematosus and rheumatoid arthritis (Drexler and Foxwell 2010).

Absence or exaggeration of TLR signaling is also associated to hematopoietic and lymphoid malignancies, and promotion of oncogenesis in general. The common effect of TLRs in these malignancies is a chronic TLR signaling caused by gain-of-function mutations, increased expression of the signaling molecules or sustained exposure to agonists (Monlish, Bhatt, and Schuettpelz 2016). The amplified signaling leads to survival and proliferation of the affected cell via the activation of specific transcription factors and resulting cytokine production as described before.

Aberrant TLR signaling frequently happens outside of their well-known role in immune cells, influencing e.g. differentiation and proliferation of hematopoietic stem cells. Continuous signaling diminishes hematopoietic stem cell capacity for self-renewal and favors myeloid differentiation, giving rise to diseases like Myelodysplastic syndromes and leukemia. Relevant aberrations include: TLR2-F217S variant or increased TRAF6 activity due to deletion of 5q in Myelodysplastic syndromes (Starczynowski et al. 2010, Wei et al. 2013). Furthermore, examples for oncogenic promotion are well described in lymphomas, leukemias and colon, breast and lung cancer mainly by overexpression of TLR signaling members linked to worse prognosis (e.g. MyD88 and TLR2) (Monlish, Bhatt, and Schuettpelz 2016, Ngo et al. 2011, Wang et al. 2013, Muzio et al. 2009).

Chapter 2: Assessing MyD88 alternative splicing in B cells and Lymphomas

2.1 Introduction

2.1.1 Myeloid differentiation primary response 88, MyD88

Myeloid differentiation primary response 88 (MyD88) is a well characterized pivotal adaptor protein participating in signaling pathways in innate and adaptive immunity. The human and murine coding sequences comprise 296 amino acids, forming a 33 kilo-Dalton protein. The sequences of the three main domains, which determine its functionality and interactions, are well conserved. The TIR domain at the C-terminus binds to the TIR-domains of all Toll-like receptors (except for TLR3) and the Interleukin-receptor members IL-1-R and IL-18-R upon receptor engagement. The N-terminal death domain (DD) interacts with downstream signaling proteins, thereby mediating the formation of a signaling complex. At last, the intermediate domain is suggested to be important for conformational changes, allowing MyD88 to transmit signal (Avbelj, Horvat, and Jerala 2011, Deguine and Barton 2014, von Bernuth et al. 2012). MyD88 has been intensely studied as the main player of the MyD88-dependent pathway in innate immune cells. However, the MyD88 somatic mutation leucine to proline in position 265 has move the attention of this pathway to adaptive immune cells, where many things remain to be discovered to understand the crucial differences limited to specific cell types (Ngo et al. 2011, Wang et al. 2014).

2.1.2 Molecular steps in MyD88 signaling complex assembly

Most of the knowledge about TLR signaling has been gained from innate immune cells like human and murine plasmacytoid or myeloid dendritic cells, primary monocyte derived macrophages and monocyte or macrophage cell lines. Thus, the downstream signaling steps of MyD88 presented in this section are the result of studies in innate immune cells.

During MyD88-dependent signaling, MyD88 functions as a scaffold protein for the interaction and activation of several serine-threonine kinases from the IL-1 receptor-associated kinase (IRAK) family. IRAK1, IRAK2, and IRAK4 are positive activators and IRAK3, also known as IRAKM, is a negative regulator. IRAKM is the only IRAK that doesn't have a kinase activity and its expression is induced, whereas others mediate their activation through self-phosphorylation events and are ubiquitously expressed (Gosu et al. 2012). The interaction between MyD88 and the IRAKs is mediated by their respective N-terminal DDs, resulting in the assembly of a multi-protein signaling complex named the

"Myddosome". A crystal structure of the DDs within the Myddosome revealed that the complex comprises six MyD88, four IRAK4 and four IRAK1 or IRAK2 molecules assembled into a helical tower-shaped structure. Furthermore, assembly of the Myddosome is thought to occur in a sequential manner: MyD88 binds IRAK4 and MyD88/IRAK4 then recruit IRAK1 or IRAK2. The assembled Myddosome complex allows the kinase domains of IRAK4 to phosphorylate themselves and IRAK1 or IRAK2, leading to IRAK1/2 autophosphorylation (Fig.1). This step-sequence suggests IRAK4 kinase activity as key point for downstream signaling (Lin, Lo, and Wu 2010). Nevertheless, Vollmer et al. proposed that IRAK1 catalytic activity turns on just by an allosteric mechanism binding to IRAK4, meaning that IRAK4 kinase activity is not necessary for IRAK1 autophosphorylation (Vollmer et al. 2017). Next, IRAK1/2 autophosphorylation prompt recruitment of the E3 ligase TRAF6 leading to MyD88-dependent activation of NF-κB, MAPKs and IRFs as described above in Section 1.3.2 (Conze et al. 2008, Lin, Lo, and Wu 2010, Schauvliege, Janssens, and Beyaert 2007).

2.1.3 MyD88 signaling variations in B cells

TLR expression in adaptive immune cells like B cells and T cells is low in comparison to innate immune cells. Nevertheless, TLRs play critical roles in the development of an efficient adaptive response. This section will focus on B cells. Expression levels of TLRs can vary depending on the B cell type, meaning that naïve B cells have very low levels of TLRs, and marginal zone B cells have the highest expression among B cell populations.

TLR-MyD88 activation in MyD88-deficient B cells has shown its involvement in promoting class-switching and antibody production including germinal center formation, and plays a role in progression of autoimmune diseases (Hess et al. 2017, Hua and Hou 2013). Recent B cell non-Hodgkin lymphoma (B-NHL) RNA sequencing studies found a common somatic mutation in MyD88's TIR-domain (p.L265P) that contributes to lymphomagenesis (Ngo et al. 2011). This finding boosted the interest to investigate similarities and differences of the MyD88 pathway in adaptive immune cells in comparison to innate immune cells. In general, the signaling pathways leading to the activation of NF-κB, MAPKs and PI3K are suggested to be the same. In fact some findings were first discovered in B cells and proved later in macrophages, e.g. BCAP regulation of PI3K activation (Ni et al. 2012, Okada et al. 2000). Thus, both types of cells have been used to solve the complete TLR-inducible signaling pathways.

However, there are several TLR events exclusive for B cells. One distinction is the cross-talk between TLR- and B cell receptor (BCR)-signaling, where TLR ligands enhance BCR signaling in the presence of low BCR antigen (Freeman et al. 2015, Wilson et al. 2015). Furthermore, both receptor pathways up-regulate the expression of transmembrane

activator and calcium-modulating cyclophilin ligand interactor (TACI) increasing the sensitivity of B cells to BAFF (B cell-activating factor) and APRIL (a proliferation-inducing ligand). Briefly, TACI-signaling inhibits B cell expansion and promotes the differentiation and survival of plasma cells, thus it is an important immune response regulatory pathway. Recent data demonstrated the direct contribution of MyD88 in activating NF-κB signals dependent on TACI. These signals can result in the expression of activation-induced cytidine deaminase (AID; an enzyme that is required for somatic hypermutation) and extrafollicular class-switch recombination in germinal centers, which are important events for antibody responses in a T cell-independent manner. Thus, MyD88 signaling in B cells is crucial for T-independent B cell responses (Rawlings et al. 2012).

Moreover, further events were elucidated based on MyD88-L265P mutation studies. The direct binding of MyD88 to BTK (Bruton's tyrosine kinase) increases BTK phosphorylation and kinase activity in MyD88-L265P diseases (Yang et al. 2013). Last, the breakthrough discovery was made that L265P mutated MyD88 can activate downstream signaling cascades without TLR engagement by spontaneous assembly of the Myddosome (Avbelj et al. 2014).

2.1.4 MyD88 signaling in Disease

The impact of MyD88-IRAK4-dependent signaling on protective immunity has been mostly elucidated using MyD88- and IRAK4-deficient mice. These mice have shown to be susceptible to a broad variety of pathogens including bacteria, viruses, fungi and parasites; not only did the knockout mice show enhanced pathogen growth *in vivo* in comparison to wild type mice, but their mortality was also increased at any age (Suzuki et al. 2002, Pennini et al. 2013). Conversely, in humans these deficiencies cause recurrent pyogenic infections, such as meningitis, osteomyelitis and sepsis by limited bacteria strains, e.g. *Streptococcus pneumoniae*, *Staphylococcus aureus* and *Pseudmomonas aeruginosa* (Picard et al. 2003, Picard et al. 2010). Although patients have been detected to have other pathogens like mycobacteria or *Toxoplasma*, these pathogens do not cause invasive infections as observed in mice. Patients carry heterozygous or even homozygous mutations in MyD88 or IRAK4 genes causing a loss-of-function phenotype. 40% of IRAK4-deficient and 37,5% of MyD88-deficient patients of all cases published to date died during infancy, strongly suggesting that the MyD88-dependent pathway is relevant in early life, but dispensable in adulthood. With simple prophylaxis such as the use of antibiotics, vaccination and IgG substitution, several individuals survived into adolescence (Picard et al. 2010, von Bernuth et al. 2012).

Although the MyD88 or IRAK4 deficiency is not limited to innate immune cells, the pathogenicity is attributed to the lack of induction of an inflammatory response coming

from these cells (Deguine and Barton 2014, von Bernuth et al. 2012). Interestingly, no gain-of-function mutations have been discovered in human innate immune cells. Continuous stimulation of TLRs and the constitutive activation of transcription factors such as NF-κB and STAT3 in innate immune cells is known to exert pro-oncogenic activity by promoting cell proliferation and cell death resistance. In addition, the resulting constant cytokine secretion attracts many type of cells, thereby establishing a perfect microenvironment for tumor formation and growth. Thus, tumorigenic pathogens, mainly viruses, use the MyD88-dependent pathway to carry out their oncogenic effects by exhorting chronic inflammation (Swann et al. 2008, Wang et al. 2014).

Interestingly, somatic mutations leading to a hyperactive phenotype are more common in adaptive immune cells. Polymorphisms in TLRs are known to increase the risk of non-Hodgkin lymphoma (Purdue et al. 2009) and the L265P mutation in MyD88 contributes to the selection of B cell-malignant clones by inhibiting apoptosis and increasing proliferation through the specific activation of NF-κB (Isaza-Correa et al. 2014). Therefore, therapeutic strategies concentrate on shutting down the MyD88-dependent pathway at the MyD88 level, since NF-κB inhibitors have strong side effects.

In this study, I am particularly interested in lymphomas described to have the somatic mutation c.794T>C in the *MYD88* gene, which changes leucin to proline at amino acid residue 265 (p.L265P) summarized in Table 1. Of special interest is Diffuse Large B cell lymphoma (DLBCL), the most common fast-growing B-NHL, which has two main subtypes: 1) Active B cell (ABC) type and 2) Germinal Center B cell (GCB) type. The ABC-DLBCL characteristics are a chronic BCR signaling due to gain-of-function mutations in the pathway and several recurrent aberrations like *BCL2* and *MYC* translocations; additionally, ~30% of ABC-DLBCL cases have the MyD88 L265P mutation (Ngo et al. 2011). Therefore, DLBCL cell lines were used as one model system in this study.

Available therapies against DLBCL are limited, and prognosis is worse for the latter subtype due to the constant acquirement of mutations and consequent resistance to treatments. Some FDA-approved examples are Ibrutinib against BTK kinase activity and Fostamatinib against Syk (spleen tyrosine kinase), targeting the BCR-signaling pathway (Sandoval-Sus, Chavez, and Dalia 2016). Still in basic research are potential MYD88 (Shiratori, Itoh, and Tohda 2017) and IRAK4 (Scott et al. 2017) inhibitors.

Table 2. List of Non-Hodgkin lymphomas with frequent MyD88 L265P mutation.

B cell malignancy	Frequency of L265P	Reference
Waldenström's Macroglobulinemia	90% (54% MGUS)	(Varettoni et al. 2013, Xu et al. 2013)
Primary central nervous B cell lymphoma	60-71%	(Montesinos-Rongen et al. 2011, Lee et al. 2017)
Primary cutaneous large B cell lymphoma, leg type	61%	(Pham-Ledard et al. 2014)
Mucosa-associated lymphoid tissue lymphoma	7-9%	(Ngo et al. 2011, Traverse-Glehen et al. 2013)
Diffuse large B cell lymphoma	6.5-8% (29% ABC subtype)	(Ngo et al. 2011, Choi et al. 2013) (Pasqualucci et al. 2011)
Chronic lymphocytic leukemia	3-4%	(Puente et al. 2011, Landau et al. 2013)
Ocular adnexal extranodal marginal zone lymphoma	7%	(Zhu et al. 2013)
Splenic marginal zone lymphoma	4-5%	(Pasqualucci et al. 2011) (Gachard et al. 2013)

2.1.5 Alternative splicing of MYD88

Constitutive (or canonical) splicing is a simple process applied to precursor messenger RNA (pre-mRNA) transcripts, in which introns are removed and exons are ligated in the order they appear in a gene to generate a single functional protein (Wang et al. 2015). RNA splicing in eukaryotes takes place in a big ribonucleoprotein complex called the spliceosome. Five small nuclear ribonucleoprotein complexes (U1, U2, U4/U6, and U5) dynamically recognize and assemble on introns to cleave and ligate RNA molecules for intron removal, generating the protein-coding mRNAs (Wahl, Will, and Luhrmann 2009). The spliceosome catalyzes splicing with high precision, but also displays high flexibility to regulatory signals for rapid responses. One of these regulatory signals is alternative splicing. Alternative splicing involves mechanical processes by which "alternative" splice sites in pre-mRNAs are selected, creating new junctions to produce multiple mature mRNAs. This allows the production of multiple proteins with potentially distinct structures and functions from a single gene (Fu and Ares 2014, Bonomi et al. 2013). Recent findings have determined that the average human gene can generate at least 3 alternatively spliced isoforms. Thus, alternative splicing is a process used across kingdoms to expand the diversity and function of the proteome (Lee and Rio 2015).

There are numerous mechanisms for alternative splicing, for example: RNA-RNA interaction from long-distance RNA, which facilitates the exchange of a common exon to an alternative exon; or most common, RNA-protein interactions, where splicing factors bind to regulatory sites such as silencers or enhancers, thereby changing splicing patterns. Systematic analysis of RNA data has revealed several types of alternative

splicing: 1) exon skipping, 2) alternative 5' and 3' splice sites within exon or intron sequences, which often lead to subtle changes in the coding sequence and 3) intron retention, which frequently generates premature termination codons (Wang et al. 2015).

MyD88 alternative splicing generates four isoforms (1, 3, 4 and 5) found in genomic and RNA sequence analysis deposited on NCBI's Reference Sequence database, besides the canonical MyD88 isoform 2. Isoforms 3, 4 and 5 are generated by exon skipping and isoform 1 by an alternative splice site within the 3rd intron. For a detailed description of MyD88 alternative isoforms see Figure 2.

Some alternative splicing events seem to be constitutive resulting in the co-existence of isoforms at constant ratios in the same cell, while others are regulated by signal responses. In the case of MyD88, its alternative splicing has been proposed to be regulated by TLR responses in macrophages, although it has been only shown for the expression of MyD88 isoform 3 (Adib-Conquy et al. 2006, Burns et al. 2003, Janssens et al. 2003). Furthermore, the splicing factors SF3A and SF3B were also found to control production of MyD88 isoform 3 in murine myeloid cells (De Arras and Alper 2013). Thus, isoform 3 remains the only isoform to be, although little studied. Therefore, an aim of this project is to elucidate the regulation of the other known but uncharacterized splice variants (Isoforms 1,4 and 5), whose so far associated knowledge is summarized in Table 3.

Alternative splicing in oncogenesis is frequently dysregulated and has been considered as another hallmark of cancer (Ladomery 2013). Alternative splicing can be frequently manipulated by polymorphisms within splice sites resulting in the generation of new isoforms which can originate or support oncogenesis (Kaida, Schneider-Poetsch, and Yoshida 2012, Wang et al. 2015). However, the here studied MyD88 alternative isoforms are not generated by polymorphisms. Nevertheless, it will be important to characterize splice isoforms of key proteins in a healthy vs. oncogenic scenario.

Table 3. Current knowledge about MyD88 isoforms

	Human	Mouse	Reference
Known sequences	1-2-3-4-5	2-3	Genbank, Uniprot
Isoform 2			
Referred as	"Canonical" sequence	"Canonical" sequence	Genbank, Uniprot
Associated with oncogenesis	MyD88 L265P mutation (hyperactive phenotype) DLBCL, CLL	MyD88 L252P mutation DLBCL-like phenotype	(Ngo et al. 2011, Avbelj et al. 2014, Knittel, Liedgens, and Reinhardt 2015)
Isoform 3			
Referred as	MyD88 short	MyD88 short	
Expression induction	Monocytes stimulated with LPS (sepsis). Bronchial epithelial cells treated with resveratrol	Monocytes and macrophages stimulated with LPS and IL-1ß. Resveratrol treatment in lung epithelial cells.	(Adib-Conquy et al. 2006, Janssens et al. 2003, Andrews et al. 2016)
Function	Tolerance to TLR2 and TLR4 re-stimulation.	Inhibit NF-κB but not JNK pathway (mouse constructs in MEF cells). Decreases inflammation in the lung of mice via inhibition of ERK1/2	(Adib-Conquy et al. 2006, Burns et al. 2003)
Molecular mechanisms	Suggested to be the same as in mouse	Sequesters Isoform 2 impairing binding to IRAK4	(Burns et al. 2003)
Isoform 1, 4 & 5			
Expression induction	Not known	Not known	
Function	Not known	Not known	

DLBCL: Diffuse Large B Cell Lymphoma; CLL: Chronic Lymphocytic Leukemia; MEF cells: murine embryonic fibroblast

2.2 Hypothesis and aims

MyD88 has been intensely studied as the main player of the MyD88-dependent pathway in innate immune cells. However, the MyD88 somatic mutation L265P has moved the attention to adaptive immune cells due to its oncogenic power. Many things about this molecule and pathway remain to be discovered to understand the crucial differences between specific cell types. The background of this project are the following facts: First, the L265P mutation confers a hyperactive phenotype leading to the constitutive activation of NF-κB which drives oncogenesis. Second, it has been shown that MyD88 isoform 3 expression can be induced by continuous stimulation with LPS, theoretically via NF-κB.

Therefore, I hypothesized that the expression of alternative isoforms is increased in B cell lymphomas versus healthy B cells. B cell lymphomas are known to have a constitutive activation of the NF-κB pathway to e.g. mediate survival. These alternative isoforms are expected to regulate MyD88 signaling possibly in a negative way as demonstrated for isoform 3 or as positive feedback loop contributing to oncogenesis. The aim of this chapter was therefore to investigate whether the expression pattern of MyD88 isoforms would change in B cell lymphomas in comparison to healthy B cells and whether any of alternative splicing products would drive oncogenesis.

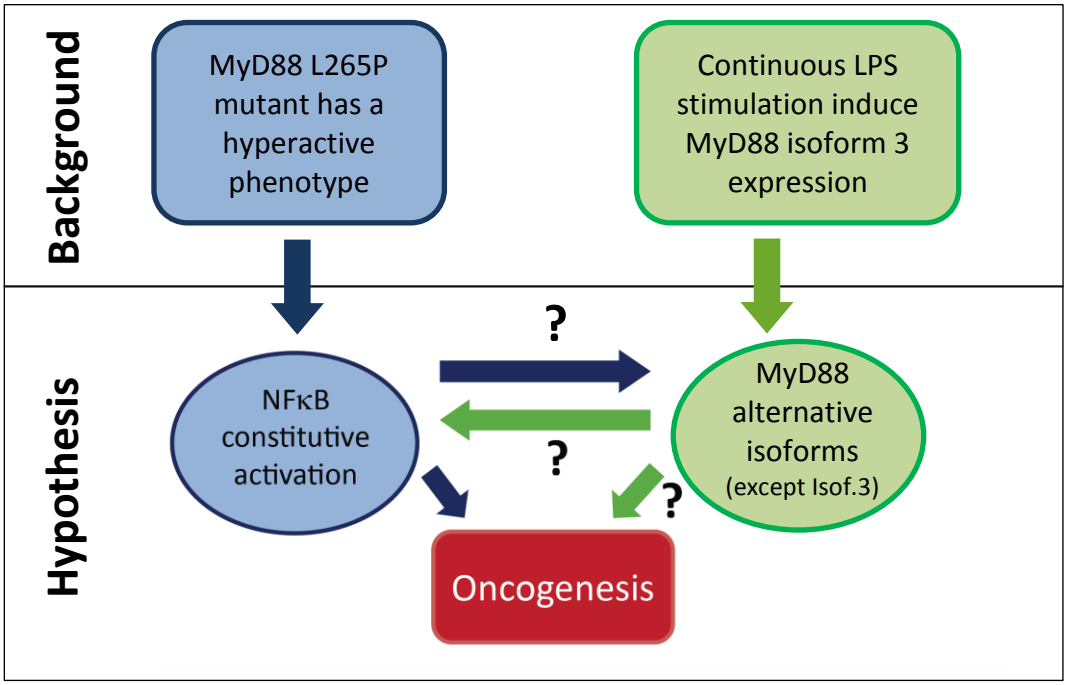

2.3 Results

MyD88 alternative splicing generates four extra isoforms besides the reference protein; only one of them has been little studied, whereas the others have so far remained annotations. Considering isoforms as different forms from the same protein, theoretically alternative isoforms can have the same or distinct function as the reference, depending on the changes at the mature mRNA and subsequent protein level. Thus, I first generated constructs of each MyD88 isoform and evaluated their ability to induce NF-κB activity to solve their function. Then, I confirmed their physiological transcription and protein expression by RNAseq data analysis and immunoblotting, using samples from several B-NHLs. I evaluated also different conditions to test how alternative splicing could be regulated, quantifying expression levels of the isoforms upon different treatments in B cells by qPCR. At last a deep analysis of the RNAseq data gave us quantitative transcription levels of the isoforms in different B-NHLs and this data gave hints of new isoforms that were not annotated before.

2.3.1 Generation of MyD88 isoforms plasmids

Genomic and RNA sequence analysis showed the existence of MyD88 alternative isoforms 1, 3, 4 and 5, which are described as "Known RefSeq" by NCBI's Reference Sequence database representing naturally occurring molecules. Therefore, this study focused first on the characterization of these reported isoforms in comparison to the isoform 2, which is here referred to as "canonical MyD88".

In comparison to canonical MyD88, isoform 1 has an alternative donor splice site 24 nt downstream of exon 3 adding 8 AA upon Lys 227 within the TIR domain, additionally exchanging R->G 236, but the TIR domain sequence remains conserved. Isoform 3 skips exon 2, isoform 4 skips exon 3 and isoform 5 excludes exons 2 and 3 (Fig.2a). The exclusion of exon 3 leads to the deletion of one nucleotide originating a frame-shift, which not only alters the amino acid sequence of the protein but introduce a premature termination codon (Fig.2a,e). Therefore, I concluded that isoforms 4 and 5 do not have a TIR domain. The different AA sequence is shown in Figure 2e and in this study this unique sequence will be called as "C-terminal region (CTR)".

To clone all isoforms, coding sequences (CDS) were extracted from the references uploaded in the NCBI nucleotide portal (Fig.2b) and were purchased or synthesized. CDS were cloned into expression vectors, which fused a StrepIII-Hemagglutinin-tag (S-HA tag) at the N-terminus of the GOI to facilitate track of the proteins, using the gateway system. Vector maps are shown in supplementary Figure S1. The AA sequence of all isoforms plasmids is schematized in Figure 2c, showing the protein domains they share. Furthermore, immunoblotting analysis demonstrated expression and correct size of the

isoforms (Fig.2d and MW in Fig.2b). These plasmids have been used in following characterization experiments.

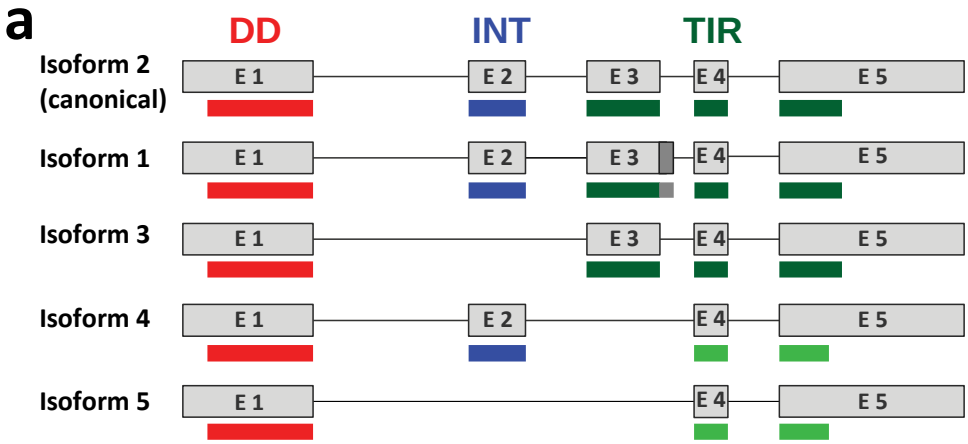

b

MyD88 Isoforms	Version	Size (bp)	No. AA	MW (kDa)	Reference
Isoform 1	WT	915	304	40,51	NM_001172567
Isoform 2	WT	891	296	39,646	NM_002468.4
Isoform 3	WT	795	264	35,998	NM_001172568.1
Isoform 4	WT	615	204	28,495	NM_001172569.1
Isoform 5	WT	480	159	23,541	NM_001172566.1

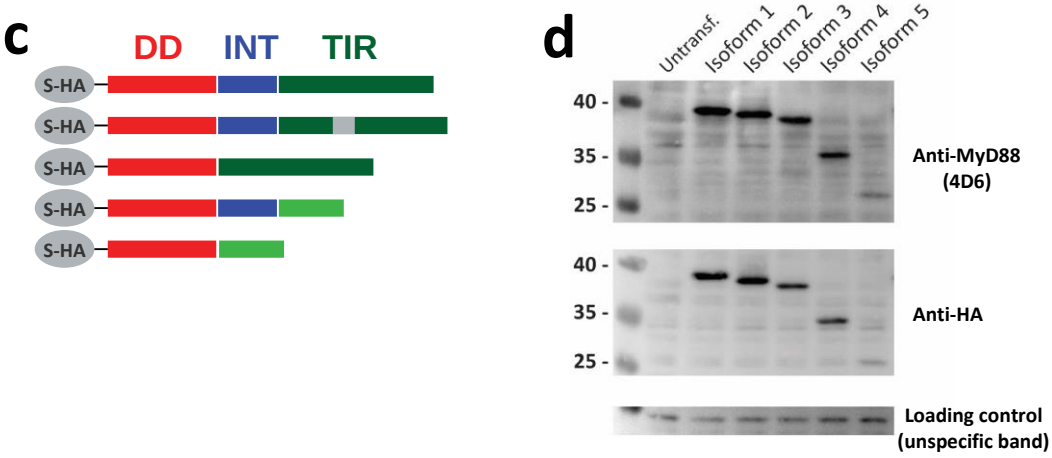

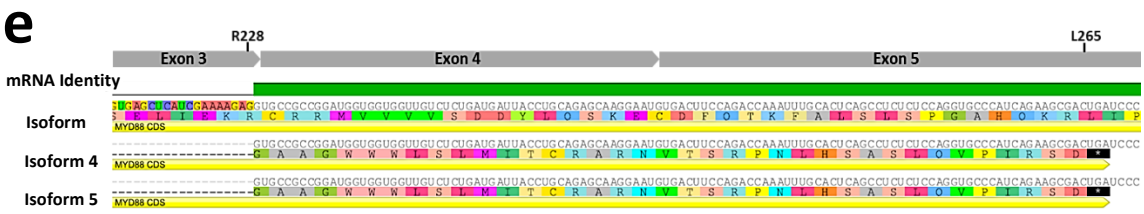

Figure 2. Generation and description of MyD88 isoforms plasmids. (a) Scheme of *MYD88* mRNA in gray blocks and coding sequence in colors according to reference sequences listed in (b). Red bar represents the death domain (DD), blue bar the intermediate domain (INT) and green the TIR domain. The light green bars show the CTR. (b) Detailed information on MyD88 isoforms. (c) Overview of MyD88 constructs highlighting the conserved domains they share. (d) Protein expression of the generated StrepIII-Hemagglutinin (S-HA)-tagged constructs transfected in HEK 293T cells showed by immunoblotting using antibodies against the DD of MyD88 and against the HA-tag. (e) Different AA sequence of exon 4 and 5 due to exon 3 exclusion in isoform 4 and 5; referred to as CTR. Black squares with an (*) represent a stop codon. Illustration done in Geneious Pro 5.5.9.

2.3.2 Ability of MyD88 isoforms to activate NF-κB

The main function of MyD88-signaling is the activation of transcription factors like NF-κB to arouse an immune response or/and support survival. Canonical MyD88 overexpression has been demonstrated to constitutively activate NF-κB in lymphomas (Ceribelli et al. 2014) and cell lines (Avbelj et al. 2014), shown by an NF-κB–dependent dual luciferase reporter assay (DLA). Therefore, I used the same assay to evaluate the NF-κB activation potential of MyD88 alternative isoforms by overexpression in the presence or absence of the endogenous MyD88, including all isoforms naturally expressed. Transient transfection of MyD88 isoforms in MyD88-deficient HEK 293T cells (known as I3A HEK293 cells, described in (Avbelj et al. 2014)) together with luciferase plasmids showed that isoforms 1, 2 and 4 induced NF-κB activation, whereas isoforms 3 and 5 demonstrated loss-of function (Fig.3a). To check if the presence of endogenous MyD88 change the activation potential of the alternative isoforms, normal HEK 293T cells were used. In this cell line, the five isoforms showed the same behavior, but the activation magnitude of isoform 1 was four times lower than the activation shown in I3A cells, suggesting a reduction of potency in the presence of endogenous MyD88 (Fig.3b). But, this last observation needs more experiments to be confirm. Moreover, in both cell lines NF-κB activation was dependent on the amount of plasmid transfected. In summary, isoform 1 and 4 can induce NF-κB activation by themselves, but isoform 3 and 5 not.

Since isoforms 3 and 5 were not able to activate signaling, and according to the literature isoform 3 has an inhibitory effect on the MyD88-dependent pathway, I also performed experiments to verify this finding. I overexpressed isoforms 3 and 5 in normal HEK 293T cells for DLA and stimulated them with flagellin, the ligand known to activate endogenous TLR5 in HEK cells. However, no inhibition effect was observed (Fig.S2). From this, I concluded that HEK cells may not be the suitable model system to study the inhibitory effect of the isoforms, because for isoform 3, it was only observed in innate immune cells.

Isoforms 4 and 5 had remained uncharacterized, because only truncated versions of MyD88 containing the DD (Loiarro et al. 2009) and DD-INT (Ceribelli et al. 2014, George et al. 2011) had been used to study the function and protein-binding of the canonical protein. Thus, the role of the shared CTR of these two isoforms has not been evaluated. Therefore, I proceeded to test if this CTR makes a difference in the isoforms functionality. For this I compared isoform 4 (Fig.3c) and isoform 5 (Fig.3d) directly with a truncated construct expressing MyD88 death domain plus intermediate domain from the canonical isoform. As observed in Figure 3c,d a MyD88 truncated version (DD-INT) is able to induce NF-κB activation like isoform 4, suggesting that the CTR does not influence the function of isoform 4. Important to mention is that the truncated version used here has Myc-Protein A as fused N-terminal tags and another backbone than the generated constructs, therefore we cannot precisely tell the function of the CTR. Thus, as short outlook the

generation of an appropriate DD-INT construct could help to assess CTR's role. Another observation is that isoform 5 protein expression is remarkably lower than isoform 4 and DD-INT (Fig.3e), suggesting that isoform 5 is not stable and might be degraded faster. Nevertheless, even higher amounts of plasmid (100 ng) did not show NF-κB activation (Fig.S2).

Together, these data suggest that isoform 1 and 4 can contribute to MyD88-dependent signaling towards NF-κB and propose the DD and INT as the main domains for signaling in overexpression conditions. Furthermore, isoform 3 and 5 cannot induce signal.

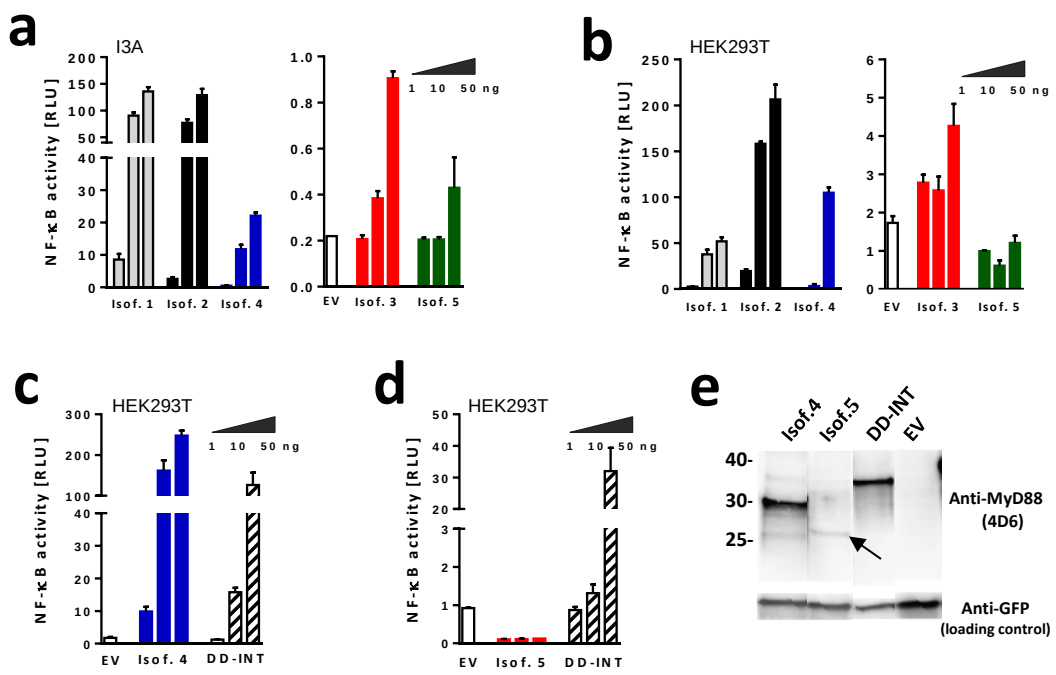

Figure 3. MyD88 isoforms have different phenotypes. (a-d) DLA measurements of NF-κB activation in (a) MyD88-defient I3A cells and (b-d) HEK 293T cells lysates upon transient transfection with MyD88 isoforms or truncated version together with NF-κB-inducible firefly luciferase and constitutive *Renilla* luciferase reporter. Cells were lysed 48 h later. Threshold for activation was set at 5 RLU. (e) Same lysates were used for immunoblotting, where eGFP served as transfection and loading control (n=1). Arrow points to isoform 5 corresponding band. Panels (a-d) are representatives of n=3 showing means+SD of triplicates. EV: empty vector; DD-INT: Death domain-intermediate domain; RLU: relative luminescence units; GFP: green fluorescent protein.

2.3.3 Physiological existence of MyD88 isoforms in healthy B cells and lymphomas

RNA sequencing data analysis determined the existence of MyD88 alternative splicing. Nevertheless, a cell-specific analysis for the presence of each isoform has not been done. Here, I chose B cells as a model, because some non-Hodgkin B cell lymphomas are known to be addictive to the MyD88-NF-κB pathway, which at least in myeloid cells can induce MyD88 alternative splicing. Therefore, I hypothesized that the chances to find alternative isoforms in B cell lymphomas are high. To test this hypothesis, together with collaborators (SH. Bernhart from University Hospital Ulm and R. Siebert from University of Leipzig), RNAseq data was analyzed from Burkitt lymphoma (BL), diffuse large B cell lymphoma (DLBCL), follicular lymphoma (FL) and FL-DLBCL samples. Because all tested lymphomas were derived from germinal center (GC) B cells, isolated GCB cells were also investigated. Additionally, naïve B cells were used as controls. To facilitate visualization of alternative splicing, RNA sequencing reads were aligned to the human genome and Sashimi Plots were generated, where exon reads are converted into density reads (y-axis) and splice junctions are represented as arcs (Fig.4a). Then, exon reads from all samples were normalized to total RNA amount and aligned to the human *MYD88* gene and corresponding annotations (Fig.4b). Next, as evidence for the existence of the differential isoforms, Sashimi plots of all samples together from naïve B cells, GCB cells and Burkitt lymphoma are presented, in which the abundance of splice junction is proportional to the width of the arcs (Fig.4c).

Sashimi plots demonstrated canonical MyD88 as the most prominent isoform, since the thickest arcs did not skip exons, and start and end at the constitutive splice sites. Furthermore, all isoforms except the canonical isoform have unique splice junctions that simplify the recognition of each alternative isoform; for example, arc in red represents isoform 3 skipping exon 2 (Fig.4c). Then, isoform 1 is represented by an arc starting at an alternative donor splice site within the intron after exon 3, isoform 4 by junction skipping exon 3 and isoform 5 by junction skipping exon 2 and 3. Interestingly, naïve B cells showed a prominent intron retention between exon 3 and 4. According to the signal, about half of the MyD88 mRNA transcripts present this intron retention event. This finding will be analyzed in detail in Section 2.2.6.

Overall, I concluded all annotated isoforms are expressed at mRNA level in B cell lymphomas and control GCB cells and naïve B cells. These isoform-specific junctions allowed quantification and deeper analysis of the Sashimi plots, which will be described in Figure 6.

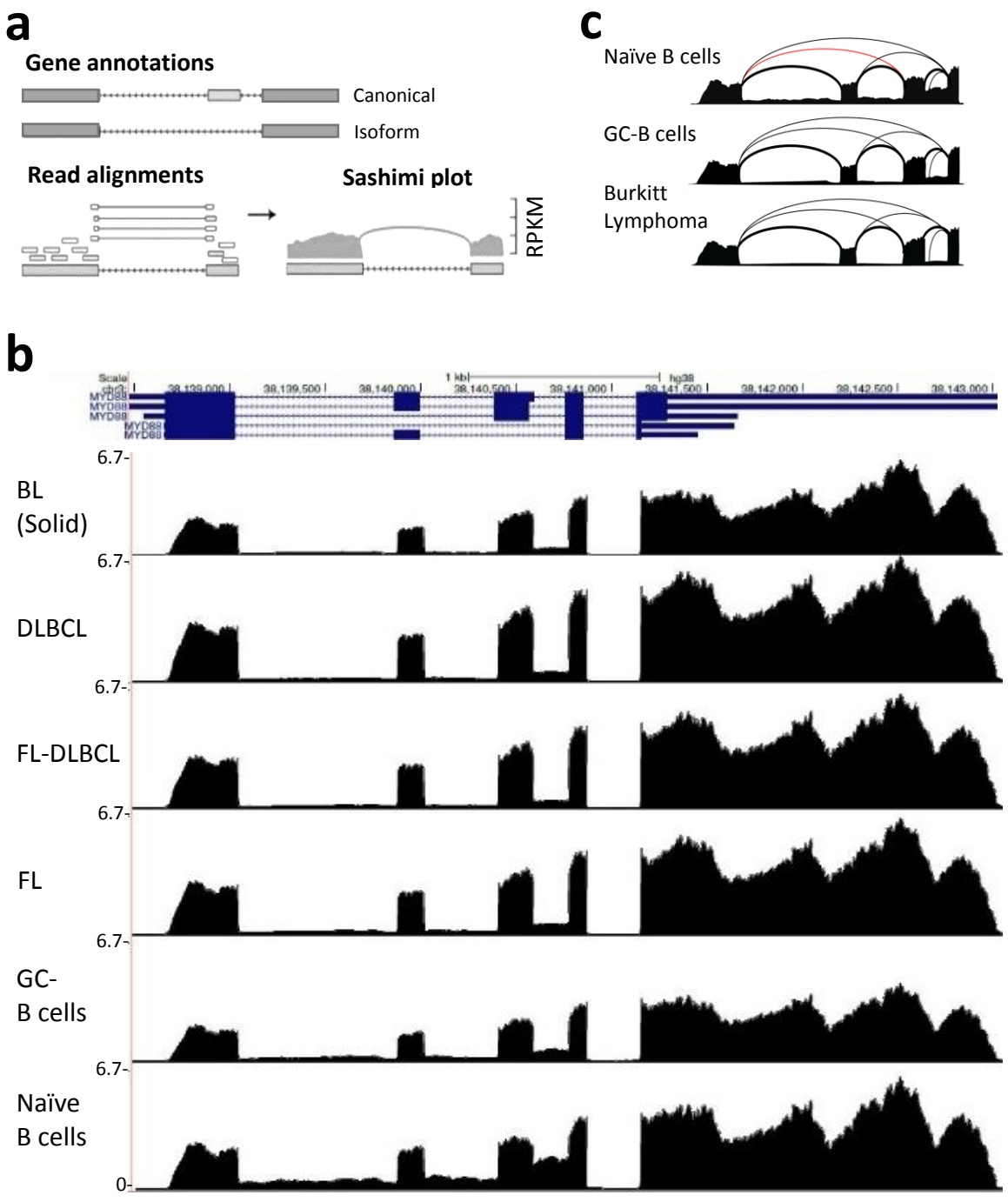

Figure 4. MyD88 isoforms are naturally occurring in B cells and lymphomas. (a) Figure adapted from (Avbelj et al. 2014, Katz et al. 2015), explaining generation of Sashimi plots. (b) RNAseq data alignment to the *MYD88* gene at hg38 using UCSC genome browser tracks. Normalized data to total expression levels (BL, n=21; DLBCL, n=72; FL, n=83; FL-DLBCL, n=14; GC-Bcells, n=5; naïve B cells, n=5). (c) Sashimi plots from naïve B cells, GCB cells and solid Burkitt lymphoma showing exon 1-4. Y axis (RPKM) represents exon reads and arcs represent exon junctions. The width of the arc is proportional to the number of junctions. RPKM: reads per kilobase million.

2.3.4 Detection of single MyD88 isoforms mRNA and protein

Upon confirming the physiological expression of the alternative isoforms in B cells, I developed a quantification system to assess their expression levels in different conditions. The aim was to test their regulation by TLR stimulation. For this purpose, I chose DLBCL immortal cell lines from both ABC and GCB types, and primary B cells as models of study. First, I designed exon spanning primers to specifically amplify and detect single isoforms (Fig.5a). To check if all primers were specific for each isoform I generated standard curves and tested each primer pair with all splice variants (Fig.S5). In summary, all primer pairs were specific with the exception of the primer pair for isoform 2 that is able to detect isoform 1 as well (data not shown). Amplification efficiencies are listed in Table 6 and Figure S5. Then, RT-qPCR was performed to determine the expression pattern of all alternative isoforms in DLBCL lines and primary B cells. Results showed that alternative isoforms are detectable in DLBCL lines but show significantly lower expression than primary B cells ($p<0.0001$). Expression levels of isoforms 4 and 5 were 2 fold and of isoform 3 were 2 to 4 fold lower than expression levels of primary B cells (Fig.5b). Thus, MyD88 alternative isoforms show lower expression in DLBCL in comparison to healthy B cells in a resting state.

Isoform 1 abundance was also tested but the amplicon had a different melting curve than the positive control, plasmid DNA encoding the sequence of isoform 1 (Fig.S2a). Because of the discrepancy isoform 1 was not included in further experiments. Interestingly, by Sanger sequencing I found that the amplicon for isoform 1, isolated from cells, contained the intron between exon 3 and 4 (Fig.S2b). At the beginning, this was thought to be a contamination of pre-mRNA, but as seen before and described later (Section 2.2.7), the observed intron retention is not an artefact, but instead a novel MyD88 isoform (Fig.7).

In addition to the transcription of MyD88 alternative isoforms, I showed by immunoblotting that all isoforms are expressed at the protein level. The detection of all variants was possible using an anti-MyD88 antibody against a sequence at the beginning of the DD, domain that all shared. Immunoblotting showed that the canonical isoform was the most abundant, and isoform 4 and 5 the least abundant (Fig.5c). Important to mention is that the detection of the alternative isoforms required excessive amounts of protein, approximately 50 µg protein per well (commonly used <20 µg).

In summary, I successfully designed primer pairs for the detection and discrimination by qPCR of all until now annotated MyD88 isoforms, except for isoform 1. Furthermore, besides low expression levels I could showed the expression of the variants at the mRNA and protein level.

2.3.5 Regulation of *MYD88* alternative splicing by TLR stimulation

To reproduce findings from the literature, in which isoform 3 expression is regulated by TLR4 activation (Adib-Conquy et al. 2006, Janssens et al. 2003), I stimulated PBMCs with LPS, CpG and Pam3CysK4 for 6, 8 and 24 h and measured MyD88 isoform abundance by qPCR. Results showed the expected increase of MyD88 isoform 3 upon LPS and CpG stimulation. Interestingly, the use of Pam3CysK4 tended to decrease the expression of all isoforms (Fig.S3).

Then, to assess if TLR4 signaling modified the expression of the isoforms, DLBCL cells were stimulated with LPS for 18 h and whole cell lysates were analyzed by immunoblotting with an anti-MyD88 antibody. THP-1 cells were used as controls, because it is a monocyte cell line in which isoform 3 according to previous studies is up-regulated upon TLR4 engagement and because *MYD88* KO THP-1 cells are available. Based on the predicted molecular sizes, all isoforms were detected, but no significant differences were found at protein level upon stimulation. Surprisingly, THP-1 cells showed also a notable expression of isoform 4 in comparison to the DLBCL cell lines (Fig.5c). A possible explanation why I could not see differences after LPS stimulation is because the ABC-DLBCL tested cell lines have a constitutive activation of NF-κB signaling (Ngo et al. 2011), thus LPS alone may not cause significant changes in the same downstream pathway and events, such as MyD88 isoforms expression. On the other hand, GCB-DLBCL cells might be unresponsive to LPS as tested in Chronic lymphocytic leukemia, another B-NHL (Jurado-Camino et al. 2015).

Since TLR signaling in B cells is important for antibody production and proliferation, I proceeded to assess the abundance of the isoforms during B cell proliferation *in vitro*. For this, I isolated human primary B cells and treated them with CpG plus IgM for 5 days as described in Lelis et al. (Lelis et al. 2017). B cells proliferated was successful as observed by four different populations in CFSE staining and FACs analysis (Fig.5d). Since we observed two populations of B cells we stained cells with CD19, a B cell marker to confirm its origin (Fig.5d). RNA was isolated at each day and analyzed for mRNA levels of the isoforms by qPCR. Unexpectedly, all MyD88 isoforms were downregulated during B cell proliferation. Isoforms showed ~2 down-regulation compared to the unstimulated B cells. Although the differences displayed no significance, the trend is obvious (Fig.5e).

Together, this data suggests that B cells reduce MyD88 overall expression and its alternative splicing when proliferating. This observation is supported by the comparison of isoform abundance between DLBCL lines and primary B cells presented previously and by statistical analysis of the RNAseq data described below.

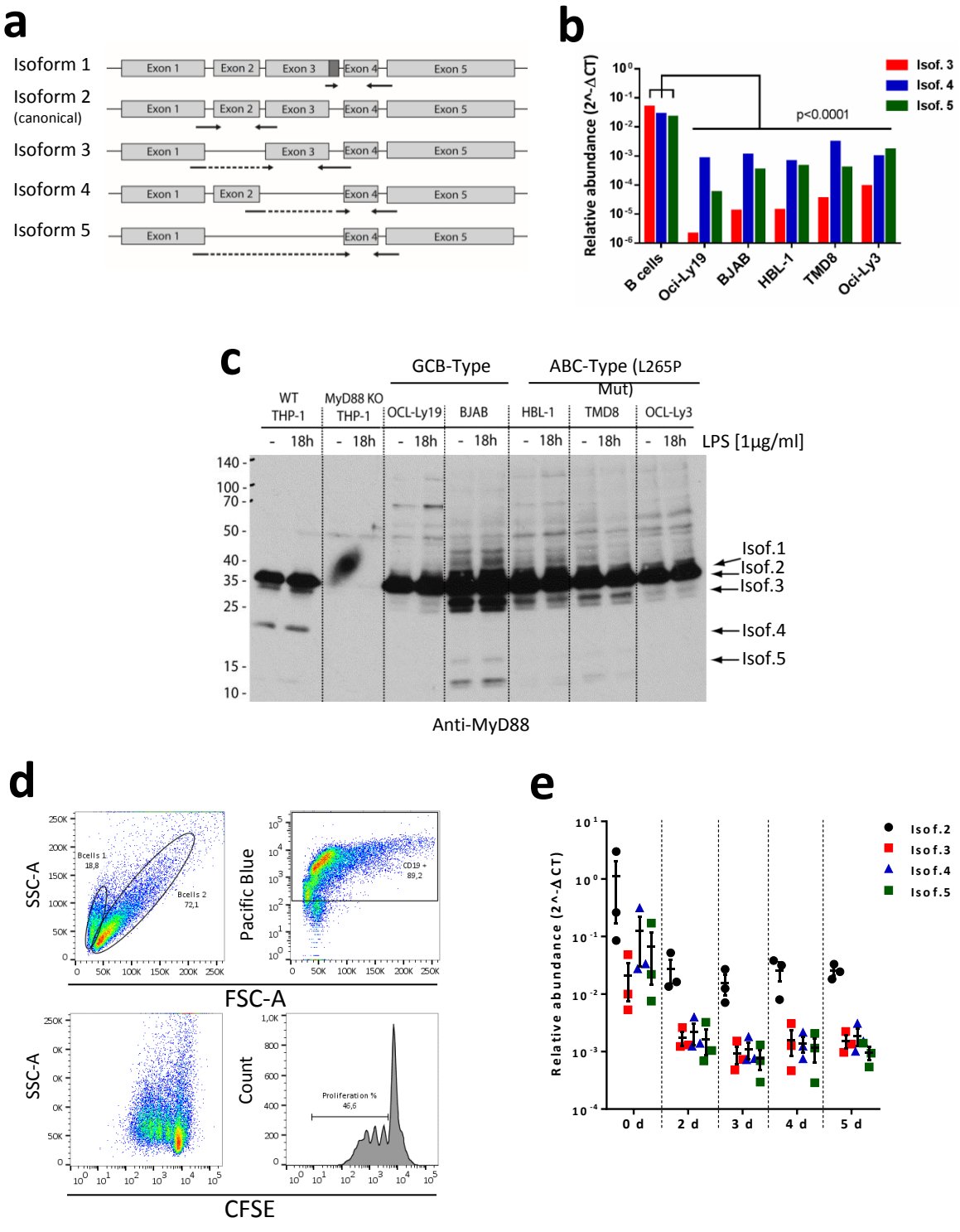

Figure 5. Regulation of *MYD88* alternative splicing by TLR stimulation. (a) RT-qPCR primer design strategy. (b) Relative abundance expression of MyD88 isoform mRNA in DLBCL lines normalized to *GAPDH* compared to healthy B cells (n=1, mean of triplicates); p values from 2way ANOVA test. (c) Expression of MyD88 isoforms assessed by anti-MyD88 immunoblot (n=1). (d) CFSE staining showing primary B cell proliferation and CD19 staining by FACs analysis; representative of n=3. (e) Relative abundance of isoform mRNA in primary B cells upon stimulation with 2,5 µg/ml CpG and 5µg/ml IgM (n=3). Shown mean+SEM from n=3.

2.3.6 Abundance of MyD88 isoforms in B cell lymphomas compared to healthy B cells

Non-Hodgkin B cell lymphomas are known to 1) overexpress MyD88 (Choi et al. 2013) and 2) have a high frequency of the hyperactive L265P mutation (Ngo et al. 2011). Both scenarios lead to constitutive NF-κB activation. I hypothesized that the expression of alternative isoforms is increased in B cell lymphomas versus healthy B cells, as observed for isoform 3 in monocytes and macrophages upon prolonged TLR4 stimulation, theoretically due to constitutive NF-κB activation (Adib-Conquy et al. 2006, Burns et al. 2003). Nevertheless, B cell proliferation *in vitro* demonstrated down-regulation of the isoforms and not the expected increased expression, suggesting that alternative splicing might be down-regulated upon prolonged TLR-BCR stimulation (Fig.5e). To extend the findings, the abundance of each MyD88 isoform in Non-Hodgkin B cell lymphomas and healthy cells was quantified using the RNAseq data presented before. Plotting the relative usage of each isoform per group of cells and lymphoma type, isoforms 1, 4 and 5 displayed significantly less abundance in lymphomas than in naïve B cells (Fig.6a,d,e). Isoforms 1, 4 and 5 mRNAs demonstrated to be 1- to 3-fold less than naïve B cells. In contrast, canonical MyD88 is 2-fold more expressed by lymphomas than healthy cells (Fig.6c) and strikingly, isoform 3 did not show significant differences (Fig.6b). Furthermore, GCB cells followed the same trend as naïve B cells using more alternative splice junctions, but with less significant data (Fig.6). Of note, no L265P cases were found in the tested samples.

Overall, alternative splicing seems to be down-regulated in oncogenic cells with the exception of isoform 3. Thus, this data suggests that B cell lymphomas use constitutive splice sites over the alternative sites. B cell lymphomas might then down-regulate alternative splicing to produce higher levels of canonical MyD88, which showed the highest activation of the pro-survival factor NF-κB. Furthermore, the stable abundance of isoform 3 implies a separate regulation for expression.

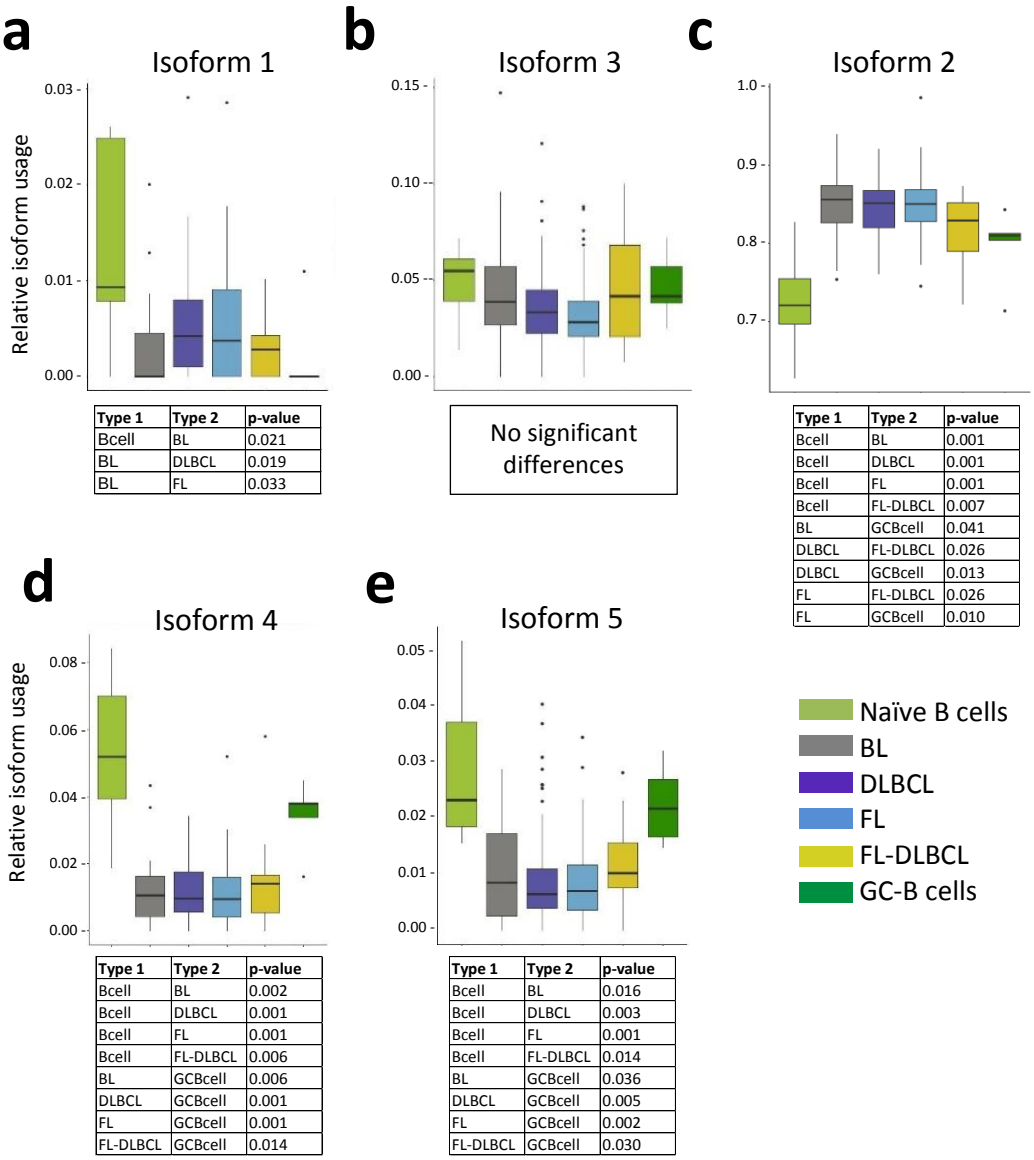

Type 1	Type 2	p-value
Bcell	BL	0.021
BL	DLBCL	0.019
BL	FL	0.033

No significant differences

Type 1	Type 2	p-value
Bcell	BL	0.001
Bcell	DLBCL	0.001
Bcell	FL	0.001
Bcell	FL-DLBCL	0.007
BL	GCBcell	0.041
DLBCL	FL-DLBCL	0.026
DLBCL	GCBcell	0.013
FL	FL-DLBCL	0.026
FL	GCBcell	0.010

Type 1	Type 2	p-value
Bcell	BL	0.002
Bcell	DLBCL	0.001
Bcell	FL	0.001
Bcell	FL-DLBCL	0.006
BL	GCBcell	0.006
DLBCL	GCBcell	0.001
FL	GCBcell	0.001
FL-DLBCL	GCBcell	0.014

Type 1	Type 2	p-value
Bcell	BL	0.016
Bcell	DLBCL	0.003
Bcell	FL	0.001
Bcell	FL-DLBCL	0.014
BL	GCBcell	0.036
DLBCL	GCBcell	0.005
FL	GCBcell	0.002
FL-DLBCL	GCBcell	0.030

Figure 6. MyD88 alternative isoforms are downregulated in B cell lymphomas.
Isoform quantification by relative abundance taking unique splice sites or junctions for each isoform: (a) exon3+20nt to exon4 = Isoform 1; (b) exon1 to exon3 = Isoform 3; (d) exon2 to exon4 = Isoform 4 and (e) exon1 to exon4 = Isoform 5. (c) Isoform 2 abundance = 1-ΣIsoforms\isoform2 abundance. Wilcoxon Mann-Whitney test was applied for statistical significance. Box-Whiskers plots and statistics were made by SH. Bernhart (University of Leipzig). BL, n=21; DLBCL, n=72; FL, n=83; FL-DLBCL, n=14; GCBcells, n=5; Bcells, n=5.

2.3.7 Discovery of novel isoforms

The initial RNAseq analysis by splice mapping revealed the presence of at least 2 novel isoforms. The most prominent newly discovered alternative splicing event is an intron retention between exon 3 and 4 (Fig.8a), event that generates a distinct splice variant with a truncated TIR-domain, here called isoform 6 (Fig.7 and Fig.8b). Furthermore, we found a novel splice site 20 nt upstream of the canonical donor site from exon 3, having a Human Splicing Finder score (HSF) of 81 (Desmet et al. 2009), creating isoform 7 (Fig.8a). A HSF score above 65 is consider a strong splice site. For isoform 7, two predicted sequences exist in GeneBank: 7.1 uses just the novel splice site and 7.2 additionally skips exon 2 (Fig.7 and Fig.8b). The use of this novel donor site shift the AA frame and causes an early stop codon and translates the exact C-terminal region determined for isoform 4 and 5 (Fig.7 and Fig.2e). Thus, the discovered splice events generate more truncated versions of MyD88. Since they have an intact DD-INT structure, they fulfill the requirements to transmit signal.

It is important to mention that intron retention is one of the rarest events of alternative splicing and often neglected, because these events may originate from contamination of pre-mRNA molecules (Ge and Porse 2014). Nevertheless, the intron retention observed here covers almost 50% of the total MyD88 transcripts, suggesting that the existence of the corresponding isoform is intentional.

Regarding the usage of the novel alternative splice sites, healthy B cells again showed a higher abundance than B cell lymphomas (Fig.8c,d). Thus, these final outcomes support the idea that lymphomas prefer the expression of the canonical MyD88 over the alternative and mainly truncated isoforms. Nevertheless, their function evaluation would be of high interest.

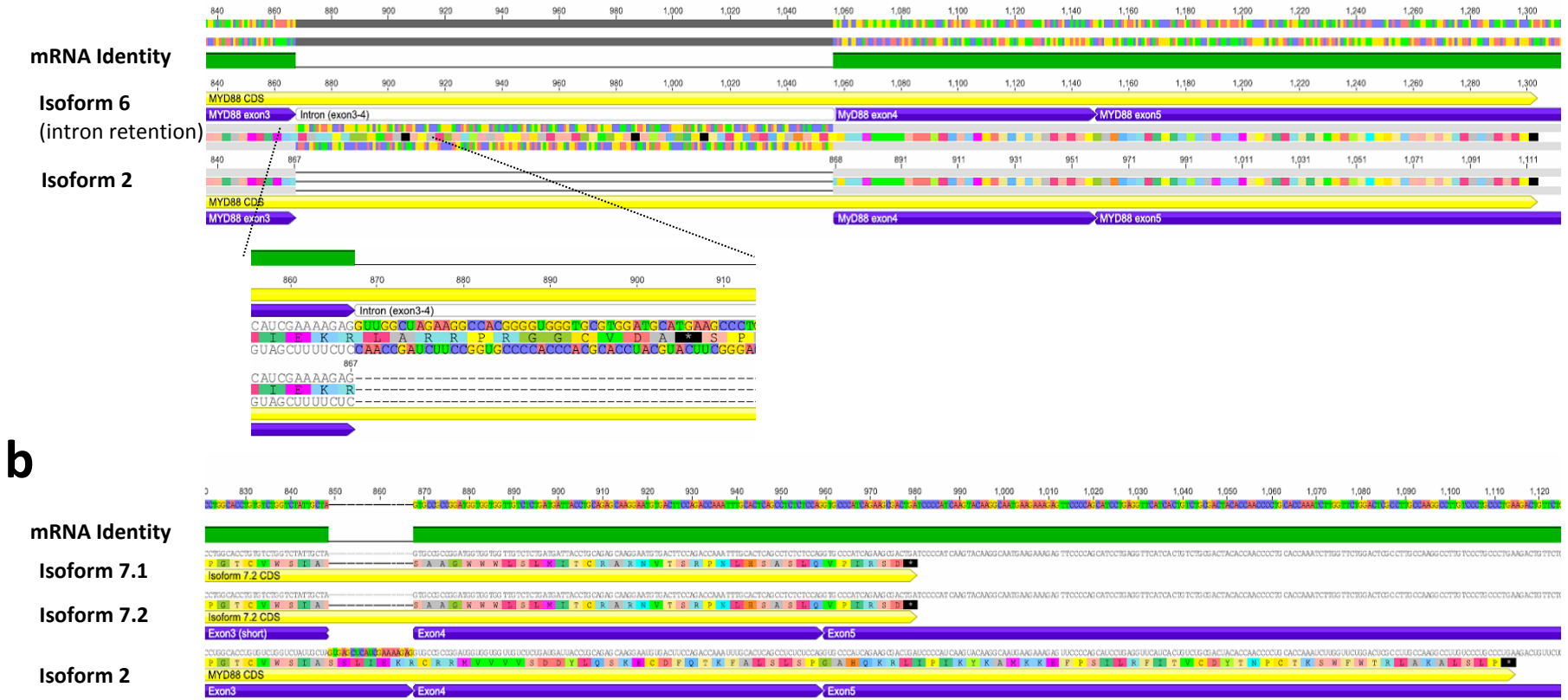

Figure 7. Illustration of isoforms 6 and 7 in comparison to the canonical MyD88 isoform. (a) Illustration of intron retention between exon 3 and 4 in isoform 6. Zoom in to show translation of intron retention which adds a premature stop codon. (b) Illustration of alternative splice site within exon 3 causing a frameshift in the AA sequence and therefore a premature stop codon. The translation of exon 4 correspond to the here called CTR. Pictures generated in Genious Pro 5.5.9. Big colored squares show AA sequence and black square with an (*) represent a stop codon.

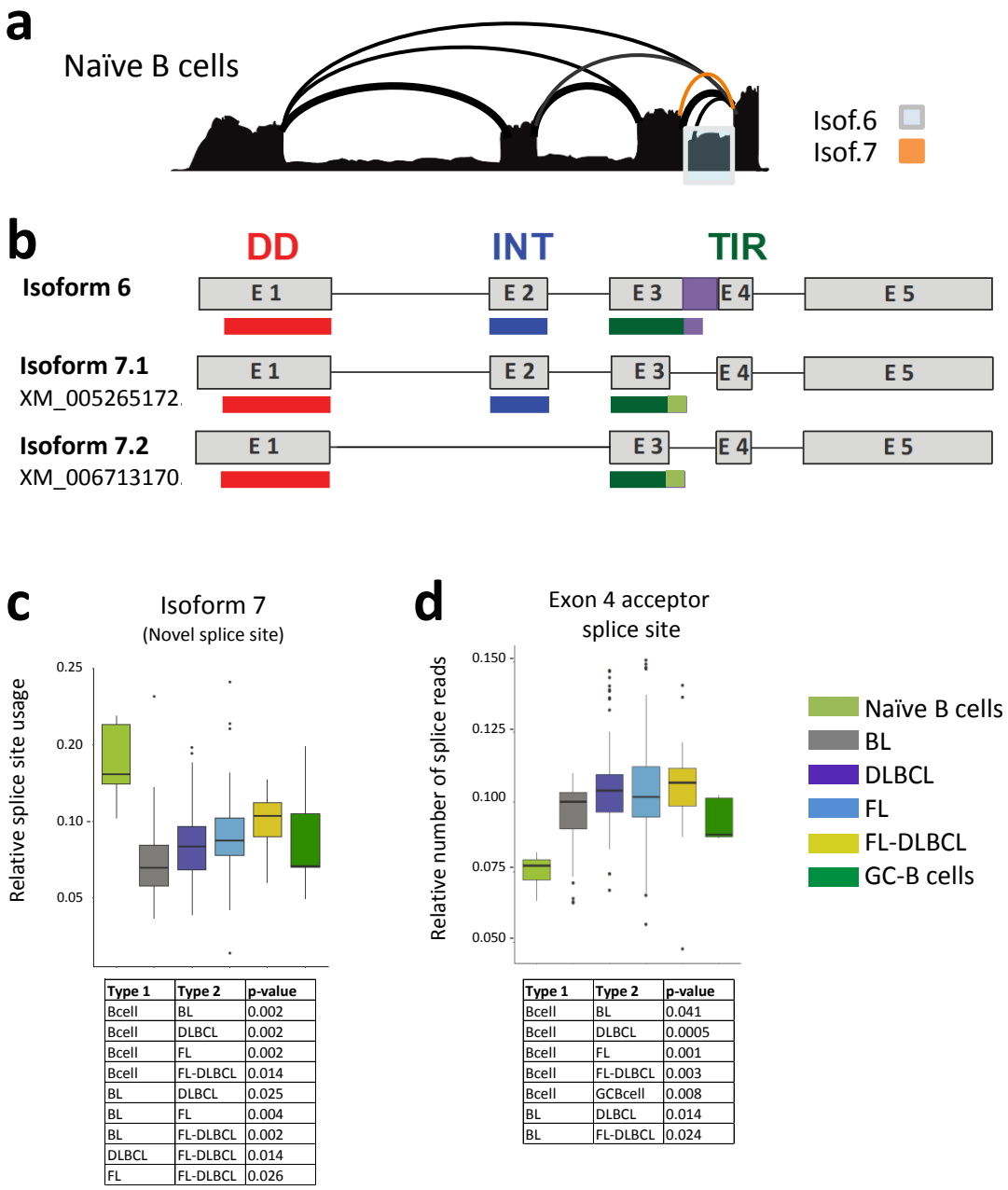

Type 1	Type 2	p-value
Bcell	BL	0.002
Bcell	DLBCL	0.002
Bcell	FL	0.002
Bcell	FL-DLBCL	0.014
BL	DLBCL	0.025
BL	FL	0.004
BL	FL-DLBCL	0.002
DLBCL	FL-DLBCL	0.014
FL	FL-DLBCL	0.026

Type 1	Type 2	p-value
Bcell	BL	0.041
Bcell	DLBCL	0.0005
Bcell	FL	0.001
Bcell	FL-DLBCL	0.003
Bcell	GCBcell	0.008
BL	DLBCL	0.014
BL	FL-DLBCL	0.024

Figure 8. Discovery of novel isoforms. (a) Sashimi plot from naïve B cells showing intron retention and the novel spice site. (b) Scaled scheme of MyD88 mRNA in gray blocks and coding sequence in colors according to domain sequences if available. Light green block represents CTR. (c-d) Isoform quantification by relative abundance taking unique splice sites for each isoform: (c) Novel site upstream of canonical donor within exon3 and (d) exon4 acceptor site. Wilcoxon Mann-Whitney test was applied for statistical significance. (c,d) Box-Whiskers plots and statistics made by SH. Bernhart (University of Leipzig). BL, n=21; DLBCL, n=72; FL, n=83; FL-DLBCL, n=14; GC-Bcells, n=5; naïve B cells, n=5.

2.3.8 Mutated MyD88 isoforms

As preliminary data, I tested if the somatic mutation c.794T>C (p.L265P) could influence the phenotype of alternative isoforms as previously shown with isoform 2 (Avbelj et al. 2014). Interestingly, mutated isoform 4 showed hyperactivity at low plasmid concentrations similar to canonical MyD88 (See arrows Fig.9a,b). However, other splice variants showed no different phenotype (Fig.9a,b). Last, the T>C exchange disrupts the original stop codon in isoforms 4 and 5 adding 8 extra AA. Thus, these extra AA could attribute the hyperactivity of isoform 4 (Fig.9c). Overall, this data confirms that Myd88 isoform 2 and suggests isoform 4 become hyperactive when introducing the corresponding L265P mutation.

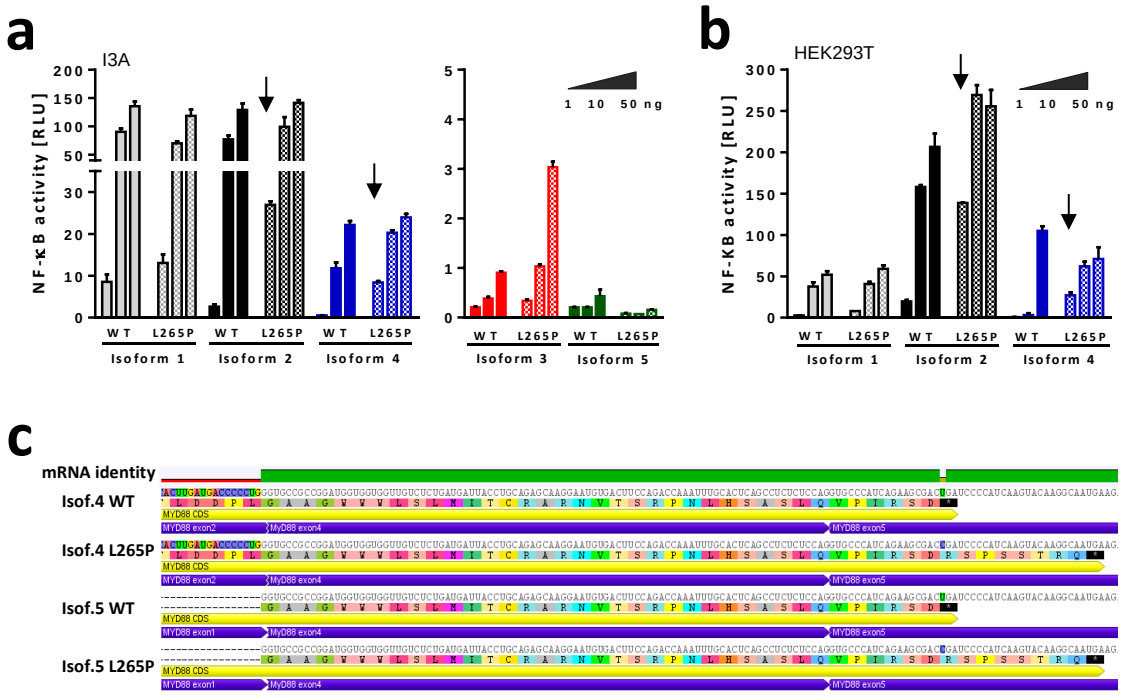

Figure 9. Myd88 isoforms 2 and 4 become hyperactive with the corresponding L265P mutation. (a,b) DLA measurements of NF-κB activation in (a) MyD88-defient I3A cells lysates or (b) HEK 293T cells lysates upon transient transfection with MyD88 isoforms in WT and mutated versions together with NF-κB-inducible firefly luciferase and constitutive *Renilla* luciferase reporter. Cells were lysed 48 h post transfection. Panels are representatives of n=3 showing means+SD of triplicates. (c) Addition of AA due to somatic mutation c.794T>C on exon 5 disrupts the original stop codon in isoforms 4 and 5. Big colored squares show AA sequence and black square with an (*) represents a stop codon. Illustration generated in Geneious Pro 5.5.9. RLU=relative luminescence units.

2.4. Discussion

MyD88 alternative splicing and its function have been little studied. To date, only isoform 3 was investigated and suggested to be a negative regulator of the MyD88 pathway in humans and mice. In general, alternative splicing has been implicated and shown to occur frequently in human cancer (Wang et al. 2015), but it is less well understood which alternative splice isoforms could contribute to the malignant state of the cells. Therefore, for MyD88, I first characterized its four alternative isoforms found in transcriptome analysis together with the canonical isoform. In luciferase reporter assays, two out of the four alternative isoforms (1 and 4), whose protein structure shared complete DD and INT domains, were able to induce NF-κB activity. These results were expected as truncated versions of canonical MyD88, designed as DD plus INT, were shown to be sufficient to transmit signal (George et al. 2011). On the other hand, constructs with separated domains, namely DD, INT and TIR alone were suggested to not induce, but instead inhibit the pathway (Loiarro et al. 2009, Avbelj, Horvat, and Jerala 2011, Fekonja, Bencina, and Jerala 2012). In my studies, I could only see the loss-of-function of isoform 5, which consists of the DD alone plus a CTR. However, the loss-of-function could also be due to a high mRNA or protein instability, as evidenced by the low signal in immunoblots. A possible explanation might be that its degradation is a result from the function of an mRNA surveillance pathway named nonsense-mediated mRNA system, which deals with transcripts with premature termination codons. This system commonly prevents the expression of C-terminal truncated proteins that could potentially have dominant negative properties (Ge and Porse 2014), as would be the case for isoform 5.

Previous studies also found that isoform 3 showed a loss-of-function and dominant negative effect on MyD88 signaling by overexpression in HEK cells and recurrent stimulation of macrophages, respectively (Avbelj, Horvat, and Jerala 2011, Adib-Conquy et al. 2006, Janssens et al. 2003). These properties were attributed to its lacking the INT, because this domain was reported to support MyD88 conformational changes critical to signal transmission (Avbelj, Horvat, and Jerala 2011). To assess the inhibitory effect of isoform 3 and potentially of isoform 5, I performed several experiments using the DLA system in flagellin-stimulated HEK cells, but I could not see suppression of TLR5 signaling by overexpression of the isoforms. As isoform 3 inhibitory effect has been only shown in macrophages, bronchial epithelial cells and fibroblast, I consider the effect could not be seen here, because it has been shown in innate immune cells, but not in other cells e.g. HEK cells. Furthermore, the negative regulation has been exclusively shown for TLR2 and TLR4 signaling (Andrews et al. 2016, Burns et al. 2003, Adib-Conquy et al. 2006). Thus, to gain knowledge about isoform 3 and 5, it will be interesting to overexpress them in B cells and check its function. TLR2 stimulation, together with isoforms overexpression in B cells would be also of high interest to assess the restrictedness of the negative effect to this TLR and rule out cell-specific effects. Also, TLR2 stimulation is often used, besides TLR9, to

induce B cell proliferation with BCR co-stimulation (Ganley-Leal, Liu, and Wetzler 2006, Bekeredjian-Ding and Jego 2009, Bekeredjian-Ding et al. 2007). Thus, in general, these conditions are a good system to further study all isoforms' function in B cells.

Next, based on knowledge from the literature that MyD88 overexpression and the hyperactive mutation L265P lead to a constitutive activation of NF-κB in B cell lymphomas and that isoform 3 expression is inducible by prolonged TLR stimulation (presumably via NF-κB), I hypothesized that B cell lymphomas addicted to NF-κB signaling (e.g. FL and ABC-DLBCL (Ngo et al. 2011, Suzuki et al. 2010)) would have higher expression of MyD88 alternative isoforms than other lymphomas (e.g. Burkitt lymphoma and GCB-DLBCL) and healthy B cells. Additionally, the hypothetically increased expression of the alternative isoforms and the ability of isoforms 1 and 4 to transduce signal could support the proposal that the alternative isoforms contribute to the activation of the pro-survival transcription factor. To test these hypotheses, I started evaluating possible regulatory conditions of MyD88 isoforms expression using CD19+ primary B cells as a healthy control and DLBCL cell lines as oncogenic samples. Overall, I could show the expression of the alternative isoforms at mRNA and protein level and interestingly the abundance of the alternative isoforms was lower in the DLBCL lines versus primary B cells. Additionally, primary B cells under proliferative conditions reduced the expression of all MyD88 isoforms. Together, both observations turned out to be the opposite of my hypothesis.

The latter finding, low MyD88 levels during proliferation, even of the canonical isoform, could be explained by a B cell subtype-specific issue. In this study, I stimulated peripheral B cells with a TLR9 and B cell receptor (BCR) agonist to mimic conditions of a B cell entering the germinal center where proliferation (Lelis et al. 2017), class-switching and differentiation to plasma cells in a T-independent manner happens, theoretically events dependent on MyD88 overexpression (Hua and Hou 2013, Rawlings et al. 2012). However, MyD88 overexpression has been observed in follicular B cells entering the germinal center, and it has not yet been measured in other B cell subtypes such as peripheral B cells under conditions of stimulation. Moreover, extrafollicular B cells are suggested to need a TACI-MyD88 signaling for germinal center events (He et al. 2010, Rawlings et al. 2012). Together, this could indicate that I observed a general down-regulation of MyD88 transcription during primary B cell proliferation because I used different stimuli and another subtype of cells. Thus, it will be worth to test the TACI-MyD88 signaling instead of the TLR9-MyD88-BCR signaling to assess the expression levels of MyD88 isoforms and clarify the discrepancy of total expression.

Furthermore, since DLBCL cell lines showed less expression of alternative isoforms than primary B cells in RT-qPCR analysis, together with collaborators I did a deep RNAseq data analysis of BL, FL, DLBCL and GCB-DLBCL samples, and germinal center and naïve B cells as controls, to have clearer results regarding my hypothesis. Data showed the natural

occurrence of the 5 previously described MyD88 isoforms and gave convincing evidence for the existence of 2 additional alternative isoforms (isoform 6 and 7). Isoform 2 exhibited higher mRNA levels (overexpression) in lymphomas than in healthy cells as expected and previous shown (Mudaliar et al. 2013, Choi et al. 2013). Nevertheless, the abundance of the alternative isoforms was in general lower in B-NHL than in healthy B cells, except for one isoform (isoform 3). To understand better these outcomes, I will discuss first how alternative splicing can be regulated.

Alternative splicing is a process by which defined "alternative" splice sites are preferred to canonical splice sites. This process can either occur constitutively or under regulatory conditions, which can be dependent on cellular stimulation or cell type. For example, MyD88 isoform 3 expression can be increased by stimulating innate immune cells with TLR ligands, whereas fibroblast growth factor receptor-2 (FGFR2) is an example for cell type-specific expression, in which one of two different isoforms is expressed in either epithelial cells (FGFR2-IIIb) or mesenchymal cells (FGFR2-IIIc) (Wagner et al. 2003, Kozlovski et al. 2017). Thus, stringent regulation of alternative splicing is crucial for the complex requirements of tissue- or signaling-dependent splicing under normal conditions. However, alternative splicing in oncogenesis is frequently manipulated leading to aberrant splicing (Sveen et al. 2016). A recent example is the expression of alternative isoforms, α, β and γ, in breast cancer of the protein DMTF1 (Tian et al. 2017, Maglic et al. 2015), which isoform b induce strong proliferation and progression of the cancer cells.

There are a wide variety of causes of alterations in the splicing process, but here I will discuss the most common ones. One cause is direct aberrations in splice factors, which can be alterations of their abundance, localization and activity. The most common example is the overexpression in many cancers of the oncogene *MYC*. MYC controls transcription of multiple splicing factors resulting in aberrant splicing of numerous genes related to lymphomagenesis discovered and reviewed by Koh and colleagues (Koh et al. 2015). Interestingly, MyD88 was not listed. Mutations in splice factors are less frequent, but have been seen in e.g. the spliceosome member SF3B1 appearing in breast cancer, melanoma and chronic lymphocytic leukemia (Alsafadi et al. 2016, Singh and Eyras 2017, Wan and Wu 2013). One of the frequent SF3B1 mutations is p.K700E, which has been proved to cause aberrant splicing (Obeng et al. 2016, Inoue and Abdel-Wahab 2016) and loss-of function (Darman et al. 2015, Wang et al. 2016). Strikingly, SF3A1 or SF3B1 knock down, mimicking loss of function, has showed to induce MyD88 isoform 3 expression in murine macrophages, as published by De Arras et al. (De Arras and Alper 2013). Therefore, the authors proposed SF3A1/SF3B1 as regulatory candidates for MyD88 alternative splicing, though they only investigated isoform 3. Despite SF3B1 mutations have been discovered in chronic lymphocytic leukemia (Wang et al. 2016, Wan and Wu 2013, Wu, Tschumper, and Jelinek 2013), which is also a B-NHL, there is no evidence that this mutation occurs in the tested B-NHLs. The second most common manipulation of

alternative splicing are polymorphisms within the affected gene. Mutations can occur in splicing enhancer/silencer elements or create new splice sites (Tazi, Bakkour, and Stamm 2009). Most of the splice site mutations that lead to human disease happen at the GT and AG dinucleotides in the 5' and 3' canonical splice sites, essential sites for exon definition. Thus, mutations at these positions result in exon skipping, activation of a cryptic splice site, or intron retention (Ward and Cooper 2010). However, in the case of MyD88, alternative splicing events occur in healthy B cells and seem not to be products of aberrations. Thus, considering all the mentioned causes of aberrant alternative splicing found in oncogenesis and the main finding that MyD88 alternative splicing is downregulated in B cell lymphomas, I conclude that MyD88 alternative splicing occurs under normal conditions and it is not a consequence of oncogenesis or NF-κB constitutive activation as hypothesized.

My study showed that alternative isoforms 1 and 4 induce NF-κB activation and based on the protein sequence of isoform 6 and 7.1 I speculate that they might too. However, why are alternative isoforms downregulated in B cell lymphomas, although the majority is able to induce signaling via NF-κB? The data presented in this thesis indicates that lymphomas prefer the expression of the canonical MyD88 over the alternative isoforms. All alternative MyD88 isoforms are truncated versions of the canonical version (with the exception of isoform 1) and they all showed less activation potential for NF-κB than canonical MyD88. Together, this suggests that lymphomas suppress alternative splicing in order to produce the most potent isoform, canonical MyD88, which has been confirmed many times to contribute to oncogenesis; for example MyD88 overexpression was associated with worst prognosis, tumor recurrence and shortened disease-free survival in DLBCL cases (Reddy et al. 2017, Choi et al. 2013). Hence, one imaginable role of the MyD88 alternative splicing is to counterbalance the potency of the canonical isoform. This idea is supported by the discovery of Rhyasen et al. and unpublished findings by Smith et al., in which another important member of the TLR pathway, IRAK4, was found to express a cancer-specific isoform in myelodysplastic syndrome (MDS) developed to acute myeloid leukemia (AML) (Rhyasen et al. 2013). This isoform lacks the N-terminal death domain, important for the interaction with MyD88 and IRAK1 (see Figure 1) but showed the ability to induce innate immune signaling. Nevertheless, Smith et al. found that MDS/AML samples predominantly express the canonical IRAK4 protein, while normal hematopoietic bone marrow cells express the truncated IRAK4. Moreover, they demonstrated that canonical IRAK4 expression is significantly associated with increased NF-κB activity and correlates with poor AML patient outcome (Smith et al. 2016). Thus, alternative splicing of MyD88 and IRAK4 seem to be downregulated by cancer in order to express the canonical isoforms, being the most potent variants. To support this idea, I performed a pilot analysis of RNAseq data from ovarian cancer samples. Similar to B cell lymphomas, MyD88 overexpression is known to exert an oncogenic effect by inducing constitutive NF-κB activation in ovarian cancer (Annunziata et al. 2010). Furthermore, it

has been demonstrated that NF-κB plays a role in the propagation and poor outcome of ovarian cancer (Annunziata et al. 2010, Alvero 2010). Preliminary analyses showed the existence of the MyD88 splice variants in ovarian cancer samples, as well as the novel isoforms (Fig.S6). But, further analysis concerning the abundance of MyD88 isoforms in comparison to healthy ovarian cells remain to be done.

Regarding isoform 3, surprisingly it showed no significant differences between the groups and remained similar in healthy and oncogenic conditions of B cells. Thus, its expression trend implies that this isoform might be regulated separately from the other splice variants. The fact that isoform 3 is the only one lacking the intermediate domain and described to have an inhibitory function, makes it very likely that its regulation is different. For example, its expression could be independent of the NF-κB pathway or regulated by distinct splicing factors as shown by SF3B1 knock down (De Arras and Alper 2013). Nevertheless, I cannot rule out the possibility of a different regulation of the isoform between myeloid cells and lymphocytes, because this study is the first to assess MyD88 alternative splicing in B cells and TLR stimulation showed downregulation of MyD88 total transcription. Its inhibitory effect plays a critical role in acute responses, since it has been linked to tolerance of TLR2 and TLR4 re-stimulation upon septic conditions in human monocytes (Adib-Conquy et al. 2006); but has not been investigated so far in oncogenesis. Thus, the regulation of MyD88 isoform 3 in oncogenesis will be of high interest since its inducible overexpression could be a potent and natural inhibitor of the MyD88-dependent pathway in the corresponding MyD88-driven B cell lymphomas.

Collectively, MyD88 alternative splicing is not an oncogenic cause and MyD88 alternative isoforms do not seem to have an oncogenic role at least in the B cell lymphomas tested in this study. Instead I propose that MyD88 alternative isoforms may play important roles in the broad functions of MyD88 in B cells (presumably before entering the germinal center or other stages) or in other cell types.

Focusing on the fast and high dynamic assembly and disassembly of the Myddosome it is likely that the alternative isoforms can support Myddosome formation. Recently, it was published by Bryant and colleagues that upon activation, TLR4/MD2 only forms dimers and not oligomers to nucleate the assembly of the Myddosome, demonstrating a stoichiometric mismatch between the receptor and the huge complex (Latty et al. 2018). As determined by the crystal structure the Myddosome contains six MyD88 death domains (Lin, Lo, and Wu 2010). Thus, TLR4 has just a transient role in the nucleating assembly (Latty et al. 2018). MyD88 alternative isoforms 1, 4, 6 and 7 can transmit signal, and interestingly isoform 6 has a truncated TIR domain and isoforms 4 and 7 do not have this domain. Because the TIR domain comprises the biggest portion of the MyD88 molecule, one could assume that the truncated isoforms (4,6 and 7) could have a steric advantage in the complex, needing less space as the canonical MyD88 and conferring

more structural flexibility to the complex. The latter publication indicated that only two TIR domains are needed for the nucleation of the Myddosome (Latty et al. 2018), thus theoretically also only 2 canonical MyD88 molecules are enough for the nucleation, opening the possibility to truncated versions to complete the complex, since the MyD88 scaffold contains six MyD88 death domains (Lin, Lo, and Wu 2010) and all alternative isoforms have this domain. Additionally, defined truncated versions of the canonical MyD88 were used to study MyD88's function and interactions with other members of the TLR-MyD88 cascade. For example, TACI was shown to bind to MyD88 in a TIR-independent manner in B cells (He et al. 2010). Thus, truncated isoforms could also mediate specific MyD88-interactions to other molecules and/or therefore induce signaling of transcription factors, apart from NF-κB, as determined by canonical MyD88 (e.g. CREB, AP-1) (Gay et al. 2014).

2.5 Conclusion

MyD88 has been associated to many different cancer types, specially to non-Hodgkin lymphomas due to overexpression and the somatic mutation L265P. These aberrations lead to a constitutive NF-κB signaling, which mediates cell survival, proliferation and maintenance of the tumor environment. Furthermore, assuming from the literature that the expression of the MyD88 alternative isoform 3 can be induced by acute TLR-signaling, e.g. during sepsis, theoretically in a NF-κB-dependent manner; I hypothesized that B cell lymphomas addictive to NF-κB signaling would have higher levels of alternative splicing than healthy B cells. Moreover, the alternative isoforms could support the oncogenic effect of MyD88. This study is the first to prove the existence of all until now annotated MyD88 isoforms, plus two novel isoforms, in primary B cells and Non-Hodgkin B cell lymphomas at the mRNA and protein level. I also showed that potentially four out of the six MyD88 variants are functional. And although the alternative isoforms did not show relevance for oncogenesis, at least in B cells, they suggest having a functional role in healthy cells, where they were highly expressed. I speculate that MyD88 alternative isoforms could participate in the Myddosome formation, signal transmission and extend protein-interactions of canonical MyD88. Thus, alternative isoforms warrant further investigation assessing their potential roles in the Myddosome assembly and the regulation of alternative splicing process as a mechanism to attenuate the oncogenic potency of canonical MyD88.

Chapter 3: Assessing Chitin-TLR2 interaction in mammals

3.1 Introduction

Chitin is the second most abundant polysaccharide in nature, having a vital role in the structural stiffness of cell walls present in exoskeleton of arthropods, the egg-shell of nematodes and the cell wall of fungi. Unlike other oligosaccharides, chitin has been described as a strong immunogenic ligand relevant in fungal infections and as an allergen associated with allergic asthma in humans (Brown et al. 2012, To et al. 2012). Additionally, although different receptors have been hypothesized to recognize chitin and mediate its multiple pathological effects, depth molecular studies describing how chitin is sensed by a receptor in innate immune cells are required (Bueter, Specht, and Levitz 2013).

3.1.1 Chitin properties and metabolism

Chitin is a linear homopolymer of β-(1,4)-linked N-acetyl-D glucosamine (GlcNAc) monomers, able to form stable microfibrils that, together with glycoproteins and β(1,3)-glucan chains, constitute the structural basis of hard cell walls from living beings. Of interest is that chitin is a component of fungal cell wall (Munro and Gow 2001). Chitin requires a complex synthesis process including seven classes of chitin synthase enzymes in fungi. Although they have shown to be redundant, their expression can vary among fungal strains and suggests being tightly regulated (Pacheco-Arjona and Ramirez-Prado 2014). The expression and activity of chitin synthases change throughout the fungal cell cycle and under stress conditions. For example, in response to lytic enzymes or oxidants within phagolysosomes of innate immune cells, chitin synthases are overexpressed to restore fungus cell integrity. Furthermore, transcriptional activation of synthases may be clinically relevant since it is a protection mechanism against antibiotics and anti-fungal drugs through thickening of the fungal cell wall (Lee et al. 2008, Lenardon, Munro, and Gow 2010).

Besides its presence in human disease vectors, like insects, and infectious pathogens, chitin alone has been determined to elicit a strong immunogenic response as an allergen and as a MAMP (Reese et al. 2007, Lee et al. 2008, Lenardon, Munro, and Gow 2010, Choi et al. 2016). Chitin is sensed by a large array of immune cells such as macrophages and eosinophils, or stromal cells like epithelial cells and keratinocytes evoking inflammation and allergy, reviewed in (Elieh Ali Komi, Sharma, and Dela Cruz 2017). Thus, to overcome chitin's pathogenicity, mammals have developed mechanisms to degrade it.

Mammals and bacteria can catabolize chitin. Chitin polymers catabolism is mediated by chitinases, e.g. human Chitotriosidase, and chitinase-like proteins e.g. breast regression

protein (BRP)-39/YKL-40 (Lee et al. 2011), which degrade chitin in two steps: 1) initial hydrolysis generating chitin oligosaccharides and 2) further break down of glycosidic bonds to dimers or monomers (Elieh Ali Komi, Sharma, and Dela Cruz 2017). Bacteria and fungi use chitinases to recycle the saccharides (Bueter, Specht, and Levitz 2013). Important in this project are two main groups of chitinases: endochitinases and exo-chitinases. Endochitinases randomly hydrolyze chitin at internal sites generating low molecular mass multimers such as chitotriose and chitotetraose or longer oligomers. On the other hand, exo-chitinases catalysis starts at the non-reducing end, breaking the oligomeric products of endochitinases, thereby generating GlcNAc monomers (Hamid et al. 2013). Incidentally, we and others (Kuusk, Sorlie, and Valjamae 2017) propose that chitinases, specially endochitinases, could degrade microbe-derived chitin-containing structures and once released, oligosaccharides could subsequently trigger an immune response. Furthermore, dysregulation in the expression, mainly increased levels, of chitinases and chitin-like proteins has been linked to inflammatory and allergic conditions such as inflammatory bowel disease and asthma (Lee et al. 2011). Therefore, in this project we aimed to assess the induction of chitin-dependent innate immunity triggered by chitin oligomers from 4 to 15 GlcNAc.

3.1.2 Chitin immune responses in mammals

In mammals, recent studies have suggested that several PRRs are responsible to regulate chitin-dependent immune responses: 1) Da Silva and colleagues (Da Silva et al. 2009) found that in macrophages, the CLRs mannose receptor and Dectin-1 trigger the production of TNFα and IL-10 in response to chitin. Additionally, 2) Da Silva et al. (Da Silva et al. 2008, Da Silva et al. 2009) also showed that TLR2 can mediate chitin-responses inducing expression of TNFα, IL-10, IL-17A and IL-17AR expression. 3) Wagener et al. (Wagener et al. 2014) using corresponding knockout mice, showed that upon chitin recognition, TLR9, a toll-like receptor member, and NOD2, a nucleotide-binding oligomerization domain-like receptor member, both down-regulate the chitin-mediated inflammation by producing the anti-inflammatory cytokine IL-10. 4) Mora-Montes et al. (Mora-Montes et al. 2011) demonstrated that chitin can block the recognition of immunogenic β-glucans on fungal pathogens by Dectin-1, a member of the C-type-lectin-like receptors. And 5) further CLRs like Mincle and mannose receptor (Wagener et al. 2014, Kottom et al. 2017, Shibata, Metzger, and Myrvik 1997) have been also suggested to sense chitin, but with high controversy.

Yet, even though the above-mentioned receptors have been associated to chitin-immune responses, the exact molecular mechanisms behind the immune response were not elucidated and the direct binding to chitin was not validated. Thus, the responsible receptor for the immunological effects of chitin remains elusive. Furthermore,

contaminants in used chitin preparations cannot be excluded and could be responsible for the immunogenic effects measured. One possible explanation for the lack of validation experiments can be chitin's highly polymeric structure. Chitin preparations in the publications cited above are 1-40 µm large, containing thousands of GlcNAc monomers (Fuchs et al. 2018). Such dimensions make it difficult to assess the chitin-receptor interaction at the molecular level, since a typical ectodomain size of a receptor is in average 8 nm (Gutmann et al. 2018). Moreover, chitin polymers are insoluble and therefore difficult to purify. On the other hand, chitin oligomers have been used to define the multimeric CEBiP/Cerk1 chitin receptor, as part of the plant innate immune response against fungal chitin (Miya et al. 2007, Liu et al. 2012). Furthermore, Schlosser et al. (Schlosser et al. 2009), discovered FIBDC1 as a mammalian chitin-receptor, found highly expressed in enterocytes of the gastrointestinal tract, using also chitin oligomers. However, this latter recognition has not been associated to an immune response so far.

Thus, here we proposed to use defined-size chitin oligomers to assess chitin-receptor interaction and the resulting immune response.

3.1.2 Toll-like receptor 2

Toll-like receptor 2 is a special TLR because it increases the variety of its ligands by forming heterodimers with TLR1, TLR6 and possibly TLR10. These TLRs are proposed to be unable to induce signal in the absence of TLR2, and likewise TLR2 is probably unable to signal without a co-receptor. TLR2 and TLR1 together identify triacylated lipopeptides, and TLR2 with TLR6 diacylated lipopeptides (Gay et al. 2014). Both lipopeptides are components from the cell-wall of Gram-positive and Gram-negative bacteria, and mycoplasma (Takeuchi et al. 2001). Thus, synthetic ligands are commonly used to engage each specific dimer, for TLR2/TLR1: Pam3CSK4 is used and for TLR2/TLR6: Pam2CSK4, FSL-1 and MALP-2 are used. FSL-1 and MALP-2 are synthetic diacylated lipopeptides derived *from Mycoplasma salivarium* and *Mycoplasma fermentans*, respectively (Shibata et al. 2000, Takeuchi et al. 2001). Not long ago, TLR10 has been shown to also dimerize with TLR2 evoking an anti-inflammatory response (Oosting et al. 2014). All TLR2 heterodimers have been proven to signal primarily in a MyD88-dependent manner; nevertheless Nilsen et al. revealed that these heterodimers can be internalized towards early endosomes, where they can signal via the TRAM/TRIF-pathway inducing the production of IFN-β and CCL4 (chemokine C-C-motif ligand 4). Additionally, in the endosomal compartment, they can induce production of CCL5 involving the kinase TBK1 and transcription factor IRF3, as well as MyD88 (Nilsen et al. 2015). Interestingly, the engagement of a TLR2/TLR10 dimer apparently fails to induce a typical pro-inflammatory response but rather inhibits the production of inflammatory cytokines like IL-6 and IFN-β. Of note TLR10 ligand remains elusive. Therefore, authors used an anti-TLR10 antibody to induce

signal. The dimer suppresses both MyD88-dependent and independent signaling (Hess et al. 2017, Oosting et al. 2014, Jiang et al. 2016) suggesting a regulating function.

Recently, CD14 and CD36 have been described as accessory molecules facilitating TLR2 responses, where CD36 binds lipopeptides and transfers them to CD14, which subsequently transfers the ligand to the TLR2 heterodimer. The proposed role of this accessory molecules is to diminish the threshold needed to activate receptor signaling (Oliveira-Nascimento, Massari, and Wetzler 2012).

Besides recognizing bacterial lipopeptides, TLR2 recognizes structures in the fungal cell wall. It senses phospholipomannans and β-mannoside chains in combination with galectin-3 (Choteau et al. 2017). Moreover, TLR2-dependent responses have been associated to lung inflammation upon inhalation of fungi and yeasts, and intestinal inflammation due to e.g. *Candida albicans* infection and treatments with zymosan (Choteau et al. 2017, Sato et al. 2003, Taylor, Richmond, and Upham 2006). Additionally, murine fungal infection models have demonstrated TLR2 as a key receptor for pathogenic fungi including: *Aspergillus fumigatus, Aspergillus niger, Cryptococcus neoformans* among others (Goodridge and Underhill 2008).

3.2 Hypothesis and aims

Studies of the chitin recognition by the immune system are relevant for therapeutic strategies against fungal infections like candidiasis, as well as arthropod related allergies for example to house dust mite allergens. Previous studies aiming to find the chitin-receptor in mammals have used chitin macroparticles with variable purity. Thus, the overall project aimed to validate the binding to suggested receptors or find a novel chitin-receptor using highly pure chitin oligomers, which would match the size of a receptor's ectodomain.

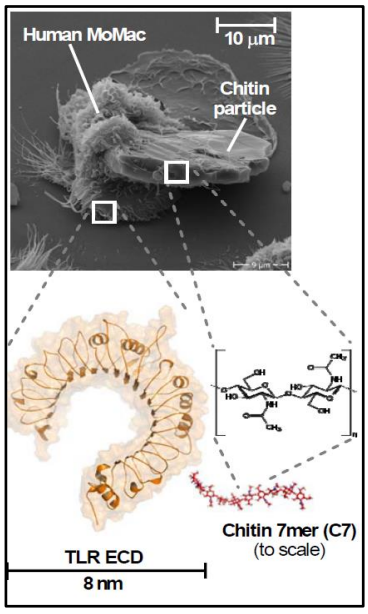

Fig.M.1a,b from manuscript. Electron micrograph of a human macrophage engulfing a crude chitin particle; size comparison of typical TLR ectodomain and seven NAG subunits.

To illustrate the challenge of studying the interaction between chitin and its receptor at a molecular level, we conducted electron microscopy studies of a macrophage incubated with the type of chitin preparation used in the literature, where we observed that chitin particles can be as big as cells. Thus, chitin oligomers would have more suitable dimensions to solve molecular chitin recognition, as shown with the schematic of a TLR ectodomain (ECD).

This thesis project is part of the findings described in a manuscript Fuchs, Cardona Gloria, 2018 with the title: *The fungal ligand chitin directly binds and signals inflammation dependent on oligomer size and TLR2*. My direct contribution to this manuscript was to confirm the found TLR2 as a chitin-receptor, to evaluate other receptors suggested by the literature and explore the chitin binding site in TLR2. Furthermore, a preliminary analysis of the involvement of TLR2 co-receptor was performed.

3.3 Results

3.3.1 Background findings in Manuscript

Although different receptors have been suggested to mediate the pleiotropic immunogenic effects of chitin, molecular studies to prove receptor interaction to chitin remain elusive. So far, chitin preparations were mainly obtained by extraction from shrimp and crab shells or fungal cell wall preparations, with a great variation in molecular size and purity.

We then first tested the immunogenic properties of chitin oligomers comprising 4 to 15 NAGs (N-acetyl-glucosamine). Results showed that oligomers ≥6 NAGs elicited pro-inflammatory cytokines in human and murine macrophages. The oligomer size with the highest immunogenic potency was a mixture of 10-15 NAGs, referred here as C10-15 (experiments done by K. Fuchs). C10-15 was able to induce secretion of pro-inflammatory cytokines from several primary immune cells, such as monocytes, macrophages and neutrophils (experiments done by other authors). Thus, this mixture was used to assess the chitin-receptor.

The following sections summarize my individual contribution to the "Fuchs, Cardona Gloria, 2018 manuscript" (Fuchs et al. 2018), supported by experiments from other authors.

3.3.2 Chitin 10-15 oligomer induce a TLR2-dependent immune response

To identify the chitin-receptor we used murine bone marrow-derived macrophages (BMDMs) from several strains of KO mice and stimulated them with C10-15 and respective control ligands. As outcome of a chitin-dependent immune response, we measured TNF-α levels in the cell supernatants. *Myd88* and *Tlr2* KO BMDMs showed a strong decrease in TNF-α production in response to C10-15 proposing TLR2 as the chitin-receptor in mammals (Fig.10a). This was supported by the involvement of TLR2 in human primary monocyte-derived macrophages (MoMacs), where we knockdown *MYD88* and *TLR2* using siRNAs. Indeed, *MYD88* and *TLR2* knockdown led to a reduction in IL-6 release following stimulation with C10-15. Similar decrease in IL-6 secretion was observed after cell treatment with the well-established TLR2 ligands Pam2CSK4 (Pam2) and Pam3CSK4 (Pam3). Cells treated with TLR2-specific siRNA showed no decrease in IL-6 secretion upon stimulation with the TLR4 ligand LPS (Fig.S7).

To confirm this finding and to establish a robust system to test chitin-dependent signaling, we co-transfected HEK 293T cells with a human TLR2 construct together with

luciferases to assess NF-κB activity by a dual-luciferase reporter assay (DLA). DLAs demonstrated a TLR2-dependent and dose-dependent response to C10-15 (Fig.10b). Of note, in all performed DLAs we stimulated the endogenously expressed TLR5 with flagellin (from *S. typhimurium*) as cell viability and TLR2-independent control.

Next, to test chitin-TLR2 molecular interaction, we pre-treated TLR2 transfected HEK 293T cells for DLA with the TLR2-inhibitor SSL3 (staphylococcal superantigen-like protein 3). SSL3 is an immune evasion protein, part of a mechanism of defense from *Staphylococcus aureus*, which prevents TLR2 stimulation by pathogen-associated lipopeptides. Koymans, et al. presented a crystal structure of SSL3 in complex with TLR2 showing that SSL3 partially covers the entrance of TLR2 binding pocket and thereby inhibits the binding of the TLR2 ligands Pam2 and Pam3 (Koymans et al. 2015). Here, we anticipated that chitin would bind to the same TLR2 binding pocket as the lipopeptides (Fig.10d). Hence, SSL3 would be expected to impair chitin binding and consequent immune response. Indeed, SSL3 abolished C10-15-induced NF-κB activation and significantly decreased Pam2 and Pam3 stimulation (Fig.10e). Likewise, this data was strengthened by other techniques illustrated in the manuscript using SSL3 and an anti-TLR2 antibody as blockers of chitin-TLR2 binding (Fuchs et al. 2018). Furthermore, the effect of SSL3 on chitin recognition is medical relevant since co-infections of *S. aureus* and pathogenic fungi such as *C. albicans* occur frequently (Morales and Hogan 2010).

Since the *Tlr2* KO showed reduced but not total abrogation of a C10-15 response (Figure 10a), we wanted to check if some of the chitin-receptors suggested by the literature were responsible for the remaining cytokine production. The here tested receptors were Dectin-1, NOD2 and TLR9, which are the view that have been directly associated to chitin (Mora-Montes et al. 2011, Wagener et al. 2014, Marakalala et al. 2013). We used the DLA system to evaluate these receptors, in which positive controls were, zymosan for Dectin-1, MDP (Muramyl dipeptide) for NOD2 and CpG for TLR9. Positive controls showed significant differences ($p<0.05$) compare to unstimulated conditions, but none of the receptors were able to induce a chitin-dependent NF-κB activation, even using a high chitin concentration (5 μM, Fig.10c). Additionally, we evaluated TNF release from WT and Dectin-1-deficient immortalized murine macrophages (*Clec7a* KO iMacs) upon chitin stimulation (Rosas et al. 2008) and deficient cells responded as efficiently as WT iMacs (in manuscript, Fig.S2d). Thus, we concluded that these tested receptors cannot directly mediate chitin-responses, at least in a NF-κB manner.

Collectively, we here confirmed TLR2 as a chitin-receptor by triggering the activation of NF-κB and the subsequent cytokine production. Furthermore, we could abrogate chitin-responses by the specific TLR2-antagonist SSL3. At last, we disproved several “chitin-receptors”, which exclusively were suggested to induce an immune response originated by chitin.

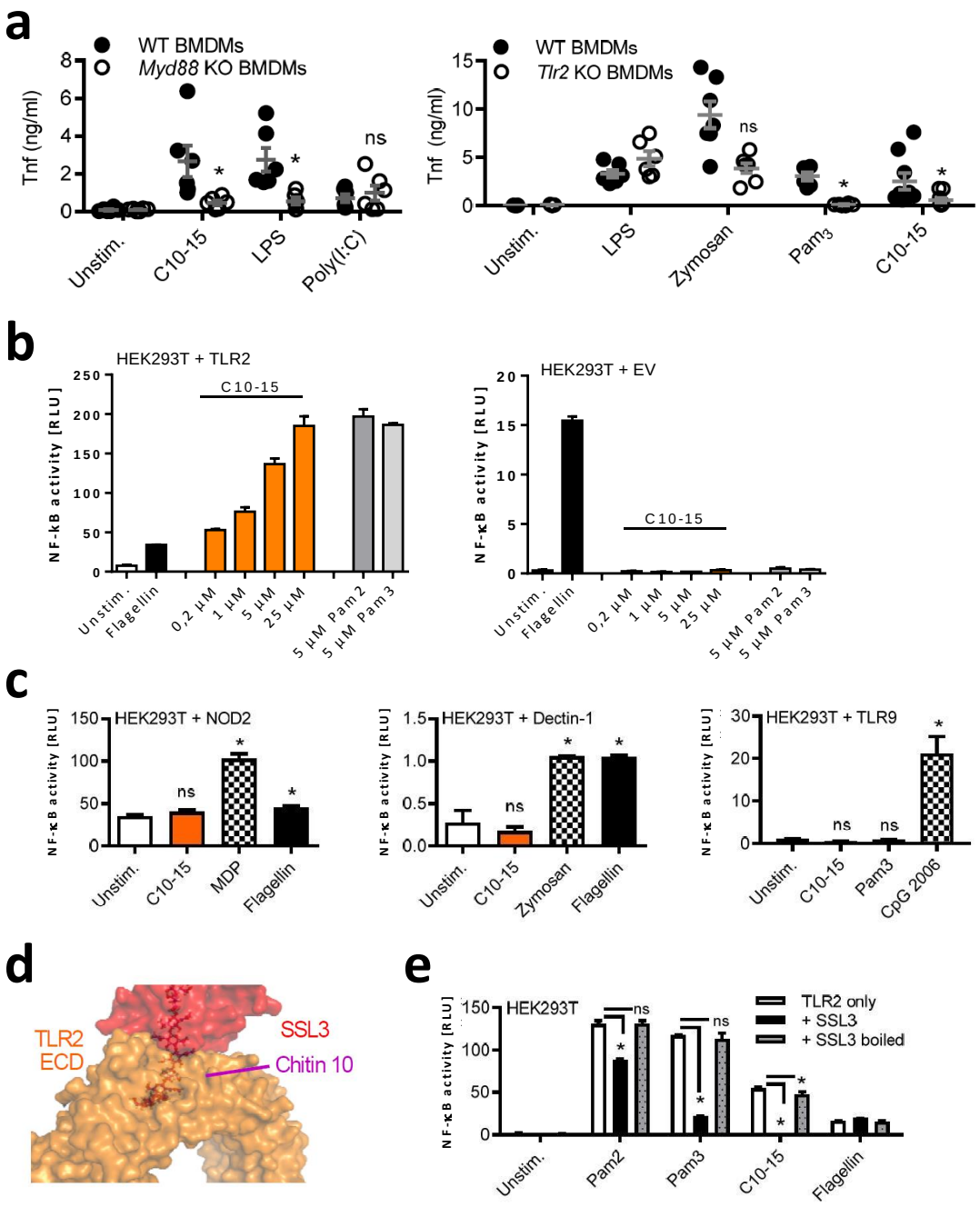

Figure 10. Chitin 10-15 oligomer induce TLR2-dependent immune response. (a) TNF released from WT or MYD88 and TLR2 KO BMDMs upon 18 h stimulation (n=6-9/group measured in 3 experiments). (b,c,e) DLA measurements of NF-κB activation in HEK 293T cells lysates upon transient transfection with (b) TLR2 and empty vector; (c) NOD2, Dectin-1 and TLR9. (e) HEK 293T cells transfected with TLR2, were treated for 30 min with SSL3 alone, then stimuli were added and incubated for further 18 h before lysis. SSL3 was boiled for 10 min at 95°C. (d) Docking of chitin 10 (magenta) into TLR2 (orange) binding pocket (close-up, pdb 2z7x) and overlaid with SSL3 (red) from SSL3-inhibited TLR2 complex (pdb 5d3i). (b,c,e) Shown mean+SD of one representative of n=2-3 independent experiments. *p<0.05 according to Student's t-test in all graphs. *Note:* (a) done by K. Fuchs, (c) done with T. Sanmuganantham and (d) by A. Weber. All from the Department of Immunology, University of Tübingen. RLU: relative luminescence units; EV: empty vector; ECD: ectodomain.

3.3.3 Chitin-TLR2 molecular recognition

Having observed that SSL3 was a potent antagonist of receptor activation, binding of chitin to the TLR2 hydrophobic pocket was investigated further. We generated TLR2 constructs with single point-mutations in residues placed at the ligand-binding domain to test their potential to induce NF-κB activity by DLA upon engagement to Pam2, Pam3 and C10-15. The position of the ligand-binding domain was determined by the TLR2/TLR1 heterodimer crystal structure comprising AA residues from position 266 to 355 (Jin et al. 2007). Residues L328, V348 and F349 are positioned in the hydrophobic core and dimer interface with TLR1. F349 is involved in mediating hydrophobic interactions with TLR1 and fixes by strong hydrogen bonds the lipopeptide backbone to the heterodimer (Jin et al. 2007), in this case Pam3. L328 exchange to K (Lysine) has been demonstrated to abolish response to TLR2 ligands: Pam3 and MALP-2 (Kajava and Vasselon 2010, Takeuchi et al. 2001). V248 mutation could influence the hydrophobic interactions of F349. Thus, mutations of these residues were expected to impair chitin-TLR2 signaling by narrowing the ligand-binding pocket (Fig.11). Indeed, almost all tested mutations: L328W, V348Y, V348W, F349W affected chitin-dependent response, except for V348L. V348L also did not block Pam2 and Pam3 responses, presumably because both, valine and leucine, have a non-polar and small structure (Fig.11d). V348 exchange to Y and W abrogated all TLR2-ligands responses (Fig.11f). Interestingly, F349W did not reduce Pam2-induced NF-κB activity (Fig.11e). This shows a specific involvement of a TLR2/TLR1 mediated response.

Together this data proved TLR2 to be an essential immune sensor for fungal-chitin and triggers the consequent activation of NF-κB. It also suggests that chitin fits similarly to Pam3 in the TLR2 hydrophobic pocket.

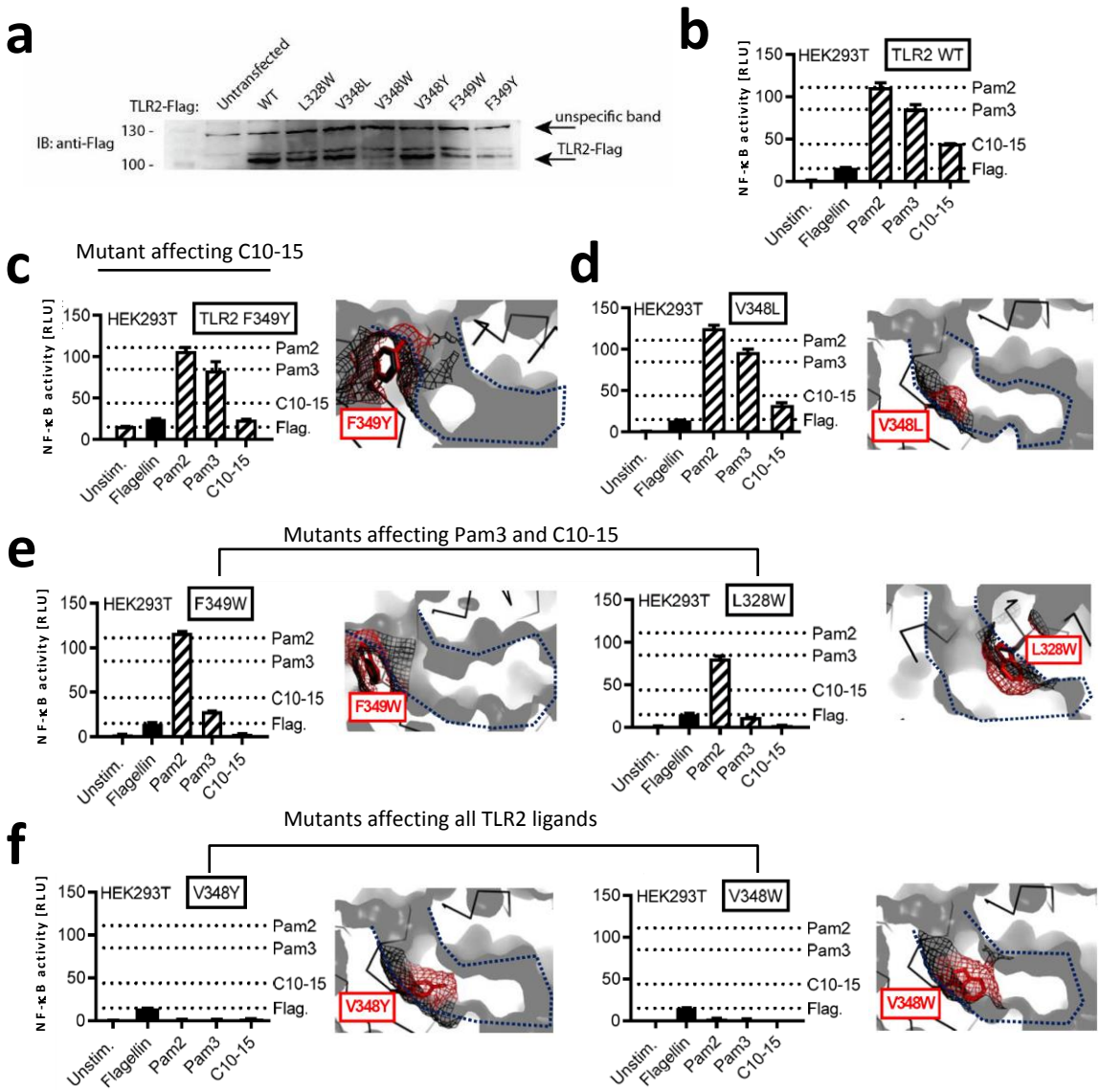

Figure 11. TLR2 mutations in the hydrophobic binding pocket. (a) TLR2 WT and mutant's protein expression assess by immunoblot with an anti-Flag antibody. (b-f) DLA measurement of NF-κB activation in HEK 293T cells lysates upon transient transfection with TLR2 constructs having the stated mutations. Panels are representatives of n=3 showing means+SD of triplicates. Dash lines represent levels stated by TLR2 WT. Mutated constructs were generated by A. Weber and M-T. Dang from University of Tübingen. (c-f) Blue dotted line delineates the hydrophobic pocket, shown in cross-section. Black mesh demonstrates original surface profile in pdb 2z7x and red mesh the predicted surface of the respective point mutant. Dockings were made in Pymol 1.4.1 by A. Weber (University of Tübingen). RLU: relative luminescence units.

3.3.4 Chitin as TLR2-ligand in the fungal cell wall preparation, zymosan

Zymosan is an insoluble preparation from the cell wall of *Saccharomyces cerevisiae* (yeast) and/or *Candida albicans* and has often been used as Dectin-1 and TLR2 stimulus. However, upon hot alkali treatment (e.g. boiling in a high concentrated sodium hydroxide suspension), it loses its capacity to induce a TLR2 response (Walachowski, Tabouret, and Foucras 2016, Dillon et al. 2006). Zymosan main constituents are polysaccharides like β-glucan and mannan, and was shown to activate macrophages, monocytes and leucocytes (Brown et al. 2002). Moreover, it is often used to induce sterile inflammation *in vivo* (Thomas et al. 2008, Malik et al. 2011) and to mimic dust toxic syndrome by inhalation of fungi or yeast inducing inflammation and immune responses in the lungs (Sato et al. 2003).

Although chitin is known as a constituent of zymosan (Fig.12a and (Di Carlo and Fiore 1958), it remained unclear which of zymosan's constituents is the TLR2 ligand and is sensitive to a hot alkali treatment (also referred to as "depletion"). Interestingly, such a treatment is also used to deacetylate chitin chains (shown in Fig.12b), converting it to the non-immunogenic chitosan (Elieh-Ali-Komi and Hamblin 2016). Hence, we hypothesized that the TLR2 ligand in zymosan preparations is chitin. Depleted zymosan (also commercially available) would lose its potency to induce TLR2-responses, while keeping its Dectin-1-dependent immunogenicity. To prove this, we performed depletion of C10-15 or zymosan and further tested their immunogenic properties. As expected, depletion treatment on chitin and zymosan abolished the NF-κB activation in TLR2-transfected HEK 293T cells (Fig.12d). Likewise, zymosan depletion significantly reduced by two fold the TLR2-dependent IL-8 secretion from primary PMNs but increased by two fold the ROS (reactive oxygen species) production, possibly due to unmasked Dectin-1 ligand produced by the treatment (Fig.12e). ROS production can be mediated by Dectin-1 and TLR2 together, but TLR2 stimulation alone produces very low amounts (Romero et al. 2016). Thus, we used it as a Dectin-1 activation read out.

We confirmed the de-acetylation of chitin by treating depleted C10-15 with a recombinant bacterial chitinase (from *Streptomyces griseus*), in order to get soluble dimers. The resulting chitin and chitosan dimers were then quantified by mass spectrometry. Spectrums showed that >90% of chitin oligomers were de-acetylated upon depletion treatment (Fig.12c). Likewise, chitin contained in zymosan was assessed in a similar way (Fig.12a).

This data confirms our hypothesis that the chitin content in zymosan, presumably at oligomeric sizes, is the main TLR2-ligand whose immunogenicity can be eliminated by depletion treatment. To our knowledge, this is the first study to identify chitin as TLR2-ligand present in zymosan.

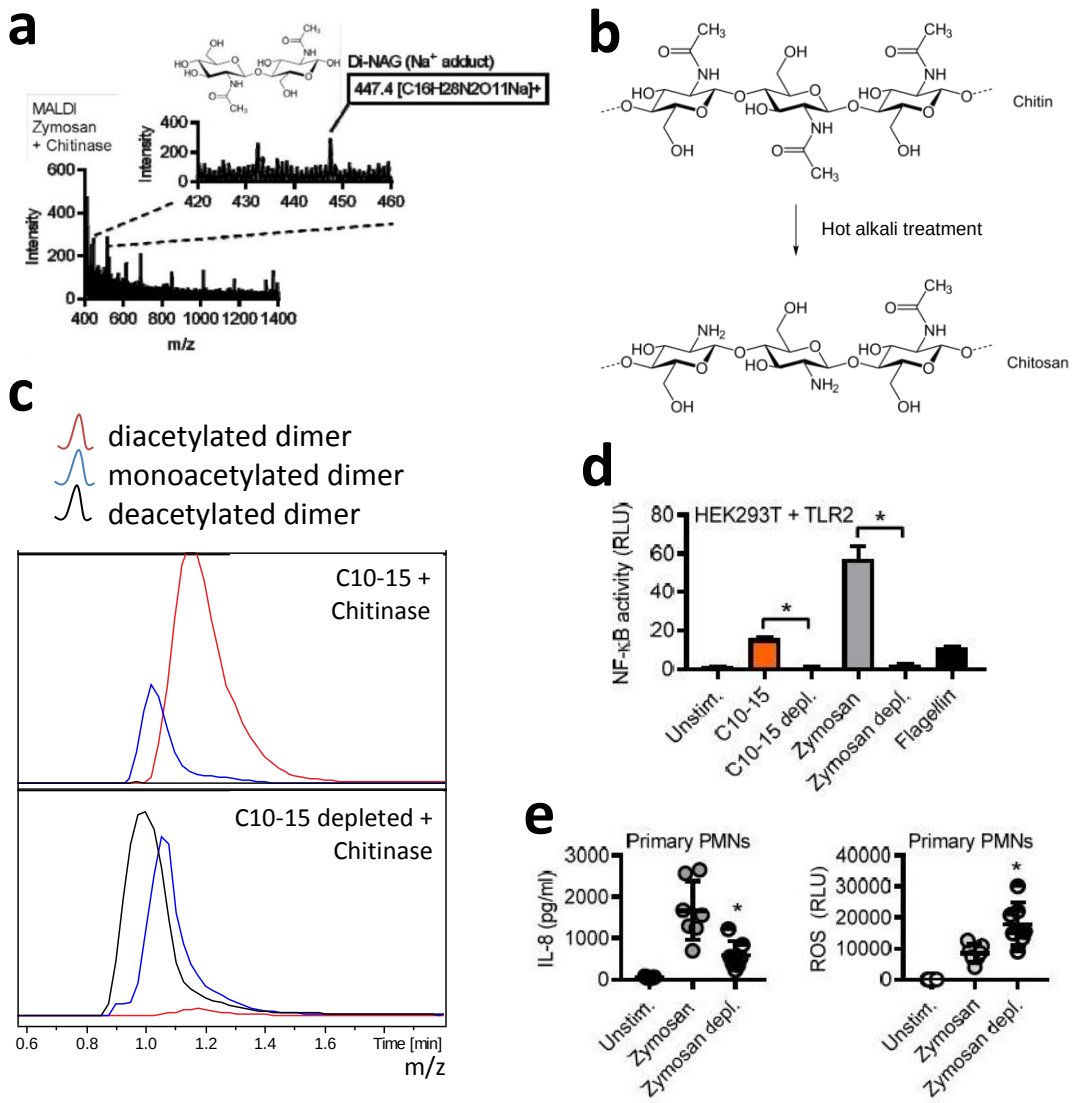

Figure 12. Chitin as TLR2-ligand in zymosan preparation. Mass spectrometry analysis of (a) zymosan and (c) C10-15 original and depleted upon treatment with bacterial chitinase to produce soluble dimers of the oligomeric chains. (b) Deacetylation reaction by hot alkali treatment and deacetylases. (d) NF-kB DLA from TLR2 transfected HEK 293T cells lysates upon 18 h stimulation and 48 h transfection, representative of n=2. (e) IL-8 and ROS production of primary PMNs upon 4-3 h stimulation, n=7. * $p<0.05$ according to Student's t-test (d) and Wilcoxon signed rank sum (e). Data presented in (e) was generated by F. Herster and (a,c) together with N. Schilling (both from the University of Tübingen). RLU: relative luminescence units.

3.3.5 TLR2 co-receptor for chitin-response in human HEK cells

TLR2 in complex with TLR1 or TLR6 recognizes triacylated and diacylated lipopetides, respectively. However, to this date, the TLR2 co-receptor for chitin recognition has not been determined. Ozinsky, et al. demonstrated that TLR2 together with TLR6 mediated macrophages activation by zymosan particles placed in phagosomes (Ozinsky et al. 2000). Thus, together with our discovery that TLR2 ligand in zymosan is chitin, these findings would suggest that chitin is recognized by the TLR2/TLR6 heterodimer. On the other hand, we noted that chitin bound to the TLR2 hydrophobic pocket similarly to Pam3, since F349W and L328W mutations affected sensing of both ligands (Fig.11). This fact would suggest a TLR2/TLR1 dimer as responsible to induce a chitin-dependent response.

Thus, to reveal which co-receptor is responsible to assist TLR2-chitin signaling, we used siRNAs to knockdown TLR1 or TLR6 in HEK 293T cells transfected with TLR2 for NF-κB di-luciferase assays. HEK 293T cells constitutively express TLR1 and TLR6, although at low levels. Nevertheless, since the single transfection of TLR2 induced NF-κB activation upon stimulation with Pam2 (TLR2/TLR6-ligand) and Pam3 (TLR2/TLR1-ligand), we took for granted that their endogenous levels were enough to mediate TLR2-dependent signaling. As negative control we knocked down TLR5, also expressed in HEK cells. Results showed that TLR1 and TLR6 knockdown significantly reduced NF-κB activity. TLR6 knockdown had the strongest effect showing ~70% decrease in NF-κB activity (Fig.13a). TLR1 knockdown showed ~55% reduction of NF-κB activity. This data suggested that both heterodimers might be equally important for chitin recognition, since endogenous expression of TLR1 and TLR6, and siRNA efficiencies could influence the reduction differences but not the signal blockage.

For further validation we used a TLR6 dominant negative (DN, p.P680H) construct to support TLR6 as a co-receptor candidate. This mutation of proline to histidine in the TIR domain confers a dominant negative function of any TLR and was first described for TLR4 (Haase et al. 2003). Using again the HEK 293T cells transfected with TLR2 for DLA, we here co-transfected TLR6 DN in overexpression amounts to theoretically form heterodimers with all available TLR2. The presence of TLR6 DN decreased chitin-dependent NF-κB activity by half, but the positive control Pam2 was only reduced 30%, and no plasmid dose-dependent effect was observed (Fig.13b). This data could support redundancy between TLR1 and TLR6. To support this idea we could test next a TLR1 DN construct in the same system.

At last, using the same system, we tested the receptor TLR10 as potential co-receptor for sensing of chitin. Two constructs of TLR10 were tested (here only one is shown, since results were the same) but none enhanced the C10-15-induced NF-κB activity in TLR2 transfected cells. Furthermore, in contradiction with the literature (Oosting et al. 2014)

neither TLR10 construct reduced Pam2 or Pam3 responses (Fig.13c). Thus, in our system TLR10 neither supported nor inhibited chitin-TLR2 response.

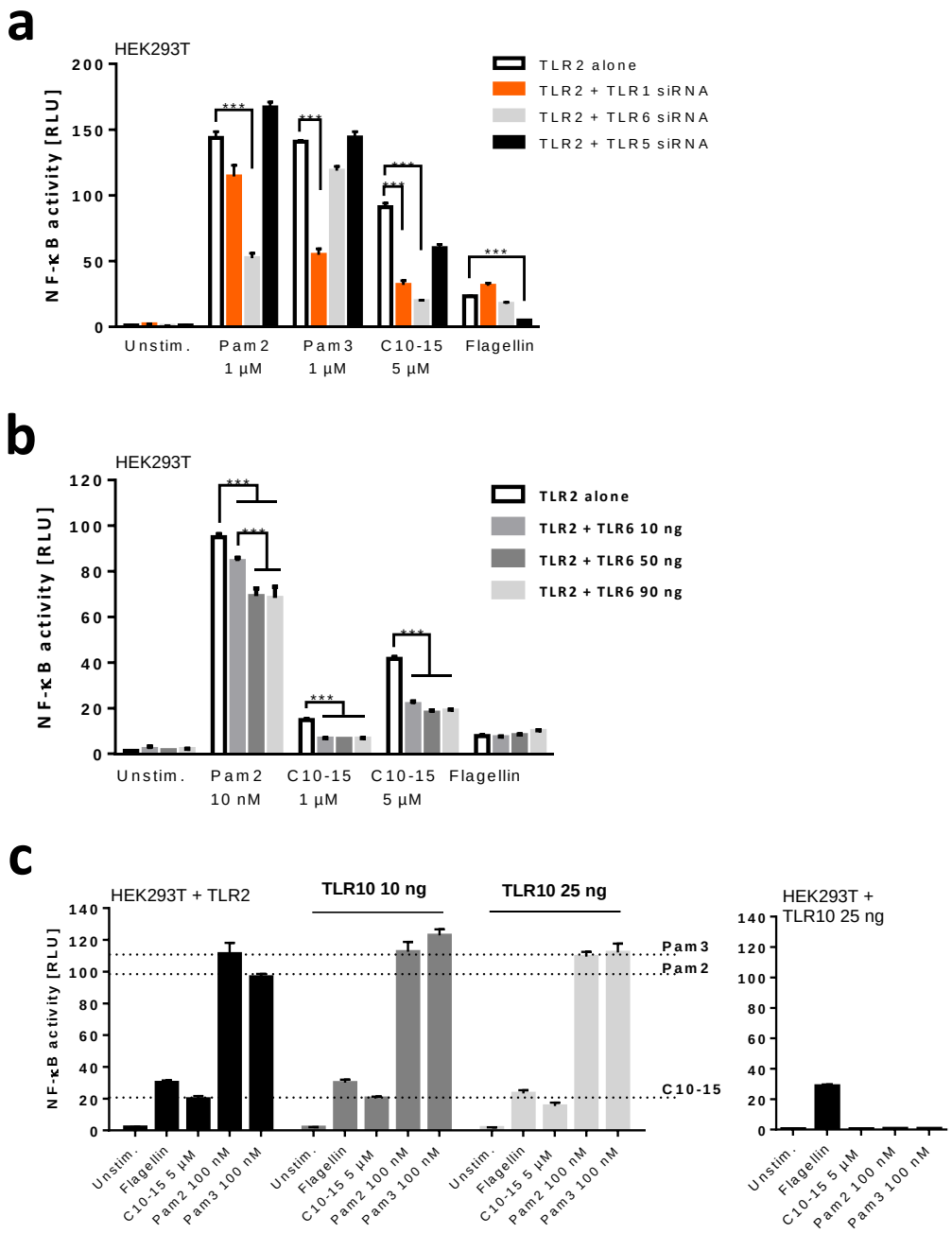

Figure 13. TLR1, TLR6 and TLR10 as potential TLR-2 co-receptor for chitin. NF-κB activity upon 18 h stimulation of HEK 293 T cells transfected with the corresponding luciferases plus (a) TLR2 and siRNAs against TLR1 TLR6 and TLR6, or (b) TLR2 and TLR6 DN, or (c) TLR2 or TLR10 alone or together. Graphs are representatives of (a) n=4, (b) n=3 and (c) n=3 and error bars are mean+SD from triplicates. *** p<0.001 according to Student's t-test. DN: dominant negative; RLU: relative luminescence units.

3.3.6 TLR2 co-receptor for chitin-response in murine BMDMs

To extend the search for the TLR2 co-receptor to the murine system, we used BMDMs (bone marrow derived macrophages) from *Tlr2*, *Tlr1* and *Tlr6* KO and wildtype mice. We stimulated differentiated macrophages for 18 h with C10-15 and used Pam2 and FSL-1 as TLR2/TLR6 controls, Pam3 as TLR2/TLR1 control and LPS as TLR2-independent stimulus. Then, as activation readout we measured secreted IL-6 amounts by ELISA. This showed no differences among KO and WT murine cells in unstimulated and LPS conditions. As expected, *Tlr2* and *Tlr1* KO BMDMs showed significantly lower IL-6 production upon Pam3 stimulation ($p \leq 0.03$); likewise, *Tlr2* and *Tlr6* KO secreted significantly lower cytokine upon Pam2 ($p \leq 0.05$) and FSL-1 ($p \leq 0.01$) stimulation in comparison to WT cells. Thus, all controls worked well. Although *Tlr1* and *Tlr6* KO BMDMs showed a trend towards a reduced response to chitin when compared to WT cells, the difference failed to be significant; only *Tlr2* KO showed a two-fold lower IL-6 levels than WT BMDMs ($p \leq 0.04$) (Fig.14).

Collectively these data proposed that chitin could use either co-receptor TLR1 or TRL6 to induce an immunogenic response, perhaps preferring TLR1 since C10-15 showed more similarities to Pam3 stimulus using the TLR2 mutants. Nevertheless, we do not discard the possibility of a still unknown TLR2 co-receptor.

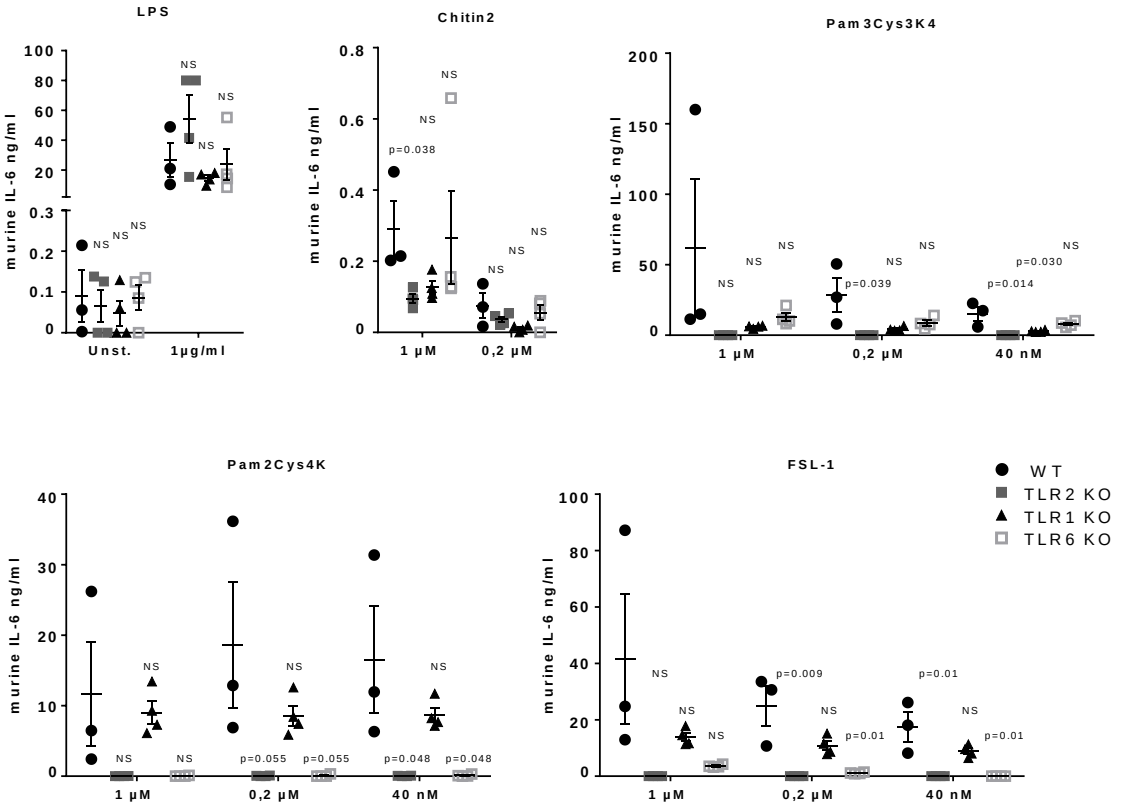

Figure 14. Assessing TLR2 co-receptor for chitin sensing in the murine system. Murine IL-6 production upon 18 h stimulation of BMDMs with the stated ligands measured by ELISA. BMDMs were differentiated with murine GM-CSF for 6 days. WT mice n=3 and others n=4. Chitin stimulus was tested in a 1:5 dilution, other stimulus at 1:20 dilution and unstimulated without dilution. P values stated are according to Student's t-test. All mice were tested in one experiment performed together with Z. Bittner and F. Herster from University of Tübingen.

3.4. Discussion

Different receptors have been proposed to mediate the sensing of chitin leading to an immune response. However, direct binding of chitin to the suggested receptors and corresponding molecular studies remained elusive. One technical limitation faced by previous studies has been the lack of defined and pure chitin. In our study, using pure chitin oligomers, we identified chitin as a TLR2 ligand.

The use of oligomeric chitin matched the dimensions of PRRs ectodomains and allowed us to show trustable molecular studies covering the chitin-TLR2 interaction. Previously, we found six NAGs to be the minimum size for induction of an immune response in mammals and this was largely increased by a mixture of 10-15 NAGs, which we used in the following experiments. Although C10-15 showed the highest immunogenicity, it is worth to discuss that we used this mixture because it is extremely difficult to 1) synthesize specific size oligomers bigger than 6 subunits, particularly in milligram scales and 2) separate them by sizes upon isolation from raw material. These limitations are attributed to the insoluble nature of chitin (Younes and Rinaudo 2015). Despite the broad occurrence of chitin in nature, the main commercial sources are crab and shrimp shells. Its industrial process by extraction from crustaceans involves many laborious steps and solubility remains a big issue (reviewed in (Younes and Rinaudo 2015)). Therefore, the most demanded chitin source is chitosan a chitin derivative used in biomedical products. Chitosan is more soluble than chitin and is generated by chitin deacetylation under alkaline conditions. Notably, its purity is of high importance since it is commonly utilized for biomedical products, in which residual proteins or pigments could cause many side effects. One example is a chitosan bandage used for the control of hemorrhage and wound healing (Burkatovskaya et al. 2008, MacIntyre, Quick, and Barnes 2011). Then, the raw source of our chitin preparation is chitosan oligomers varying from 10 to 15 subunit sizes, which were acetylated according to well established protocols (Bueter et al. 2011) and treated to be endotoxin free. Together, all these arguments support the quality and purity from the here used oligomeric chitin lacking other potential components that could cause an immune response. Interestingly, such chitin oligomers were used before to discover the chitin-receptor in plants (Kaku et al. 2006). Moreover, we and others (Kuusk, Sorlie, and Valjamae 2017) propose that chitinases, specially endochitinases, could degrade pathogen-derived chitin-containing structures and once released, oligosaccharides (e.g. C6-15) could subsequently trigger an immune response. Together, the oligomeric chitin used in this study is a good tool to approach the aimed molecular studies.

C10-15 allowed us to define TLR2 as a decisive receptor for chitin and the major player in the subsequent inflammatory response in human and murine immune cells. However, murine *Tlr2* KO BMDMs did not show complete abrogation of chitin responses raising the possibility that another receptor might be involved. Dectin-1 (Da Silva et al. 2009), TLR9

and NOD2 (Wagener et al. 2014) were candidates suggested by others, which we also tested here. But, they failed to induce the activation of NF-κB upon chitin stimulation in HEK 293T cells and *Dectin-1* KO iMacs; therefore, we discarded them as potential mediators of the residual immune signal in *Tlr2* KO cells. Nevertheless, we cannot rule out the possibility that they could regulate chitin-signaling as it was proposed for Dectin-1. For example, it was demonstrated that chitin blocks Dectin-1 binding and response to ß-glucans from *Candida albicans* cell wall (Mora-Montes et al. 2011); and that differences in the levels of cell-wall chitin influence the capacity of Dectin-1 to control *C. albicans* infection (Marakalala et al. 2013). Furthermore, there are several publications suggesting that Dectin-1 and TLR2 synergize inflammatory responses, e.g. TNFα or ROS secretion, triggered by each receptor (Goodridge and Underhill 2008, Ferwerda et al. 2008). Other probable receptors, not tested here, might be Mincle, DC-SIGN (SIGNR1 homolog) and the mannose receptor, all CLRs, which also recognize sugars and have been shown to be involved in fungal recognition (Mora-Montes et al. 2011, Takahara et al. 2012, Wells et al. 2008), nevertheless their association to chitin remains to be assess. For example, *Mincle* KO macrophages were already used to show Mincle sensing of *C. albicans* by Well, et al. (Wells et al. 2008) and the mannose receptor (*MR*) KO has been generated (Lee et al. 2002) and tested again in response to *C. albicans* (van de Veerdonk et al. 2009). Thus, chitin-response experiments could be done by stimulating the corresponding KO innate immune cells with the here used C10-15 to rule out or associate these receptors directly to chitin.

More importantly, we proved here the direct binding of chitin to TLR2. Using direct mutagenesis, we could modify the TLR2-binding pocket and block TLR2-ligand responses including chitin. Furthermore, we confirmed this result by utilizing the TLR2-antagonist SSL3. The direct binding was also supported by microscale thermophoresis analysis measuring the binding of chitin to recombinant TLR2 and by TLR2 staining in *C. albicans* cells measured by flow cytometry analysis (in manuscript). Collectively, we are the first to show chitin-TLR2 direct sensing and binding at the molecular level. Of interest, the inhibition of chitin recognition by SSL3 warrants further analysis in *S. aureus/C. albicans* co-infections (Morales and Hogan 2010), since it could attenuate host response against concomitant fungal infection in a chitin-TLR2-dependent manner.

At last, we aimed to find the TLR2 co-receptor responsible to mediate the chitin-induced TLR2 activation. Our knockdown and knockout experiments of the main TLR2 co-receptors, i.e. TLR1 and TLR6, did not show an exclusive preference. Although one study showed that TLR2-response to zymosan requires TLR6 (Ozinsky et al. 2000), we speculate that TLR2 might use both co-receptors for the sensing of chitin. Potentially, chitin-TLR2 complex might be more stable with TLR1 since TLR2 mutants in the binding pocket impaired Pam3 and C10-15 similarly. Nevertheless, the idea of another still unknown TLR2 co-receptor is imaginable. Preliminary data showed that double KO of TLR1 and TLR6 in

HEK cells, which stably express TLR2, were unable to induce NF-κB activation when stimulated with C10-15. But single KO reduced chitin-responses by 50% compared to TLR2 HEK cells (not shown). We also do not exclude that immune cells might express co-receptors that are absent in HEK cells. Therefore, we suggest that TLR1 and TLR6 remain the main candidates and warrant further research. Of immediate importance would be to test in our DLA system a TLR1 dominant negative construct, expecting a chitin-response reduction of 50% as observed for TLR6 DN to confirm redundancy and performed double knockdown or/and knockout of TLR1 and TLR6 in e.g. macrophages to rule out the existence of another co-receptor.

Overall, our study resolved the missing link between 1) fungal immunogenicity and the previously observed TLR2 response in murine infection models (Cunha, Romani, and Carvalho 2010, Goodridge and Underhill 2008) and 2) house dust mite allergic symptoms mediated by TLR2 (Ryu et al. 2013). Thus, this project raises the possibility to use chitin oligomers as tools for further research about fungal infections and chitin-related allergies, which now could concentrate on chitin-TLR2 binding and activation. Moreover, the confirmed chitin-TLR2 interaction can become an attractive target for the development of molecules against the TLR2 hydrophobic core to treat chitin-related pathologies, since our study demonstrated a chitin-response reduction with SSL3-peptides and TLR2 blocking antibody treatments.

3.5 Conclusion

Chitin preparations used in previous studies, in which different chitin-receptors had been proposed, were large chitin particles and with variable purities. Thus, findings remain to be confirmed and assess by different approaches. Here, we used defined and pure chitin oligomers to confirm the chitin recognition by the Toll-like receptor 2 and disproved other previously suggested candidates. Furthermore, we are the first to provide conclusive molecular evidence for a direct TLR2-chitin interaction and to identify chitin as TLR2-ligand present in zymosan. Finally, we demonstrated that the chitin-TLR2 complex could use both TLR1 and TLR6 as co-receptor. Hence, inflammation and allergic symptoms in fungal infection and asthma could now be attributed to the recognition of chitin by TLR2 in immune cells and the resulting potent inflammatory response. Thus, our study highlights chitin oligomers as a valuable tool to study fungi-host interactions and the TLR2-chitin interaction as an attractive target for the development of novel therapies in chitin-related pathologies and fungal diseases.

Chapter 4: Materials and Methods

4.1 General Methods

4.1.1 Cell maintenance

Cell culture media used here were Dulbecco´s modified Eagle's medium (DMEM) and RPMI-1640 from Sigma Aldrich, and alpha-MEM from Gibco. For supplements heat-inactivated fetal calf serum (FCS) from Biowest; penicillin, streptomycin, L-glutamine from Gibco were used. For harvesting, Dulbecco´s Phosphate Buffered Saline (DPBS) and Trypsin from Gibco were utilized. Human serum was obtained from fresh blood from the same donor whose B cells were isolated. All cell lines were maintained at 37 °C and 5% CO_2 in a humidified incubator. Maintenance media are summarized in the table below.

Table 4. Maintenance medium used during experiments

Cell type	Medium	Supplements
HEK 293 T WT and MyD88-deficient (I3A)	DMEM	10% (vol/vol) heat-inactivated FCS, 100 U/ml penicillin, 100 µg/ml streptomycin and 2 mM L-glutamine
DLBCL cell lines		
BJAB, TMD8, HBL-1 and Oci-Ly3	RPMI-1640	20% (vol/vol) heat-inactivated FCS, 100 U/ml penicillin, 100 µg/ml streptomycin and 2 mM L-glutamine
Oci-Ly19	alpha-MEM	10% (vol/vol) heat-inactivated FCS, 100 U/ml penicillin, 100 µg/ml streptomycin and 2 mM L-glutamine
Human primary cells		
PBMCs, Monocyte-derived macrophages and Neutrophils	RPMI-1640	10% (vol/vol) heat-inactivated FCS, 100 U/ml penicillin, 100 µg/ml streptomycin and 2 mM L-glutamine
B cells	RPMI-1640	10% (vol/vol) human serum, 100 U/ml penicillin, 100 µg/ml streptomycin and 2 mM L-glutamine
Murine cells		
Bone-marrow derived macrophages	RPMI-1640	10% (vol/vol) heat-inactivated FCS, 100 U/ml penicillin, 100 µg/ml streptomycin and 2 mM L-glutamine

4.1.2 Human primary cells isolation and analysis

PBMCs

Human peripheral blood mononuclear cells (PBMCs) were purified from whole blood or buffy coats (University Hospital Tübingen Transfusion Medicine) using Biocoll density gradient (Millipore) and subsequently washed twice with DPBS. PBMCs were resuspended and maintained for experiments in supplemented RPMI and rested at least 4 h prior to stimulation. 5x10^6 cells were stimulated with the stated ligands and concentration for 0, 6, 12 and 18 h, then cells were lysed in RLT buffer + β-mercaptoethanol (Qiagen) for RT-qPCR experiments described below.

B cells

Primary B cells were isolated from PBMCs by negative selection using B Cell Isolation Kit II (Miltenyi Biotec), according to instructions with the following modifications: I resuspended cells in 17 µl Buffer, used 8 µl of Biotin-Antibody Cocktail (10 min), 15 µl of Anti-Biotin MicroBeads (15 min) per 10^7 PBMCs. B cell isolation always reached >90% purity and cells were seeded in supplemented RPMI with human serum and rested for at least 4 h before the experiment. 5x10^6 cells were stimulated for 0, 2, 3, 4, 5 days with 2,5 µg/ml CpG 2006 and 5 µg/mL IgM and processed for RT-qPCR, or 1x10^6 cells were stained on day 0 with carboxyfluorescein-succinimidyl ester (CFSE, Life Technologies) to track cell proliferation. Purity of the isolated cells was assessed by flow cytometry on a BD FACSCanto™ II system staining cells with anti-CD19 Pacific Blue, anti-CD3 FITC, anti-CD14 PE und anti-CD11b APC (Biolegend). Graphs were done with software FlowJo PC version 10.

Human monocyte-derived macrophages (MoMacs)

Human macrophages were generated by purifying monocytes out of PBMCs using anti-CD14 microbeads (Miltenyi Biotec, >90% purity). Monocytes were differentiated in complete RPMI supplemented with human recombinant GM-CSF (Prepro Tech) for 6 days as described (Verreck et al., 2004). On day 5, cells were collected and plated in 96 well plate-format (100,000 cells/well). For knockdown experiments, MoMacs were transfected with 35 nM of corresponding siRNA (Table 7, GE Dharmacon) using Viromer Blue (Biozol). On day 6 cells were stimulated for 18 h with C10-15, LPS, Pam2 and Pam3. Supernatants were collected and analyzed for human IL-6 levels by ELISA.

Neutrophils

Fresh whole blood from healthy donors collected in EDTA tubes was processed to isolate neutrophils. Briefly, whole blood cells were separated depending on their density using Biocoll (Millipore); the resulting pellet below the Biocoll phase contains mainly neutrophils. The neutrophil-erythrocyte pellet was treated twice with 1x Ammonium chloride buffer for erythrocyte-lysis (10X Stock: 1.54 M NH_4Cl, 100 mM $KHCO_3$ and 1 mM EDTA adjusted to pH 7.3); the first treatment was for 20 min and second for 10 min at

4°C. Cells were resuspended in complete RPMI, seeded immediately in 24-well plates for experiments and rested for 1 h. Cells more than 95% pure and not pre-activated were used. For ROS assays, 2x10^5 neutrophils in 100 µl were mixed with 100 µl DCF (2',7'-dichlorofluorescein; final concentration 10 µM) plus ligands and DCF fluorescence was measured every 5 min for 3 hours using the Fluorstar Optima plate reader at 37°C (BMG Labtech). Only the last fluorescence value was used for the graphs. For human IL-8 ELISA, 1x10^6 cells were plated and stimulated for 4 h and supernatants were collected.

4.1.3 Immunoblotting

Expression of endogenous proteins and proteins derived from plasmids was checked by Western Blot. For this, whole cell lysates (WCL) were obtained by washing cells once with PBS and resuspending cells with either passive lysis buffer from Promega or with RIPA buffer (20 mM Tris-HCl pH 7.4, 150 mM NaCl, 1 mM EDTA, 10% glycerol, 0.1% SDS, 1% Triton X-100 and 0.5% deoxycholate) supplemented with PhosSTOP, EDTA-free protease inhibitor cocktail (both from Roche) and 0.1 µM PMSF. WCL were mixed with reducing agent and loading buffer (Novex, Thermo Fisher) and boiled 5 min at 95°C for denaturation. Samples were run on 10% or 12% Tris-glycine gels with SDS buffer (25 mM Tris-base, 250 mM glycine and 0.1% SDS), loading corresponding volumes to ~20 µg protein onto the gel. Separated proteins were transferred onto nitrocelullose membranes (GE Healthcare, 0.2 µm) and blocked at room temperature in 10 ml of 5% BSA (wt/vol) in Tris-buffered saline solution with 0.1% (vol/vol) Tween-20 (TBS-T). Subsequently, nitrocellulose membranes were incubated with 5 ml diluted specific primary antibodies in 5% BSA in TBS-T overnight at 4°C with rotation. On the next day, membranes were washed 3 times with TBS-T for 5 min each and then incubated with the corresponding secondary antibodies diluted in 8 ml 5% BSA in TBS-T for 1 h at RT with rotation. After incubation with the secondary antibodies, membranes were washed 3 times with TBS-T, 5 min each wash. Detection was done by chemiluminescence (Peqlab) and development using a CCD (charge-coupled device) camera to capture the luminescent signals. Pictures were analyzed and edited in Phusion (Peqlab) and Adobe Illustrator programs. Information regarding all the antibodies used, including dilutions, can be found in Table 5.

4.1.4 Dual NF-κB Luciferase assay in HEK 293T cells

75,000 HEK 293T (WT or MyD88-deficient I3A) cells were plated (24-well format, Greiner Bio One) and incubated overnight to allow adherence. On the next day, cells were transiently transfected with the following amounts of plasmid DNA per well: 100 ng EGFP as a transfection control, 100 ng of firefly luciferase under the NF-κB promoter and 10 ng of *Renilla* luciferase under a constitutive promoter. Additionally, varying amounts of plasmid encoding the gene of interest were added. For the tested chitin-receptors 10-25 ng were used. For MyD88 isoforms 1-100 ng were used. Each set of transfections was

adjusted with empty vector to equal amount of total variable plasmid (100 ng) and was accompanied by negative controls containing the corresponding empty vector at the same total amount of variable plasmid (for a list of plasmids, see Table 8). Transfection was performed using Lipofectamine 2000 (Thermo Fisher) with a total volume of 50 µl per well as supplier instructions. Transfections and pre-dilutions were prepared using OptiMEM. If stimulation was required, after 32 h incubation, the medium was discarded and exchanged with fresh complete DMEM with or without the ligands to be tested. Cells were stimulated for 18 h and measurements were carried out immediately. Supplier information and the concentrations of all ligands are summarized in Table 6. For MyD88 splice variant analysis, measurements were performed 48 h post transfection. To analyze luciferase activity, cells were washed in PBS and subsequently lysed in passive lysis buffer (Promega). Lysates were harvested by centrifugation and 10 µl of lysate was used to measure luciferase activity on a FluoStar luminescence plate-reader (BMG Labtech), which automatically added the corresponding substrates, Luciferase Assay Reagent II for the firefly luciferase and Stop & Glo Reagent to quench the firefly luciferase and initiate reaction for *Renilla* luciferase, both reagents from Promega. Analysis settings were chosen as recommended in the Dual-Luciferase Reporter Assay System by Promega. Graphs and statistics were done in GraphPad Prism version 6.

4.2 MyD88 alternative splicing Methods

4.2.1 MyD88-isoforms plasmids

To study the expression of all MyD88 isoforms and their ability to induce NF-κB activation, expression constructs were generated in pTO-N-SH vector using the Gateway cloning system (Thermo Fisher). The coding sequences (CDS) of MyD88 isoforms 3, 4 and 5 (NCBI accession numbers NM_001172568.1, NM_001172569.1 and NM_001172566.1, respectively) were synthesized by the company Genewiz and cloned into a pDONR207 vector. MyD88 isoform 1 (NM_001172567.1) was purchased from Harvard Plasmids (HsCD00296025) in a pDONR221 vector. To clone the CDS in the pTO-N-SH destination vector, an LR-reaction was performed according to kit instructions (Gateway® LR Clonase® II Enzyme mix, Thermo Fisher). pTO-N-SH vector, a destination vector from the Gateway system, adds a fused StrepIII-Hemagglutinin tag at the N-terminus of the gene of interest (vector map Fig.S1a). The final destination vectors were transformed in the DH5 alpha *E.coli* strain and to prove the correct insertion of the CDS a BsgI (New England Biolabs) digestion was made from at least 3 resulted colonies (300 ng plasmid and 5 units enzyme in 1X Buffer Tango, 1 h at 37°C). The colonies that showed the right digestion pattern in 1% Agarose gel were tested for protein expression by immunoblotting and used for further experiments. For plasmids' detailed origin information see Table 8. Expression plasmid map example in Figure S1.

The corresponding L265P mutation and corresponding insertion, depending on the isoform, were introduced to the CDS of the MyD88 isoforms using the QuikChange II XL site-directed mutagenesis kit (Agilent) according to the manufacturer's instructions using the primers listed in Table 9. Mutagenesis primers were designed in Geneious software 5.5.9 following the requirements stated in the kit. The introduction of the exact desired mutation to the isoforms was confirmed by Sanger sequencing (GATC Biotech).

4.2.2 B cell immunohistochemistry

The protocol for proliferation staining of human B cells was kindly provided by F. Lelis from D. Hartl's group at the University Hospital of Tübingen. A stock solution of 1 mM CFSE was diluted in 5625 µl PBS, then 1 ml B cells (resuspended in PBS, 2.5x10^6/ml) with 1.5 ml CFSE dilution were mixed and incubated 12 min at 37°C. To remove any free dye, 4 ml FCS + 8.5 ml RPMI medium were added. The tube was centrifuged at 350 x g for 5 min to pellet the cells, which were then resuspended at 1x10^6/ml in the corresponding medium for primary B cells (see Table 4). B cells were stained with CFSE immediately upon isolation and stimulated for 5 days with 2.5 µg/ml CpG 2006 and 5 µg/mL IgM. On day 5, B cells were washed by centrifugation with PBS and stained with anti-CD19 Pacific Blue (Biolegend, diluted 1:1000 in PBS). After staining, cells were washed again with PBS and analyzed on a BD FACSCanto™ II system with 488 nm excitation for CFSE and 405 nm for Pacific Blue. Graphs were generated using FlowJo PC version 10.

4.2.3 Primers and qPCR analysis

5x10^6 cells per condition were seeded at the beginning of the experiments. Following treatment, cells were washed once with DPBS and lysed in 350 µl RLT buffer + β-mercaptoethanol at -80 °C. Total RNA isolation was performed by a Qiacube robot using reagents from the RNeasy Mini Kit from Qiagen including DNA digestion (RNase-Free DNase Set, Qiagen). mRNA transcription to cDNA was done manually using High Capacity RNA-to-cDNA Kit from Thermo Fisher. Quantitative PCR was performed in 10 µl total volume containing 20 ng cDNA, 0.3 µM of forward primer and 0.3 µM of reverse primer, 1x SYBR Green (FastStart Universal SYBR Green Master Rox, Sigma) and RNA-free water. Each sample was analyzed in triplicates in a real-time cycler (Thermo QuantStudio 7 Flex, Thermo Fisher). The cycling profile applied was: 10 min/95 °C; 40 cycles of 95 °C/15 s and 60 °C/1 min, followed by a continuous melt curve stage from 50°C to 95°C.

Primers generated to discriminate the MyD88 isoforms were situated at the exon junctions and fulfill compatibility requirements with the SYBR Green mix, which were evaluated in the program Geneious Pro version 5.5.9 and the publicly available software Primer3 (http://bioinfo.ut.ee/primer3-0.4.0/). Primer sequences and more details are found in Table 10. Standard curves were done using the same cycling profile as explained

above utilizing plasmids as templates, which were diluted 1 to 5 six times. Results were analyzed with the QuantStudio 6 and 7 Flex software and graphs and statistics were generated using GraphPad Prism version 6.

4.2.4 RNAseq data analysis

RNAseq libraries from 190 B cell lymphoma samples, including Burkitt's Lymphoma (BL, n=21), Follicular Lymphoma (FL, n=83), Diffuse Large B cell Lymphoma (DLBCL, n=72), and FL-DLBCL (n=14) were acquired by the German ICGC MMMLSeq consortium and were uploaded as part of several publications to the European genome-phenom archive at EBI: https://www.ebi.ac.uk/ega/home. Naïve B cells (B cells, n=5) and germinal center B cells (GC B cells, n=5) libraries were used as control data and were made public in the same way. Details for library preparation can be found under the access ID listed in Table S3 and related papers: Hübschmann, D. et al.; Lopez, C. et al. both unpublished and others cited (Hezaveh et al. 2016, Kretzmer et al. 2015, Richter et al. 2012). To visualize alternative splicing events, RNA sequencing data was mapped onto the human hg38 reference genome using Segemehl version 2.0 alpha. Segemehl is a tool that maps splicing sites into the gene of interest and provides a list of all spliced reads as an output (Hoffmann et al. 2014). Splice reads overlapping with the human MYD88 gene were counted and visualized in Sashimi Plots based on UCSC genome browser tracks. The Sashimi Plots show genomic reads converted into density reads (y-axis, units) aligned to the genomic coordinates (x-axis), where arcs represent read junction. Their width is proportional to the number of reads aligned to the junctions of the splice sites (Yarden Katz, 2015). A compositional data approach used in the DIEGO software (Doose et al. 2018) was applied to analyze differential splicing patterns of the MYD88 gene: the support number of every splice junction is considered relative to all splice junctions of the MYD88 gene, and possible variations are analyzed using Wilcoxon's rank sum test as implemented in R. Boxplot graphics were generated using R's ggplot2.

A novel splice site within exon 3 (20 nucleotides upstream of a canonical donor) found in segemehl mapping showed a Human Splicing Finder (HSF) score of 81. Typically, a score above 65 is considered a strong splice site (Desmet et al. 2009). This was confirmed using BLAT (UCSD). For intron retention analysis, we applied the number of spliced reads/number of total reads on MYD88 as a proxy.

RNAseq analysis was performed by SH. Bernhart at the Interdisciplinary Centre for Bioinformatics, University of Leipzig, and coordinated by R. Siebert from the Institute of Human Genetics, University Hospital of Ulm.

4.3 Chitin-TLR2 interaction Methods

4.3.1 Receptors plasmids

Many of the plasmids expressing PPRs used in this study were kind gifts from different research laboratories and are summarized in Table 8 and Table S2. Mutations in the hydrophobic binding pocket of TLR2 were introduced using the QuikChange II XL site-directed mutagenesis kit (Agilent) following the manufacturer's instructions. Primer design was done by A. Weber (see Table 9) and mutagenesis by T-M. Dang (both from Department of Immunology, University of Tübingen). Correct introduction of the desired mutations was confirmed by automated Sanger sequencing (GATC Biotech).

4.3.2 siRNAs mediated knock-down of TLRs in HEK 293T

HEK 293T cells were transfected with plasmids used for NF-κB DLA, using as a variable plasmid TLR2 (10 ng/well) described in Section 4.1.4. siRNA pools to knock-down TLR1, TLR6 and TLR5 were transfected together with the plasmids using Lipofectamine 2000. Supplier and catalog IDs are listed in Table 7. Final concentration of siRNA per well from a 24 well-plate was 20 nM. After one day of transfection cells were stimulated with the corresponding ligands for 18 h and lysates were prepared to measure NF-κB activity by luminescence. Knock-down efficiency was evaluated by qPCR showing a stable reduction of ~70% of the targeted mRNA molecules after 24 and 48 h of transfection (not shown, tested by T. Sanmuganantham and S. Dickhöfer).

4.3.3 ELISA (enzyme-linked immunosorbent assay)

Cytokines in supernatants were measured by ELISA as per the manufacturer's instructions using triplicate points. Human IL-6 and IL-8, murine IL-6 and TNF ELISA kits were from BioLegend. Briefly, coating antibody was applied to high binding 96 well plates (half area, from Greiner Bio-One) and incubated overnight at 4°C. On the next day, plates were washed three times with PBS. Plates were blocked with BSA for 1 h at RT and subsequently washed with PBS; then supernatants were added using the corresponding dilutions listed below. Sample supernatants were incubated at RT for 2 h. A third washing step was applied, biotinylated detection antibody was added and incubated for 1 h followed by three washes and the addition of Avidin-HRP for 30 min. A final washing step was done, the substrate solutions were added and incubated for 5-20 min. Finally, the stop solution (sulfuric acid) was added and absorbance was measured on a standard plate reader. Antibody and reagent concentrations were applied as recommended.

For murine IL-6 and TNF ELISA, BMDMs supernatants were diluted as followed: for LPS, Pam2, Pam3 and FSL-1 stimulations 1:20; for C10-15 1:5 and unstimulated conditions were not diluted. Supernatants from TLR2 KO BMDMs were also not diluted when

stimulated with TLR2-ligands. For human IL-8 ELISA 1:3 dilutions of the supernatants were appropriate.

4.3.4 Chitin preparation

Chitin 10-15 subunits length, referred in the figures as C10-15, was produced by acetylating chitosan oligomers from the same length as previous described (Bueter et al. 2011). In detail, >95% pure chitosan with a molecular weight of 2000-3000 g/mol, equivalent to 10-15 subunits (from Pure Science), was resuspended in freshly prepared 1 M sodium bicarbonate, then 97% acetic anhydride was added, and the preparation was incubated at RT for 20 min, followed by incubation at 100° C for 10 min. The resulting chitin was washed with DPBS until pH was neutralized and then washed with water to remove salt content. C10-15 acetylation degree was assessed by ESI and analysis was kindly done by C. Täumer (Protein Center Tübingen, University of Tübingen). A degree of acetylation of >90% was achieved.

For cell culture experiments, the generated C10-15 was treated with Polymyxin B (Thermo Fisher) to remove endotoxin. At least 3 washes with Polymyxin B at a concentration of 2 mg/ml were done for 3 h each. Endotoxin levels were tested using the limulus amoebocyte lysate (LAL) assay (Lonza, CH) achieving endotoxin levels below 0.25 EU/ml (25 pg/ml LPS) in final dilutions.

4.3.5 Chitin and zymosan depletion

C10-15 and zymosan depletion was performed by hot-alkali treatment, treatment that causes de-acetylation converting chitin in chitosan. In detail, C10-15 (1 mM) and zymosan (10 mg/ml) dissolved in water were the starting material. First, 500 µg (50 µl) of zymosan or ~600 µg (200 µl) C10-15 were pelleted by centrifugation at maximum speed and the supernatant was removed. The insoluble fraction was resuspended in 2 ml 10 M NaOH and boiled at 95°C for 1 h. After cooling down the reaction at RT, the suspensions were washed 3 times (or more) with sterile DPBS to obtain a neutral pH and then washed twice with sterile water to remove salt contains. The reagents were resuspended in endotoxin-free water (Braun) at the starting concentrations for further experiments.

To check the deacetylation of C10-15 and chitin content in zymosan upon depletion, we treated depleted reagents with a chitinase from *Streptomyces griseus* (Sigma), an exo-chitinase that cuts out N-acetylglucosamine dimers (di-NAG). For this, we mixed 30 µl C10-15 1 mM or 100 µg zymosan in water, added volatile pyridine/glacial acetic acid buffer (pH 6.5) to a final concentration of 20 mM and 0.25 units Chitinase per 50 µl reaction and incubated for 18 h at 37°C. Then, preparations were centrifuged and supernatants, containing highly soluble di-NAGs and the resulting glucosamine dimers,

were measured by MALDI upon evaporation of the buffer. MALDI analyses were kindly done by N. Schilling (Institute of Organic chemistry, University of Tübingen).

4.3.6 In silico docking of TLR2-chitin interactions and modeling of TLR2 mutations

The molecular structure of human TLR2 was extracted from PDB entry 2z7x (Jin et al. 2007) using AutoDOCK software. Dockings were focused on the hydrophobic cavity of TLR2, where lipopeptide ligands and chitin bind. The TLR2-chitin 10 (10 NAGs) complex was generated based on results obtained from the docking of chitin 5 with additional manual adjustments, changing the orientation of the NAG chain while keeping the binding position. The TLR2-SSL3 structure was from PDB entry 5d3i (Koymans et al. 2015) and the docking and modeling studies were carried out by M. Frank from Biognos, Sweden. Figures showing the position and effects of mutated residues were generated in Pymol 1.4.1. (Schrödinger) by A. Weber (Department of Immunology, University of Tübingen). For further setting information see manuscript Fuchs et al.,2018 (Fuchs et al. 2018).

4.3.7 Mice and bone marrow derived macrophages (BMDMs)

Upon sacrificing of the mice using CO_2 and excision of femurs and tibia, bones were opened by cutting the edges from the bones with sterile surgical scissors, the bone marrow flushed out using insulin syringes and the isolated bone marrow maintained in RPMI medium supplemented with EDTA (2 mM). The bone marrow cells were washed once with complete RPMI, passed through a 70 µm strainer to obtain a single-cell suspension and were differentiated in complete RPMI for 6 days supplemented with 10% vol/vol supernatant of L929 culture containing GM-CSF. Here, 3x10^7 cells were plated in 10 cm petri dishes with a 10 ml total volume for differentiation. The resulting BMDMs were harvested on day 6, seeded in 96 well plates (100,000 cells/well) in complete RPMI and stimulated the next day for 18 h using ligands and concentrations stated in the figures (ligand information see Table 6). Supernatants were analyzed for murine TNF or IL-6 levels by ELISA.

Excised femurs and tibia from *Tlr2*, *Tlr1* and *Tlr6* KO mice, all from mice with a C57BL/6 background, were a gift from T. Roger (Centre hospitalier universitaire Vaudois, Lausanne, Switzerland). *Myd88* and *Tlr2* KO mice, originally a gift from H. Wagner (Ludwigs-Maximilian University, Munich), and C57BL/6 WT were maintained and sacrificed in the local animal facility (Department of Immunology, University of Tübingen) using CO_2 and following local institutional guidelines and protocols. All mice were 14-16 weeks old. Experiments using *Tlr2*, *Tlr1* and *Tlr6* KO mice BMDMs were done together with Z. Bittner and F. Herster (Department of Immunology, University of Tübingen).

Table 5. List of antibodies for immunoblotting.

Antibodies	Host species	Working dilution	Manufacturer (Cat.#)	Blocking	Blotting
Primary					
Anti-Flag	Rabbit	1:1000	Sigma, (F7425)	5% BSA, 1h RT	5% BSA, 4°C O/N
Anti-GFP	Rabbit	1:2000	Sigma, (G1544)	5% BSA, 1h RT	5% BSA, 4°C O/N
Anti-HA, C29F4	Rabbit	1:1000	Cell Signaling (#3724)	5% BSA, 1h RT	5% BSA, 4°C O/N
Anti-MyD88, 4D6	Mouse	1:1000	Thermo Fisher (MA5-16231)	5% Milk, 1h RT	5% BSA, 4°C O/N
Anti-MyD88, D80F5	Rabbit	1:1000	Cell Signaling (#4283)	5% BSA, 1h RT	5% BSA, 4°C O/N
Secondary					
Anti-mouse, HRP conjugated	Goat	1:4000	Promega (W4028)		5% BSA, 2h RT
Anti-rabbit HRP conjugated	Goat	1:4000	Vector Laboratories (PI-1000)		5% BSA, 2h RT

BSA: Bovine serum albumin; RT: room temperature; O/N: over night

Table 6. List of Ligands and Inhibitors.

Receptor	Ligand/Inhibitor	Concentration	Catalog ID	Origin
TLR2	C-10-15 (chitosan)	0,5 to 10 µM	OC28900	Carbosynth, self-acetylated
	Zymosan	100 µg/ml	tlrl-zyn	Invivogen
	Zymosan depleted	100 µg/ml	tlrl-dzn	Invivogen
	C-5	0,2 to 10 µM	55/14-0050	Isosep
	SSL3, staphylococcal superantigen-like 3	10 nM		Koymans et al., 2015; SSLΔ3 (residues 134-326)
TLR2-TLR1	Pam3CSK4	10 pM to 5 µM	tlrl-pms	Invivogen
TLR2-TLR6	Pam2CSK4	1 pM to 5 µM	tlrl-pm2s-1	Invivogen
TLR9	CpG 2006	1 to 2.5 µg/ml		TIB MOLBIOL, Berlin
TLR5	Flagellin	50 ng/ml	tlrl-stfla	Invivogen
NOD 2	Muramyl dipeptide (MDP)	200 nM	tlrl-mdp	Invivogen
Dectin-1	Zymosan	100 µg/ml	tlrl-zyn	Invivogen
BCR	Anti-human IgM, Fc5µ	5 µg/mL	309-005-095	Jackson ImmunoResearch
TLR4	Polymyxin B	10 µg/ml	21850029	Thermo Fisher

Table 7. List of siRNA pools used for knock-down experiments

Name of siRNA pool	Catalog ID
siGENOME Human TLR1 (7096) siRNA-SMARTpool	M-008086-01
siGENOME Human TLR6 (10333) siRNA-SMARTpool	M-005156-01
siGENOME Human TLR5 (7100) siRNA-SMARTpool	M-008089-01
siGENOME Non-Targeting Pool#1	D-001206-13-05
siGENOME H TLR2 (7097) siRNA -SMART pool	M-005120-03-005
ON-TARGETplus MYD88 siRNA - SMARTpool	L-004769-00-0005

all pools from Dharmacon, GE Healthcare

Table 8. List of plasmids.

Gene to be expressed	Tag	Backbone	Resistance	Origin	Notes	Internal ID
Original MYD88 plasmids, also used for qPCR						
MYD88 Isoform 1 - WT	N.A.	pDONR221	Kanamycin	Harvard plasmids ID: HsCD00296025	lacks first 13 AA, closed construct	pEX 502
MYD88 Isoform 2 - WT	N.A.	pDONR207	Gentamycin	Generated by O. Wolz	lacks first 13 AA, closed construct	pOW 011
MYD88 Isoform 3 - WT	N.A.	pDONR207	Gentamycin	GOI[§] by GENEWIZ	closed construct	pEX 503
MYD88 Isoform 4 - WT	N.A.	pDONR207	Gentamycin	GOI by GENEWIZ	closed construct	pEX 504
MYD88 Isoform 5 - WT	N.A.	pDONR207	Gentamycin	GOI by GENEWIZ	closed construct	pEX 505
MYD88 Isoform 1 - L265P	N.A.	pDONR207	Gentamycin	This study	pEX-502 after mutagenesis	pYCG 054
MYD88 Isoform 2 - L265P	N.A.	pDONR207	Gentamycin	Generated by O. Wolz	lacks first 13 AA, closed construct	pOW 012
MYD88 Isoform 3 - L265P	N.A.	pDONR207	Gentamycin	This study	pEX-503 after mutagenesis	pYCG 060
MYD88 Isoform 4 - L265P	N.A.	pDONR207	Gentamycin	This study	pEX-504 after mutagenesis	pYCG 056
MYD88 Isoform 5 - L265P	N.A.	pDONR207	Gentamycin	This study	pEX-505 after mutagenesis	pYCG 059
Expression MYD88 plasmids						
MYD88 Isoform 1 - WT	N-SHA*	pTO-N-SH	Ampicillin	This study		pYCG 030
MYD88 Isoform 2 - WT	N-SHA	pTO-N-SH	Ampicillin	Generated by O. Wolz		pOW 030
MYD88 Isoform 3 - WT	N-SHA	pTO-N-SH	Ampicillin	This study		pYCG 033
MYD88 Isoform 4 - WT	N-SHA	pTO-N-SH	Ampicillin	This study		pYCG 036
MYD88 Isoform 5 - WT	N-SHA	pTO-N-SH	Ampicillin	This study		pYCG 038
MYD88 Isoform 1 - L265P	N-SHA	pTO-N-SH	Ampicillin	This study		pYCG 171
MYD88 Isoform 2 - L265P	N-SHA	pTO-N-SH	Ampicillin	Generated by O.Wolz		pOW 031
MYD88 Isoform 3 - L265P	N-SHA	pTO-N-SH	Ampicillin	This study		pYCG 174
MYD88 Isoform 4 - L265P	N-SHA	pTO-N-SH	Ampicillin	This study		pYCG 177
MYD88 Isoform 5 - L265P	N-SHA	pTO-N-SH	Ampicillin	This study		pYCG 180
MyD88 (Isof. 2) DD-INT	ProtA-Myc	pT-Rex-DEST30	Ampicillin	Generated by J.George	Stop codon at AA 157, used in (George et al. 2011)	pJG-072

Gene to be expressed	Tag	Backbone	Resistance	Origin	Notes	Internal ID
PRRs, expression plasmids						
TLR2 - WT	N-Flag^{+}	pcDNA3	Ampicillin	Gift from I. Bekeredjian-Ding		pEX 073
TLR2 - L328W	N-Flag	pcDNA3	Ampicillin	Generated by M.Dang	pEX 073 after mutagenesis	pMD 068
TLR2 - V348L	N-Flag	pcDNA3	Ampicillin	Generated by M.Dang	pEX 073 after mutagenesis	pMD 069
TLR2 - V348W	N-Flag	pcDNA3	Ampicillin	Generated by M.Dang	pEX 073 after mutagenesis	pMD 070
TLR2 - V348Y	N-Flag	pcDNA3	Ampicillin	Generated by M.Dang	pEX 073 after mutagenesis	pMD 071
TLR2 - F349W	N-Flag	pcDNA3	Ampicillin	Generated by M.Dang	pEX 073 after mutagenesis	pMD 072
TLR2 - F349Y	N-Flag	pcDNA3	Ampicillin	Generated by M.Dang	pEX 073 after mutagenesis	pMD 073
TLR6 - P680H	HA	pcDNA 3.1	Ampicillin	Gift from L.Quintana	Dominant negative mutation	pEX 634
TLR10	HA	pCMV	Ampicillin	Gift from U.Hasan		pEX 681
TLR10	YFP	pcDNA 3.1	Ampicillin	Internal Stock		pEX 679
TLR9	N-Flag	pcDNA 3.1	Ampicillin	Gift from A. Dalpke		pEX 013
NOD-2	N-Flag	pCMV	Kanamycin	Gift from T. Kufer		pEX 621
Dectin-1 (BGR-A)	None	pcDNA	Ampicillin	Gift from G. Brown		pEX 619
Others						
NF-κB reporter	N.A.	pNF-kB	Ampicillin	Stratagene	Firefly luciferase reporter gene the under control of NF-κB p65 consensus promotor sequence	
Renilla Luciferase	N.A.	pRL-TK	Ampicillin	Promega	Renilla luciferase, continuous expression	
eGFP	N.A.	pC1-EGFP	Ampicillin	Gift from S.Dempe		pEX 008
Empty	N.A.	pTO-N-SH	Ampicillin	Gift from A. Pichlmaira	Adds N-terminal SHA- tag	pEX 144
Empty	N.A.	pcDNA3	Ampicillin	Addgene	Adds N-terminal Flag- tag	pEX 021

All gene sequences are human sequences otherwise stated. More details about Names and Institutions see Table S1.
N.A.: No applicable; §GOI: Gene of interest; * N-SHA: fused StrepIII-Hemagglutinin tag at the N-terminus; +N-Flag: fused Flag tag at the N-terminus.

Table 9. Sequences of mutagenesis primers.

Primer name	Sequence (5‘ to 3‘)	Internal ID	Designed by
Mutagenesis primers for all MYD88 splice variants plasmids			
L265P- Forward	gcccatcagaagcgaccgatccccatcaagtac	AWm460	Hui Wang
L265P- Reverse	gtacttgatggggatcggtcgcttctgatgggc	AWm461	Hui Wang
Mutagenesis (insertion*) primers for MYD88 splice variant 4 and 5			
Myd88_insert_Fwd	ccatcagaagcgactgatccccatcaagtacaaggcaatgaagaaaggacccagctttc	AWm537	In this study
Myd88_insert_Rev	gaaagctgggtcctttcttcattgccttgtacttgatggggatcagtcgcttctgatgg	AWm538	In this study
Mutagenesis primers for TLR2 constructs			
L328W-Forward	aagtgaatataaagtgctccaatcataaaataagtaaaaccttggaatatgcagcct	AWm543	A. Weber
L328W-Reverse	aggctgcatattccaaggttttacttattttatgattggagcactttatattcactt	AWm544	A. Weber
V348L-Forward	aagtaaacaaggaaccagaaaaagtttactgttttctactgtgattc	AWm545	A. Weber
V348L-Reverse	gaatcacagtagaaaacagtaaacttttctggttccttgtttactt	AWm546	A. Weber
V348W-Forward	aatgttgtgaaagtaaacaaggaaccagaaaccatttactgttttctactgtgattcttttaactc	AWm547	A. Weber
V348W-Reverse	gagttaaaagaatcacagtagaaaacagtaaatggtttctggttccttgtttactttcacaacatt	AWm548	A. Weber
V348Y-Forward	gtaaacaaggaaccagaaaatatttactgttttctactgtgattcttttaactctttc	AWm549	A. Weber
V348Y-Reverse	gaaagagttaaaagaatcacagtagaaaacagtaaatattttctggttccttgtttac	AWm550	A. Weber
F349W-Forward	gtgaaagtaaacaaggaaccagccaaactttactgttttctactgtgattcttttaac	AWm551	A. Weber
F349W-Reverse	gttaaaagaatcacagtagaaaacagtaaagtttggctggttccttgtttactttcac	AWm552	A. Weber
F349Y-Forward	gtaaacaaggaaccagataaactttactgttttctactgtgattctttta	AWm553	A. Weber
F349Y-Reverse	taaaagaatcacagtagaaaacagtaaagtttatctggttccttgtttac	AWm554	A. Weber

*Insertion of 30 bp to the end of CDS of variant 4 and 5 due to interruption of the natural stop codon when having L265P mutation.
Hui Wang, alumna Department of Immunology, University of Tübingen.

Table 10. Sequences and information of primers used for qPCR.

Detection	Forward primer (5' to 3')	Info primer	Reverse primer (5' to 3')	Info primer	Amplicon size	Efficiency
MYD88 Variant 1	agaggttggctagaaggcc ID: AWq_029	Lenght: 19 GC%: 57.89 Tm: 58.70°C Exon:4	gcacctggagagaggctg ID: AWq_030	Lenght: 18 GC%: 66.67 Tm: 59.64°C Exon:4-5	124 bp	105%
MYD88 Variant 2	cccagcattgaggaggattgc ID: AWq_031	Lenght: 21 GC%: 57.14 Tm: 61.36°C Exon:1-2	ctcaggcatatgccccaggg ID: AWq_037	Lenght: 20 GC%: 65 Tm: 62.42°C Exon: 2-3	159 bp	n.av.
MYD88 Variant 3	tgggacccagcattgggc ID: AWq_046	Lenght: 18 GC%: 66.67 Tm: 62.38 Exon: 1-3	tccttgctctgcaggtaatc ID: AWq_047	Lenght: 20 GC%: 50 Tm: 57.3 Exon:4	247 bp	66.39%
MYD88 Variant 4	atgacccccctgggtgcc ID: AWq_035	Lenght: 17 GC%: 70.59 Tm: 61.04°C Exon:2-4	gcacctggagagaggctg ID: AWq_030	Lenght: 18 GC%: 66.67 Tm: 59.42°C Exon:4-5	104 bp	106%
MYD88 Variant 5	ggacccagcattggtgcc ID: AWq_036	Lenght: 18 GC%: 66.67 Tm: 61.07°C Exon:1-4	gcacctggagagaggctg ID: AWq_030	Lenght: 18 GC%: 66.67 Tm: 59.42°C Exon:4-5	109 pb	108%
GAPDH	agccacatcgctcagacac Awq_026	Lenght: 19 Exon:2	gcccaatacgaccaaatcc Awq_027	Lenght: 19 Exon:3	66 bp	75.4%

n.av.= not available

Appendix

A.1 Supplementary Figures

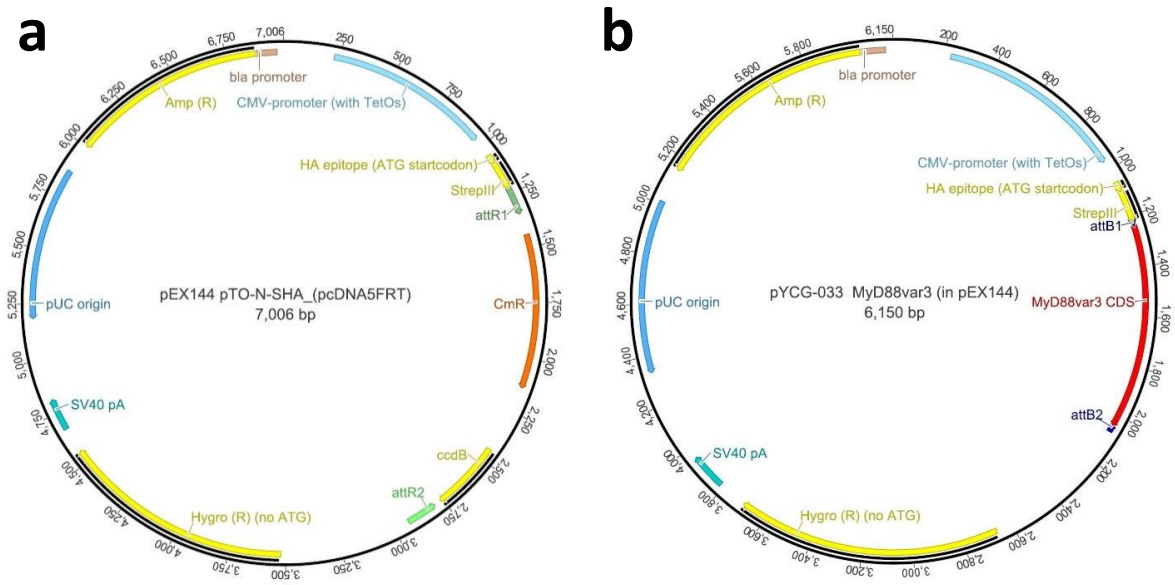

Figure S1. Plasmid maps from (a) empty destination vector pTO-N-SH, modified from pCDNA5/FRT and (b) after cloning of the CDS of MyD88 isoform 3. Maps generated in Geneious Pro version 5.5.9.

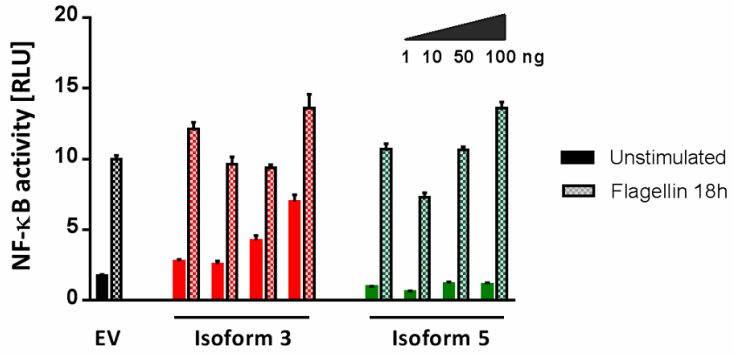

Figure S2. Assesing MyD88 isoform 3 and 5 potential inhibitory effect. DLA measurements of NF-κB activation in HEK 293T cells lysates upon transient transfection with four different amounts of MyD88 isoforms 3 and 5, together with NF-κB-inducible firefly luciferase and constitutive *Renilla* luciferase reporter. Cells were stimulated for 18 h with flagellin upon 32 h transfection. Threshold for activation was set at 5 RLU. Graph is representative of n=3 showing means+SD of triplicates. EV: empty vector; RLU: relative luminescence units.

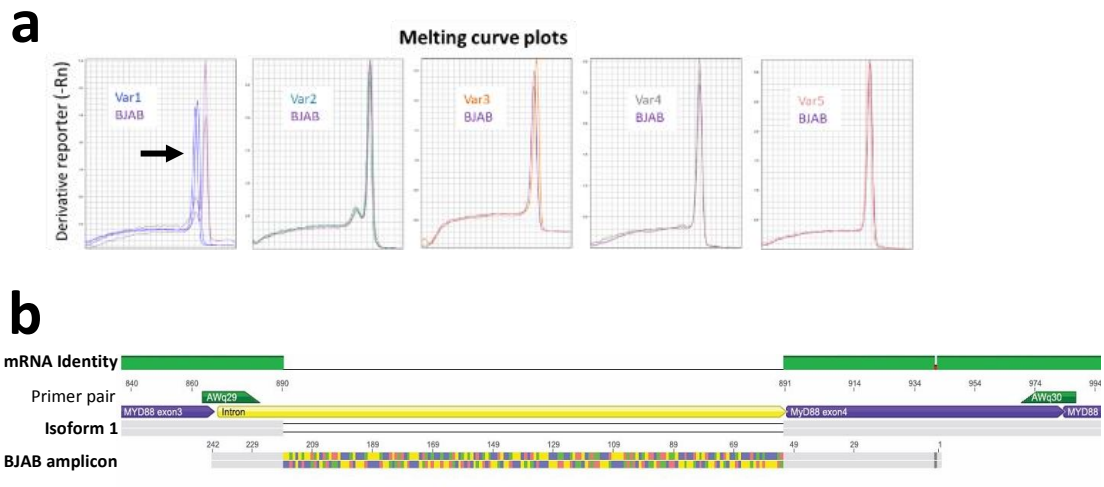

Figure S5. Primer pair generated an amplicon of unexpected length for MyD88 isoform 1. (a) Melting curves of amplicons for MyD88 isoforms 1 to 5 (left to right) for BJAB cells or entry vectors for the different MyD88 isoforms. RT-qPCR was performed using SybrGreen and primers specific for isoforms 1-5 of MyD88 (Table 10). Melting curves from BJAB sample (violet curve) and entry vectors from all MyD88 isoforms (blue for variants 1,2,4 and red for variants 3,5) are compared. Arrow points at the different melting curves from isoform 1. (b) Sequence alignment of isoform 1 reference (NM_001172567.1) and sequence of amplicon of BJAB sample from (a). Picture generated in Geneious Pro version 5.5.9.

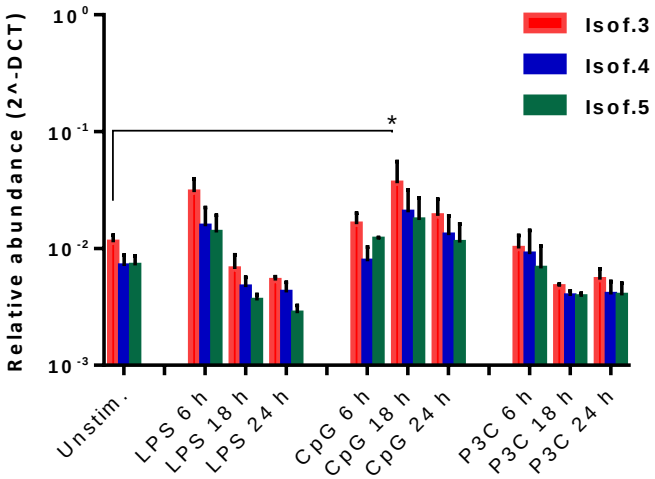

Figure S8. Increased mRNA expression of MyD88 isoform 3 upon TLR stimulation. mRNA quantification of MyD88 isoforms (isof.) in human PBMCs stimulated as indicated, n=3. PBMCs were isolated from fresh blood and stimulated in a reverse time point schedule. Upon stimulation cells were lysed and RNA was isolated and transcribed to cDNA. mRNA quantification was done by RT-qPCR using primers described in Table 10. Shown mean+SEM; *p<0.05 according to Two-way ANOVA; variables: isoform and stimuli.

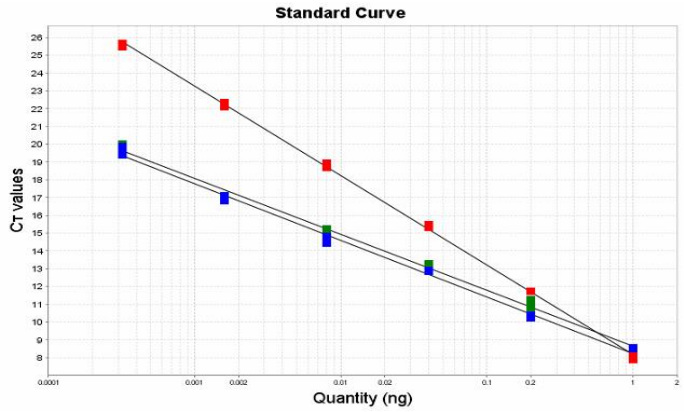

Reporter	Target	Slope	Y-intercept	r^2	Efficiency %
SYBR	Isoform 3	-4.522	8.422	0.974	66.392
SYBR	Isoform 4	-3.187	8.218	0.995	105.961
SYBR	Isoform 5	-3.138	8.644	0.994	108.288

Figure S11. Example of Standard curves from RT-qPCR primers. Primers sequences described in Table 10. Templates were generated constructs listed in Table 8. Tritation was done with consecutive 1:5 dilutions. Values are triplicates.

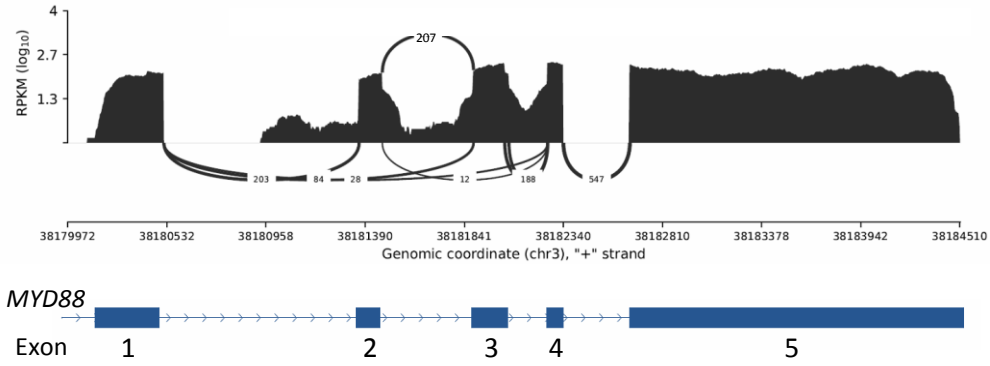

Figure S14. Representative Sashimi plot out of 72 Ovarian cancer samples; RNA seq data obtain from ICGC libraries. Y axis (RPKM) represent exon reads and arcs represent exon junctions. The width of the arc is proportional to the number of junctions. RPKM: reads per kilobase million. Plot done by S. Fillinger from ObiQ, University of Tübingen

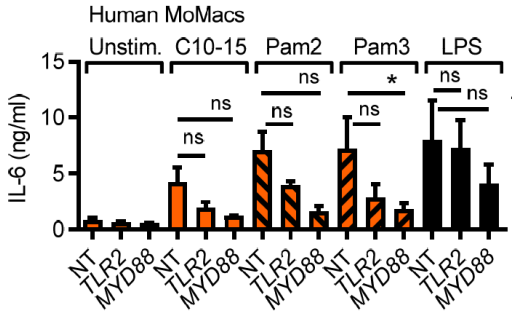

Figure S17. TLR2 knockdown in human macrophages showed reduced chitin-response. IL-6 released from human primary monocyte-derived macrophages (MoMacs, n=5) treated with non-targeting (NT), TLR2- or MyD88-specific siRNA. Data represents (mean+SEM) combined from 'n' biological replicates. * $p<0.05$ according to Wilcoxon signed rank sum. Experiments done by M. Dang and K. Fuchs from University of Tübingen. Materials and Methods described in the manuscript.

A.2 Supplementary Tables

Table S1. List of references from table 1.

TLR	References for ligands
TLR2	(Sato et al. 2003, O'Neill, Golenbock, and Bowie 2013, Leadbetter et al. 2002, Opal and Huber 2002, Erridge 2010)
TLR2 with TLR1	(Ozinsky et al. 2000, Aliprantis et al. 1999, O'Neill, Golenbock, and Bowie 2013)
TLR2 with TLR6	(Takeuchi et al. 2001, Buwitt-Beckmann et al. 2005, Shibata et al. 2000, O'Neill, Golenbock, and Bowie 2013, Li et al. 2001)
TLR3	(O'Neill, Golenbock, and Bowie 2013, Liu and Ji 2014, Green et al. 2012)
TLR4 with MD2	(O'Neill, Golenbock, and Bowie 2013, Liu and Ji 2014, Opal and Huber 2002)
TLR5	(O'Neill, Golenbock, and Bowie 2013)
TLR7	(O'Neill, Golenbock, and Bowie 2013, Green et al. 2012)
TLR8	(O'Neill, Golenbock, and Bowie 2013)
TLR9	(O'Neill, Golenbock, and Bowie 2013, Liu and Ji 2014)
TLR10 (human)	(Regan et al. 2013)
TLR11 (mouse)	(O'Neill, Golenbock, and Bowie 2013, Liu and Ji 2014)
TLR11 with TLR12 (mouse)	(Yarovinsky, Hieny, and Sher 2008, Raetz et al. 2013)
TLR13 (mouse)	(Wang, Chai, and Wang 2016, Hidmark, von Saint Paul, and Dalpke 2012)

Table S2. List of Names and Institutions of persons providing certain plasmids.

Names; Institutions
Alexander Dalpke; Medical Microbiology, Heidelberg University, Germany
Andreas Pichlmair; Max Planck Institute, Munich, Germany
Gordon Brown; Aberdeen University, UK
Goutham Pattabiraman; UCONN health Center, US
Lluis Quintana-Murci; Institut Pasteur, Paris, France
Isabel Bekeredjian-Ding; Medical Microbiology, Heidelberg University, Germany
Julie George; (alumna) University of Tübingen, Germany
Minh-Truong Dang; University of Tübingen, Germany
Olaf-Oliver Wolz; (Doctoral thesis) University of Tübingen, Germany
Sebastian Dempe; Krebsforschungszentrum, Heidelberg, Germany
Thomas Kufer; Hohenheim University, Germany
Uzma Hassan; University of London, United Kingdom

Table S3. Public IDs from RNAseq data

ID #	Origin
4118819-bcell	Bcell
4122131-bcell	Bcell
4149880-bcell	Bcell
4160735-bcell	Bcell
4174884-bcell	Bcell
4118819-gcbcell	GCBcell
4122131-gcbcell	GCBcell
4149880-gcbcell	GCBcell
4160735-gcbcell	GCBcell
4174884-gcbcell	GCBcell
4110996	BL_solid
4112512	BL_solid
4119027	BL_solid
4125240	BL_solid
4127766	BL_solid
4130003	BL_solid
4133511	BL_solid
4144633	BL_solid
4146289	BL_solid
4162611	BL_solid
4163741	BL_solid
4177434	BL_solid
4177856	BL_solid
4178518	BL_solid
4182393	BL_solid
4186812	BL_solid
4189998	BL_solid
4190495	BL_solid
4193278	BL_solid
4194218	BL_solid
4194891	BL_solid
4101316	DLBCL
4102009	DLBCL
4104105	DLBCL
4105746	DLBCL

ID #	Origin
4107137	DLBCL
4107559	DLBCL
4107990	DLBCL
4108101	DLBCL
4109808	DLBCL
4111326	DLBCL
4113140	DLBCL
4113971	DLBCL
4114033	DLBCL
4115001	DLBCL
4116268	DLBCL
4117030	DLBCL
4119279	DLBCL
4120157	DLBCL
4120193	DLBCL
4121621	DLBCL
4122063	DLBCL
4124188	DLBCL
4124791	DLBCL
4128849	DLBCL
4128852	DLBCL
4130051	DLBCL
4130194	DLBCL
4130865	DLBCL
4131257	DLBCL
4133263	DLBCL
4134434	DLBCL
4135099	DLBCL
4135278	DLBCL
4137230	DLBCL
4138464	DLBCL
4138527	DLBCL
4139696	DLBCL
4140531	DLBCL
4140544	DLBCL

ID #	Origin
4141476	DLBCL
4145528	DLBCL
4146301	DLBCL
4147968	DLBCL
4157186	DLBCL
4158933	DLBCL
4159421	DLBCL
4161781	DLBCL
4163639	DLBCL
4166940	DLBCL
4167381	DLBCL
4167925	DLBCL
4168738	DLBCL
4169012	DLBCL
4170577	DLBCL
4171586	DLBCL
4171810	DLBCL
4171946	DLBCL
4173863	DLBCL
4176046	DLBCL
4176133	DLBCL
4176325	DLBCL
4177842	DLBCL
4179894	DLBCL
4181460	DLBCL
4183136	DLBCL
4184094	DLBCL
4188879	DLBCL
4189035	DLBCL
4193638	DLBCL
4193646	DLBCL
4197155	DLBCL
4198519	DLBCL
4199714	DLBCL

ID #	Origin
4100049	FL
4101626	FL
4101815	FL
4103141	FL
4103627	FL
4105105	FL
4105782	FL
4108588	FL
4108988	FL
4108992	FL
4109142	FL
4109956	FL
4110378	FL
4112447	FL
4112817	FL
4113191	FL
4113825	FL
4118156	FL
4119463	FL
4119702	FL
4120879	FL
4121263	FL
4121361	FL
4121974	FL
4123945	FL
4124432	FL
4124542	FL
4124795	FL
4126692	FL
4128355	FL
4128435	FL
4128477	FL
4128970	FL
4131095	FL

ID #	Origin
4131738	FL
4134005	FL
4136095	FL
4138059	FL
4138652	FL
4138885	FL
4139212	FL
4139483	FL
4144366	FL
4145056	FL
4145391	FL
4147081	FL
4147360	FL
4148261	FL
4148771	FL
4149246	FL
4150549	FL
4151028	FL
4158268	FL
4158483	FL
4158726	FL
4159170	FL
4160069	FL
4160468	FL
4162154	FL
4163297	FL
4164330	FL
4165379	FL
4166503	FL
4170686	FL
4171706	FL
4171908	FL
4174905	FL
4175837	FL

ID #	Origin
4177406	FL
4177601	FL
4177810	FL
4177844	FL
4177987	FL
4178655	FL
4181037	FL
4184011	FL
4187640	FL
4188800	FL
4188900	FL
4189200	FL
4190929	FL
4198542	FL
4199848	FL
4199996	FL
4100636	FL-DLBCL
4110120	FL-DLBCL
4111337	FL-DLBCL
4131213	FL-DLBCL
4131744	FL-DLBCL
4132950	FL-DLBCL
4136702	FL-DLBCL
4144131	FL-DLBCL
4144951	FL-DLBCL
4145177	FL-DLBCL
4177376	FL-DLBCL
4183924	FL-DLBCL
4184437	FL-DLBCL
4186613	FL-DLBCL

A.3 Statutory Declaration

Hereby I affirm that I wrote this Doctoral thesis with the topic

"Molecular studies on *MYD88* alternative splicing in oncogenesis and Toll-like receptor 2 recognition of fungal chitin "

independently and that I used no other aids than those cited.
In each individual case, I have clearly identified the source of the passages that are taken paraphrased from other works and the linked manuscript. Moreover, I acknowledge the work done by collaborators.
I affirm that I performed the scientific studies according to the principles of good scientific practice.

Yamel Cardona Gloria

_____

Tübingen, Germany

References

Adib-Conquy, M., C. Adrie, C. Fitting, O. Gattolliat, R. Beyaert, and J. M. Cavaillon. 2006. "Up-regulation of MyD88s and SIGIRR, molecules inhibiting Toll-like receptor signaling, in monocytes from septic patients." *Crit Care Med* 34 (9):2377-85. doi: 10.1097/01.CCM.0000233875.93866.88.

Akira, S., K. Takeda, and T. Kaisho. 2001. "Toll-like receptors: critical proteins linking innate and acquired immunity." *Nat Immunol* 2 (8):675-80. doi: 10.1038/90609.

Aliprantis, A. O., R. B. Yang, M. R. Mark, S. Suggett, B. Devaux, J. D. Radolf, G. R. Klimpel, P. Godowski, and A. Zychlinsky. 1999. "Cell activation and apoptosis by bacterial lipoproteins through toll-like receptor-2." *Science* 285 (5428):736-9.

Alsafadi, S., A. Houy, A. Battistella, T. Popova, M. Wassef, E. Henry, F. Tirode, A. Constantinou, S. Piperno-Neumann, S. Roman-Roman, M. Dutertre, and M. H. Stern. 2016. "Cancer-associated SF3B1 mutations affect alternative splicing by promoting alternative branchpoint usage." *Nat Commun* 7:10615. doi: 10.1038/ncomms10615.

Alvero, A. B. 2010. "Recent insights into the role of NF-kappaB in ovarian carcinogenesis." *Genome Med* 2 (8):56. doi: 10.1186/gm177.

Andrews, C. S., S. Matsuyama, B. C. Lee, and J. D. Li. 2016. "Resveratrol suppresses NTHi-induced inflammation via up-regulation of the negative regulator MyD88 short." *Sci Rep* 6:34445. doi: 10.1038/srep34445.

Annunziata, C. M., H. T. Stavnes, L. Kleinberg, A. Berner, L. F. Hernandez, M. J. Birrer, S. M. Steinberg, B. Davidson, and E. C. Kohn. 2010. "Nuclear factor kappaB transcription factors are coexpressed and convey a poor outcome in ovarian cancer." *Cancer* 116 (13):3276-84. doi: 10.1002/cncr.25190.

Avbelj, M., S. Horvat, and R. Jerala. 2011. "The role of intermediary domain of MyD88 in cell activation and therapeutic inhibition of TLRs." *J Immunol* 187 (5):2394-404. doi: 10.4049/jimmunol.1100515.

Avbelj, M., O. O. Wolz, O. Fekonja, M. Bencina, M. Repic, J. Mavri, J. Kruger, C. Scharfe, M. Delmiro Garcia, G. Panter, O. Kohlbacher, A. N. Weber, and R. Jerala. 2014. "Activation of lymphoma-associated MyD88 mutations via allostery-induced TIR-domain oligomerization." *Blood* 124 (26):3896-904. doi: 10.1182/blood-2014-05-573188.

Bekeredjian-Ding, I., S. Inamura, T. Giese, H. Moll, S. Endres, A. Sing, U. Zahringer, and G. Hartmann. 2007. "Staphylococcus aureus protein A triggers T cell-independent B cell proliferation by sensitizing B cells for TLR2 ligands." *J Immunol* 178 (5):2803-12.

Bekeredjian-Ding, I., and G. Jego. 2009. "Toll-like receptors--sentries in the B-cell response." *Immunology* 128 (3):311-23. doi: 10.1111/j.1365-2567.2009.03173.x.

Bernard, N. J., and L. A. O'Neill. 2013. "Mal, more than a bridge to MyD88." *IUBMB Life* 65 (9):777-86. doi: 10.1002/iub.1201.

Bonomi, S., S. Gallo, M. Catillo, D. Pignataro, G. Biamonti, and C. Ghigna. 2013. "Oncogenic alternative splicing switches: role in cancer progression and prospects for therapy." *Int J Cell Biol* 2013:962038. doi: 10.1155/2013/962038.

Braza, F., S. Brouard, S. Chadban, and D. R. Goldstein. 2016. "Role of TLRs and DAMPs in allograft inflammation and transplant outcomes." *Nat Rev Nephrol* 12 (5):281-90. doi: 10.1038/nrneph.2016.41.

Brown, G. D., D. W. Denning, N. A. Gow, S. M. Levitz, M. G. Netea, and T. C. White. 2012. "Hidden killers: human fungal infections." *Sci Transl Med* 4 (165):165rv13. doi: 10.1126/scitranslmed.3004404.

Brown, G. D., P. R. Taylor, D. M. Reid, J. A. Willment, D. L. Williams, L. Martinez-Pomares, S. Y. Wong, and S. Gordon. 2002. "Dectin-1 is a major beta-glucan receptor on macrophages." *J Exp Med* 196 (3):407-12.

Brubaker, S. W., K. S. Bonham, I. Zanoni, and J. C. Kagan. 2015. "Innate immune pattern recognition: a cell biological perspective." *Annu Rev Immunol* 33:257-90. doi: 10.1146/annurev-immunol-032414-112240.

Bueter, C. L., C. K. Lee, V. A. Rathinam, G. J. Healy, C. H. Taron, C. A. Specht, and S. M. Levitz. 2011. "Chitosan but not chitin activates the inflammasome by a mechanism dependent upon phagocytosis." *J Biol Chem* 286 (41):35447-55. doi: 10.1074/jbc.M111.274936.

Bueter, C. L., C. A. Specht, and S. M. Levitz. 2013. "Innate sensing of chitin and chitosan." *PLoS Pathog* 9 (1):e1003080. doi: 10.1371/journal.ppat.1003080.

Burkatovskaya, M., A. P. Castano, T. N. Demidova-Rice, G. P. Tegos, and M. R. Hamblin. 2008. "Effect of chitosan acetate bandage on wound healing in infected and noninfected wounds in mice." *Wound Repair Regen* 16 (3):425-31. doi: 10.1111/j.1524-475X.2008.00382.x.

Burns, K., S. Janssens, B. Brissoni, N. Olivos, R. Beyaert, and J. Tschopp. 2003. "Inhibition of interleukin 1 receptor/Toll-like receptor signaling through the alternatively spliced, short form of MyD88 is due to its failure to recruit IRAK-4." *J Exp Med* 197 (2):263-8.

Buwitt-Beckmann, U., H. Heine, K. H. Wiesmuller, G. Jung, R. Brock, S. Akira, and A. J. Ulmer. 2005. "Toll-like receptor 6-independent signaling by diacylated lipopeptides." *Eur J Immunol* 35 (1):282-9. doi: 10.1002/eji.200424955.

Ceribelli, M., P. N. Kelly, A. L. Shaffer, G. W. Wright, W. Xiao, Y. Yang, L. A. Mathews Griner, R. Guha, P. Shinn, J. M. Keller, D. Liu, P. R. Patel, M. Ferrer, S. Joshi, S. Nerle, P. Sandy, E. Normant, C. J. Thomas, and L. M. Staudt. 2014. "Blockade of oncogenic IkappaB kinase activity in diffuse large B-cell lymphoma by bromodomain and extraterminal domain protein inhibitors." *Proc Natl Acad Sci U S A* 111 (31):11365-70. doi: 10.1073/pnas.1411701111.

Choi, J. P., S. M. Lee, H. I. Choi, M. H. Kim, S. G. Jeon, M. H. Jang, Y. K. Jee, S. Yang, Y. J. Cho, and Y. K. Kim. 2016. "House Dust Mite-Derived Chitin Enhances Th2 Cell Response to Inhaled Allergens, Mainly via a TNF-alpha-Dependent Pathway." *Allergy Asthma Immunol Res* 8 (4):362-74. doi: 10.4168/aair.2016.8.4.362.

Choi, J. W., Y. Kim, J. H. Lee, and Y. S. Kim. 2013. "MYD88 expression and L265P mutation in diffuse large B-cell lymphoma." *Hum Pathol* 44 (7):1375-81. doi: 10.1016/j.humpath.2012.10.026.

Choteau, L., H. Vancraeyneste, D. Le Roy, L. Dubuquoy, L. Romani, T. Jouault, D. Poulain, B. Sendid, T. Calandra, T. Roger, and S. Jawhara. 2017. "Role of TLR1, TLR2 and TLR6 in the modulation of intestinal inflammation and Candida albicans elimination." *Gut Pathog* 9:9. doi: 10.1186/s13099-017-0158-0.

Conze, D. B., C. J. Wu, J. A. Thomas, A. Landstrom, and J. D. Ashwell. 2008. "Lys63-linked polyubiquitination of IRAK-1 is required for interleukin-1 receptor- and toll-like receptor-mediated NF-kappaB activation." *Mol Cell Biol* 28 (10):3538-47. doi: 10.1128/MCB.02098-07.

Coussens, L. M., and Z. Werb. 2001. "Inflammatory cells and cancer: think different!" *J Exp Med* 193 (6):F23-6.

Cunha, C., L. Romani, and A. Carvalho. 2010. "Cracking the Toll-like receptor code in fungal infections." *Expert Rev Anti Infect Ther* 8 (10):1121-37. doi: 10.1586/eri.10.93.

Da Silva, C. A., C. Chalouni, A. Williams, D. Hartl, C. G. Lee, and J. A. Elias. 2009. "Chitin is a size-dependent regulator of macrophage TNF and IL-10 production." *J Immunol* 182 (6):3573-82. doi: 10.4049/jimmunol.0802113.

Da Silva, C. A., D. Hartl, W. Liu, C. G. Lee, and J. A. Elias. 2008. "TLR-2 and IL-17A in chitin-induced macrophage activation and acute inflammation." *J Immunol* 181 (6):4279-86.

Darman, R. B., M. Seiler, A. A. Agrawal, K. H. Lim, S. Peng, D. Aird, S. L. Bailey, E. B. Bhavsar, B. Chan, S. Colla, L. Corson, J. Feala, P. Fekkes, K. Ichikawa, G. F. Keaney, L. Lee, P. Kumar, K. Kunii, C. MacKenzie, M. Matijevic, Y. Mizui, K. Myint, E. S. Park, X. Puyang, A. Selvaraj, M. P. Thomas, J. Tsai, J. Y. Wang, M. Warmuth, H. Yang, P. Zhu, G. Garcia-Manero, R. R. Furman, L. Yu, P. G. Smith, and S. Buonamici. 2015. "Cancer-Associated SF3B1 Hotspot Mutations Induce Cryptic 3' Splice Site Selection through Use of a Different Branch Point." *Cell Rep* 13 (5):1033-45. doi: 10.1016/j.celrep.2015.09.053.

De Arras, L., and S. Alper. 2013. "Limiting of the innate immune response by SF3A-dependent control of MyD88 alternative mRNA splicing." *PLoS Genet* 9 (10):e1003855. doi: 10.1371/journal.pgen.1003855.

Deguine, J., and G. M. Barton. 2014. "MyD88: a central player in innate immune signaling." *F1000Prime Rep* 6:97. doi: 10.12703/P6-97.

den Haan, J. M., R. Arens, and M. C. van Zelm. 2014. "The activation of the adaptive immune system: cross-talk between antigen-presenting cells, T cells and B cells." *Immunol Lett* 162 (2 Pt B):103-12. doi: 10.1016/j.imlet.2014.10.011.

Desmet, F. O., D. Hamroun, M. Lalande, G. Collod-Beroud, M. Claustres, and C. Beroud. 2009. "Human Splicing Finder: an online bioinformatics tool to predict splicing signals." *Nucleic Acids Res* 37 (9):e67. doi: 10.1093/nar/gkp215.

Di Carlo, F. J., and J. V. Fiore. 1958. "On the composition of zymosan." *Science* 127 (3301):756-7.

Dillon, S., S. Agrawal, K. Banerjee, J. Letterio, T. L. Denning, K. Oswald-Richter, D. J. Kasprowicz, K. Kellar, J. Pare, T. van Dyke, S. Ziegler, D. Unutmaz, and B. Pulendran. 2006. "Yeast zymosan, a stimulus for TLR2 and dectin-1, induces regulatory antigen-presenting cells and immunological tolerance." *J Clin Invest* 116 (4):916-28. doi: 10.1172/JCI27203.

Doose, Gero, Stephan H. Bernhart, Rabea Wagener, and Steve Hoffmann. 2018. "DIEGO: detection of differential alternative splicing using Aitchison's geometry." *Bioinformatics* 34 (6):1066-1068. doi: 10.1093/bioinformatics/btx690.

Drexler, S. K., and B. M. Foxwell. 2010. "The role of toll-like receptors in chronic inflammation." *Int J Biochem Cell Biol* 42 (4):506-18. doi: 10.1016/j.biocel.2009.10.009.

Elieh-Ali-Komi, D., and M. R. Hamblin. 2016. "Chitin and Chitosan: Production and Application of Versatile Biomedical Nanomaterials." *Int J Adv Res (Indore)* 4 (3):411-427.

Elieh Ali Komi, D., L. Sharma, and C. S. Dela Cruz. 2017. "Chitin and Its Effects on Inflammatory and Immune Responses." *Clin Rev Allergy Immunol*. doi: 10.1007/s12016-017-8600-0.

Erridge, C. 2010. "Endogenous ligands of TLR2 and TLR4: agonists or assistants?" *J Leukoc Biol* 87 (6):989-99. doi: 10.1189/jlb.1209775.

Ewald, S. E., B. L. Lee, L. Lau, K. E. Wickliffe, G. P. Shi, H. A. Chapman, and G. M. Barton. 2008. "The ectodomain of Toll-like receptor 9 is cleaved to generate a functional receptor." *Nature* 456 (7222):658-62. doi: 10.1038/nature07405.

Fekonja, O., M. Bencina, and R. Jerala. 2012. "Toll/interleukin-1 receptor domain dimers as the platform for activation and enhanced inhibition of Toll-like receptor signaling." *J Biol Chem* 287 (37):30993-1002. doi: 10.1074/jbc.M112.376186.

Ferwerda, G., F. Meyer-Wentrup, B. J. Kullberg, M. G. Netea, and G. J. Adema. 2008. "Dectin-1 synergizes with TLR2 and TLR4 for cytokine production in human primary monocytes and macrophages." *Cell Microbiol* 10 (10):2058-66. doi: 10.1111/j.1462-5822.2008.01188.x.

Frank, M. M. 2010. "Complement disorders and hereditary angioedema." *J Allergy Clin Immunol* 125 (2 Suppl 2):S262-71. doi: 10.1016/j.jaci.2009.10.063.

Freeman, S. A., V. Jaumouille, K. Choi, B. E. Hsu, H. S. Wong, L. Abraham, M. L. Graves, D. Coombs, C. D. Roskelley, R. Das, S. Grinstein, and M. R. Gold. 2015. "Toll-like receptor ligands sensitize B-cell receptor signalling by reducing actin-dependent spatial confinement of the receptor." *Nat Commun* 6:6168. doi: 10.1038/ncomms7168.

Fu, X. D., and M. Ares, Jr. 2014. "Context-dependent control of alternative splicing by RNA-binding proteins." *Nat Rev Genet* 15 (10):689-701. doi: 10.1038/nrg3778.

Fuchs, Katharina, Yamel Cardona Gloria, Olaf-Oliver Wolz, Franziska Herster, Lokesh Sharma, Carly Dillen, Christoph Täumer, Sabine Dickhöfer, Zsofia Bittner, Truong-Minh Dang, Anuragh Singh, Daniel Haischer, Maria A Schlöffel, Kirsten J Koymans, Tharmila Sanmuganantham, Milena Krach, Nadine A Schilling, Felix Frauhammer, Lloyd Miller, Thorsten Nürnberger, Salomé LeibundGut-Landmann, Andrea A Gust, Boris Macek, Martin Frank, Cécile Gouttefangeas, Charles S Dela-Cruz, Dominik Hartl, and Alexander Weber. 2018. "The fungal ligand chitin directly binds and signals inflammation dependent on oligomer size and TLR2." *bioRxiv*. doi: 10.1101/270405.

Gachard, N., M. Parrens, I. Soubeyran, B. Petit, A. Marfak, D. Rizzo, M. Devesa, M. Delage-Corre, V. Coste, M. P. Laforet, A. de Mascarel, J. P. Merlio, K. Bouabdhalla, N. Milpied, P. Soubeyran, A. Schmitt, D. Bordessoule, M. Cogne, and J. Feuillard. 2013. "IGHV gene features and MYD88 L265P mutation separate the three marginal zone lymphoma entities and Waldenstrom macroglobulinemia/lymphoplasmacytic lymphomas." *Leukemia* 27 (1):183-9. doi: 10.1038/leu.2012.257.

Ganley-Leal, L. M., X. Liu, and L. M. Wetzler. 2006. "Toll-like receptor 2-mediated human B cell differentiation." *Clin Immunol* 120 (3):272-84. doi: 10.1016/j.clim.2006.04.571.

Gay, N. J., M. F. Symmons, M. Gangloff, and C. E. Bryant. 2014. "Assembly and localization of Toll-like receptor signalling complexes." *Nat Rev Immunol* 14 (8):546-58. doi: 10.1038/nri3713.

Ge, Y., and B. T. Porse. 2014. "The functional consequences of intron retention: alternative splicing coupled to NMD as a regulator of gene expression." *Bioessays* 36 (3):236-43. doi: 10.1002/bies.201300156.

George, J., P. G. Motshwene, H. Wang, A. V. Kubarenko, A. Rautanen, T. C. Mills, A. V. Hill, N. J. Gay, and A. N. Weber. 2011. "Two human MYD88 variants, S34Y and R98C, interfere with MyD88-IRAK4-myddosome assembly." *J Biol Chem* 286 (2):1341-53. doi: 10.1074/jbc.M110.159996.

Goodridge, H. S., and D. M. Underhill. 2008. "Fungal Recognition by TLR2 and Dectin-1." *Handb Exp Pharmacol* (183):87-109. doi: 10.1007/978-3-540-72167-3_5.

Gordon, S. 2016. "Phagocytosis: An Immunobiologic Process." *Immunity* 44 (3):463-475. doi: 10.1016/j.immuni.2016.02.026.

Gosu, V., S. Basith, P. Durai, and S. Choi. 2012. "Molecular evolution and structural features of IRAK family members." *PLoS One* 7 (11):e49771. doi: 10.1371/journal.pone.0049771.

Green, N. M., K. S. Moody, M. Debatis, and A. Marshak-Rothstein. 2012. "Activation of autoreactive B cells by endogenous TLR7 and TLR3 RNA ligands." *The Journal of biological chemistry* 287 (47):39789-99. doi: 10.1074/jbc.M112.383000.

Gregersen, P. K., and T. W. Behrens. 2006. "Genetics of autoimmune diseases--disorders of immune homeostasis." *Nat Rev Genet* 7 (12):917-28. doi: 10.1038/nrg1944.

Gurtler, C., M. Carty, J. Kearney, S. A. Schattgen, A. Ding, K. A. Fitzgerald, and A. G. Bowie. 2014. "SARM regulates CCL5 production in macrophages by promoting the recruitment of transcription factors and RNA polymerase II to the Ccl5 promoter." *J Immunol* 192 (10):4821-32. doi: 10.4049/jimmunol.1302980.

Gutmann, T., K. H. Kim, M. Grzybek, T. Walz, and U. Coskun. 2018. "Visualization of ligand-induced transmembrane signaling in the full-length human insulin receptor." *J Cell Biol*. doi: 10.1083/jcb.201711047.

Haase, R., C. J. Kirschning, A. Sing, P. Schrottner, K. Fukase, S. Kusumoto, H. Wagner, J. Heesemann, and K. Ruckdeschel. 2003. "A dominant role of Toll-like receptor 4 in the signaling of apoptosis in bacteria-faced macrophages." *J Immunol* 171 (8):4294-303.

Hamid, R., M. A. Khan, M. Ahmad, M. M. Ahmad, M. Z. Abdin, J. Musarrat, and S. Javed. 2013. "Chitinases: An update." *J Pharm Bioallied Sci* 5 (1):21-9. doi: 10.4103/0975-7406.106559.

He, B., R. Santamaria, W. Xu, M. Cols, K. Chen, I. Puga, M. Shan, H. Xiong, J. B. Bussel, A. Chiu, A. Puel, J. Reichenbach, L. Marodi, R. Doffinger, J. Vasconcelos, A. Issekutz, J. Krause, G. Davies, X. Li, B. Grimbacher, A. Plebani, E. Meffre, C. Picard, C. Cunningham-Rundles, J. L. Casanova, and A. Cerutti. 2010. "The transmembrane activator TACI triggers immunoglobulin class switching by activating B cells through the adaptor MyD88." *Nat Immunol* 11 (9):836-45. doi: 10.1038/ni.1914.

Hess, N. J., S. Jiang, X. Li, Y. Guan, and R. I. Tapping. 2017. "TLR10 Is a B Cell Intrinsic Suppressor of Adaptive Immune Responses." *J Immunol* 198 (2):699-707. doi: 10.4049/jimmunol.1601335.

Hezaveh, K., A. Kloetgen, S. H. Bernhart, K. D. Mahapatra, D. Lenze, J. Richter, A. Haake, A. K. Bergmann, B. Brors, B. Burkhardt, A. Claviez, H. G. Drexler, R. Eils, S. Haas, S.

Hoffmann, D. Karsch, W. Klapper, K. Kleinheinz, J. Korbel, H. Kretzmer, M. Kreuz, R. Kuppers, C. Lawerenz, E. Leich, M. Loeffler, L. Mantovani-Loeffler, C. Lopez, A. C. McHardy, P. Moller, M. Rohde, P. Rosenstiel, A. Rosenwald, M. Schilhabel, M. Schlesner, I. Scholz, P. F. Stadler, S. Stilgenbauer, S. Sungalee, M. Szczepanowski, L. Trumper, M. A. Weniger, R. Siebert, A. Borkhardt, M. Hummel, J. I. Hoell, and Icgc Mmml- Seq Project. 2016. "Alterations of microRNA and microRNA-regulated messenger RNA expression in germinal center B-cell lymphomas determined by integrative sequencing analysis." *Haematologica* 101 (11):1380-1389. doi: 10.3324/haematol.2016.143891.

Hidmark, A., A. von Saint Paul, and A. H. Dalpke. 2012. "Cutting edge: TLR13 is a receptor for bacterial RNA." *J Immunol* 189 (6):2717-21. doi: 10.4049/jimmunol.1200898.

Hoffmann, S., C. Otto, G. Doose, A. Tanzer, D. Langenberger, S. Christ, M. Kunz, L. M. Holdt, D. Teupser, J. Hackermuller, and P. F. Stadler. 2014. "A multi-split mapping algorithm for circular RNA, splicing, trans-splicing and fusion detection." *Genome Biol* 15 (2):R34. doi: 10.1186/gb-2014-15-2-r34.

Hua, Z., and B. Hou. 2013. "TLR signaling in B-cell development and activation." *Cell Mol Immunol* 10 (2):103-6. doi: 10.1038/cmi.2012.61.

Inoue, D., and O. Abdel-Wahab. 2016. "Modeling SF3B1 Mutations in Cancer: Advances, Challenges, and Opportunities." *Cancer Cell* 30 (3):371-373. doi: 10.1016/j.ccell.2016.08.013.

Isaza-Correa, J. M., Z. Liang, A. van den Berg, A. Diepstra, and L. Visser. 2014. "Toll-like receptors in the pathogenesis of human B cell malignancies." *J Hematol Oncol* 7:57. doi: 10.1186/s13045-014-0057-5.

Iwanaszko, M., and M. Kimmel. 2015. "NF-kappaB and IRF pathways: cross-regulation on target genes promoter level." *BMC Genomics* 16:307. doi: 10.1186/s12864-015-1511-7.

Iwasaki, A., and R. Medzhitov. 2010. "Regulation of adaptive immunity by the innate immune system." *Science* 327 (5963):291-5. doi: 10.1126/science.1183021.

Iwasaki, A., and R. Medzhitov. 2015. "Control of adaptive immunity by the innate immune system." *Nat Immunol* 16 (4):343-53. doi: 10.1038/ni.3123.

Janeway, C.A. Jr; Travers, P.; Walport, M.; et al. 2001. *Immunobiology: The Immune System in Health and Disease.* 5th edition ed. New York: Garland Science.

Janssens, S., K. Burns, E. Vercammen, J. Tschopp, and R. Beyaert. 2003. "MyD88S, a splice variant of MyD88, differentially modulates NF-kappaB- and AP-1-dependent gene expression." *FEBS Lett* 548 (1-3):103-7.

Jiang, S., X. Li, N. J. Hess, Y. Guan, and R. I. Tapping. 2016. "TLR10 Is a Negative Regulator of Both MyD88-Dependent and -Independent TLR Signaling." *J Immunol* 196 (9):3834-41. doi: 10.4049/jimmunol.1502599.

Jin, M. S., S. E. Kim, J. Y. Heo, M. E. Lee, H. M. Kim, S. G. Paik, H. Lee, and J. O. Lee. 2007. "Crystal structure of the TLR1-TLR2 heterodimer induced by binding of a tri-acylated lipopeptide." *Cell* 130 (6):1071-82. doi: 10.1016/j.cell.2007.09.008.

Jurado-Camino, T., R. Cordoba, L. Esteban-Burgos, E. Hernandez-Jimenez, V. Toledano, J. A. Hernandez-Rivas, E. Ruiz-Sainz, T. Cobo, M. Siliceo, R. Perez de Diego, C. Belda, C. Cubillos-Zapata, and E. Lopez-Collazo. 2015. "Chronic lymphocytic leukemia: a paradigm of innate immune cross-tolerance." *J Immunol* 194 (2):719-27. doi: 10.4049/jimmunol.1402272.

Kaida, D., T. Schneider-Poetsch, and M. Yoshida. 2012. "Splicing in oncogenesis and tumor suppression." *Cancer Sci* 103 (9):1611-6. doi: 10.1111/j.1349-7006.2012.02356.x.

Kajava, A. V., and T. Vasselon. 2010. "A network of hydrogen bonds on the surface of TLR2 controls ligand positioning and cell signaling." *J Biol Chem* 285 (9):6227-34. doi: 10.1074/jbc.M109.063669.

Kaku, H., Y. Nishizawa, N. Ishii-Minami, C. Akimoto-Tomiyama, N. Dohmae, K. Takio, E. Minami, and N. Shibuya. 2006. "Plant cells recognize chitin fragments for defense signaling through a plasma membrane receptor." *Proc Natl Acad Sci U S A* 103 (29):11086-91. doi: 10.1073/pnas.0508882103.

Katz, Y., E. T. Wang, J. Silterra, S. Schwartz, B. Wong, H. Thorvaldsdottir, J. T. Robinson, J. P. Mesirov, E. M. Airoldi, and C. B. Burge. 2015. "Quantitative visualization of alternative exon expression from RNA-seq data." *Bioinformatics* 31 (14):2400-2. doi: 10.1093/bioinformatics/btv034.

Kawakami, K., S. Kohno, J. Kadota, M. Tohyama, K. Teruya, N. Kudeken, A. Saito, and K. Hara. 1995. "T cell-dependent activation of macrophages and enhancement of their phagocytic activity in the lungs of mice inoculated with heat-killed Cryptococcus neoformans: involvement of IFN-gamma and its protective effect against cryptococcal infection." *Microbiol Immunol* 39 (2):135-43.

Knittel, G., P. Liedgens, and H. C. Reinhardt. 2015. "Targeting ATM-deficient CLL through interference with DNA repair pathways." *Front Genet* 6:207. doi: 10.3389/fgene.2015.00207.

Koblansky, A. A., D. Jankovic, H. Oh, S. Hieny, W. Sungnak, R. Mathur, M. S. Hayden, S. Akira, A. Sher, and S. Ghosh. 2013. "Recognition of profilin by Toll-like receptor 12 is critical for host resistance to Toxoplasma gondii." *Immunity* 38 (1):119-30. doi: 10.1016/j.immuni.2012.09.016.

Koh, C. M., M. Bezzi, D. H. Low, W. X. Ang, S. X. Teo, F. P. Gay, M. Al-Haddawi, S. Y. Tan, M. Osato, A. Sabo, B. Amati, K. B. Wee, and E. Guccione. 2015. "MYC regulates the core pre-mRNA splicing machinery as an essential step in lymphomagenesis." *Nature* 523 (7558):96-100. doi: 10.1038/nature14351.

Kottom, T. J., D. M. Hebrink, P. E. Jenson, V. Nandakumar, M. Wuthrich, H. Wang, B. Klein, S. Yamasaki, B. Lepenies, and A. H. Limper. 2017. "The Interaction of Pneumocystis with the C-Type Lectin Receptor Mincle Exerts a Significant Role in Host Defense against Infection." *J Immunol* 198 (9):3515-3525. doi: 10.4049/jimmunol.1600744.

Koymans, K. J., L. J. Feitsma, T. H. Brondijk, P. C. Aerts, E. Lukkien, P. Lossl, K. P. van Kessel, C. J. de Haas, J. A. van Strijp, and E. G. Huizinga. 2015. "Structural basis for inhibition of TLR2 by staphylococcal superantigen-like protein 3 (SSL3)." *Proc Natl Acad Sci U S A* 112 (35):11018-23. doi: 10.1073/pnas.1502026112.

Kozlovski, I., Z. Siegfried, A. Amar-Schwartz, and R. Karni. 2017. "The role of RNA alternative splicing in regulating cancer metabolism." *Hum Genet* 136 (9):1113-1127. doi: 10.1007/s00439-017-1803-x.

Kretzmer, H., S. H. Bernhart, W. Wang, A. Haake, M. A. Weniger, A. K. Bergmann, M. J. Betts, E. Carrillo-de-Santa-Pau, G. Doose, J. Gutwein, J. Richter, V. Hovestadt, B. Huang, D. Rico, F. Juhling, J. Kolarova, Q. Lu, C. Otto, R. Wagener, J. Arnolds, B. Burkhardt, A. Claviez, H. G. Drexler, S. Eberth, R. Eils, P. Flicek, S. Haas, M. Humme, D. Karsch, H. H. D. Kerstens, W. Klapper, M. Kreuz, C. Lawerenz, D. Lenzek, M. Loeffler, C. Lopez, R. A. F. MacLeod, J. H. A. Martens, M. Kulis, J. I. Martin-Subero, P. Moller, I. Nage, S. Picelli, I. Vater, M. Rohde, P. Rosenstiel, M. Rosolowski, R. B.

Russell, M. Schilhabel, M. Schlesner, P. F. Stadler, M. Szczepanowski, L. Trumper, H. G. Stunnenberg, R. Kuppers, O. Ammerpohl, P. Lichter, R. Siebert, S. Hoffmann, and B. Radlwimmer. 2015. "DNA methylome analysis in Burkitt and follicular lymphomas identifies differentially methylated regions linked to somatic mutation and transcriptional control." *Nat Genet* 47 (11):1316-1325. doi: 10.1038/ng.3413.

Kuusk, S., M. Sorlie, and P. Valjamae. 2017. "Human Chitotriosidase Is an Endo-Processive Enzyme." *PLoS One* 12 (1):e0171042. doi: 10.1371/journal.pone.0171042.

Ladomery, M. 2013. "Aberrant alternative splicing is another hallmark of cancer." *Int J Cell Biol* 2013:463786. doi: 10.1155/2013/463786.

Landau, D. A., S. L. Carter, P. Stojanov, A. McKenna, K. Stevenson, M. S. Lawrence, C. Sougnez, C. Stewart, A. Sivachenko, L. Wang, Y. Wan, W. Zhang, S. A. Shukla, A. Vartanov, S. M. Fernandes, G. Saksena, K. Cibulskis, B. Tesar, S. Gabriel, N. Hacohen, M. Meyerson, E. S. Lander, D. Neuberg, J. R. Brown, G. Getz, and C. J. Wu. 2013. "Evolution and impact of subclonal mutations in chronic lymphocytic leukemia." *Cell* 152 (4):714-26. doi: 10.1016/j.cell.2013.01.019.

Latty, S. L., J. Sakai, L. Hopkins, B. Verstak, T. Paramo, N. A. Berglund, E. Cammorota, P. Cicuta, N. J. Gay, P. J. Bond, D. Klenerman, and C. E. Bryant. 2018. "Activation of Toll-like receptors nucleates assembly of the MyDDosome signaling hub." *Elife* 7. doi: 10.7554/eLife.31377.

Leadbetter, E. A., I. R. Rifkin, A. M. Hohlbaum, B. C. Beaudette, M. J. Shlomchik, and A. Marshak-Rothstein. 2002. "Chromatin-IgG complexes activate B cells by dual engagement of IgM and Toll-like receptors." *Nature* 416 (6881):603-7. doi: 10.1038/416603a.

Lee, C. G., C. A. Da Silva, C. S. Dela Cruz, F. Ahangari, B. Ma, M. J. Kang, C. H. He, S. Takyar, and J. A. Elias. 2011. "Role of chitin and chitinase/chitinase-like proteins in inflammation, tissue remodeling, and injury." *Annu Rev Physiol* 73:479-501. doi: 10.1146/annurev-physiol-012110-142250.

Lee, C. G., C. A. Da Silva, J. Y. Lee, D. Hartl, and J. A. Elias. 2008. "Chitin regulation of immune responses: an old molecule with new roles." *Curr Opin Immunol* 20 (6):684-9. doi: 10.1016/j.coi.2008.10.002.

Lee, J. H., H. Jeong, J. W. Choi, H. Oh, and Y. S. Kim. 2017. "Clinicopathologic significance of MYD88 L265P mutation in diffuse large B-cell lymphoma: a meta-analysis." *Sci Rep* 7 (1):1785. doi: 10.1038/s41598-017-01998-5.

Lee, S. J., S. Evers, D. Roeder, A. F. Parlow, J. Risteli, L. Risteli, Y. C. Lee, T. Feizi, H. Langen, and M. C. Nussenzweig. 2002. "Mannose receptor-mediated regulation of serum glycoprotein homeostasis." *Science* 295 (5561):1898-901. doi: 10.1126/science.1069540.

Lee, Y., and D. C. Rio. 2015. "Mechanisms and Regulation of Alternative Pre-mRNA Splicing." *Annu Rev Biochem* 84:291-323. doi: 10.1146/annurev-biochem-060614-034316.

Lelis, F. J. N., J. Jaufmann, A. Singh, K. Fromm, A. C. Teschner, S. Poschel, I. Schafer, S. Beer-Hammer, N. Rieber, and D. Hartl. 2017. "Myeloid-derived suppressor cells modulate B-cell responses." *Immunol Lett* 188:108-115. doi: 10.1016/j.imlet.2017.07.003.

Lenardon, M. D., C. A. Munro, and N. A. Gow. 2010. "Chitin synthesis and fungal pathogenesis." *Curr Opin Microbiol* 13 (4):416-23. doi: 10.1016/j.mib.2010.05.002.

Li, H., G. Yang, F. Ma, T. Li, H. Yang, J. H. Rombout, and L. An. 2017. "Molecular characterization of a fish-specific toll-like receptor 22 (TLR22) gene from common carp (Cyprinus carpio L.): Evolutionary relationship and induced expression upon immune stimulants." *Fish Shellfish Immunol* 63:74-86. doi: 10.1016/j.fsi.2017.02.009.

Li, M., D. F. Carpio, Y. Zheng, P. Bruzzo, V. Singh, F. Ouaaz, R. M. Medzhitov, and A. A. Beg. 2001. "An essential role of the NF-kappa B/Toll-like receptor pathway in induction of inflammatory and tissue-repair gene expression by necrotic cells." *J Immunol* 166 (12):7128-35.

Lin, S. C., Y. C. Lo, and H. Wu. 2010. "Helical assembly in the MyD88-IRAK4-IRAK2 complex in TLR/IL-1R signalling." *Nature* 465 (7300):885-90. doi: 10.1038/nature09121.

Liu, T., and R. R. Ji. 2014. "Toll-Like Receptors and Itch." In *Itch: Mechanisms and Treatment*, edited by E. Carstens and T. Akiyama. Boca Raton (FL).

Liu, T., Z. Liu, C. Song, Y. Hu, Z. Han, J. She, F. Fan, J. Wang, C. Jin, J. Chang, J. M. Zhou, and J. Chai. 2012. "Chitin-induced dimerization activates a plant immune receptor." *Science* 336 (6085):1160-4. doi: 10.1126/science.1218867.

Loiarro, M., G. Gallo, N. Fanto, R. De Santis, P. Carminati, V. Ruggiero, and C. Sette. 2009. "Identification of critical residues of the MyD88 death domain involved in the recruitment of downstream kinases." *J Biol Chem* 284 (41):28093-103. doi: 10.1074/jbc.M109.004465.

Lu, Y. C., W. C. Yeh, and P. S. Ohashi. 2008. "LPS/TLR4 signal transduction pathway." *Cytokine* 42 (2):145-51. doi: 10.1016/j.cyto.2008.01.006.

Ma, Z., and B. Damania. 2016. "The cGAS-STING Defense Pathway and Its Counteraction by Viruses." *Cell Host Microbe* 19 (2):150-8. doi: 10.1016/j.chom.2016.01.010.

Maarschalk-Ellerbroek, L. J., A. I. Hoepelman, J. M. van Montfrans, and P. M. Ellerbroek. 2012. "The spectrum of disease manifestations in patients with common variable immunodeficiency disorders and partial antibody deficiency in a university hospital." *J Clin Immunol* 32 (5):907-21. doi: 10.1007/s10875-012-9671-6.

MacIntyre, A. D., J. A. Quick, and S. L. Barnes. 2011. "Hemostatic dressings reduce tourniquet time while maintaining hemorrhage control." *Am Surg* 77 (2):162-5.

Maglic, D., D. B. Stovall, J. M. Cline, E. A. Fry, A. Mallakin, P. Taneja, D. L. Caudell, M. C. Willingham, G. Sui, and K. Inoue. 2015. "DMP1beta, a splice isoform of the tumour suppressor DMP1 locus, induces proliferation and progression of breast cancer." *J Pathol* 236 (1):90-102. doi: 10.1002/path.4504.

Malik, P., S. Z. Berisha, J. Santore, C. Agatisa-Boyle, G. Brubaker, and J. D. Smith. 2011. "Zymosan-mediated inflammation impairs in vivo reverse cholesterol transport." *J Lipid Res* 52 (5):951-7. doi: 10.1194/jlr.M011122.

Marakalala, M. J., S. Vautier, J. Potrykus, L. A. Walker, K. M. Shepardson, A. Hopke, H. M. Mora-Montes, A. Kerrigan, M. G. Netea, G. I. Murray, D. M. Maccallum, R. Wheeler, C. A. Munro, N. A. Gow, R. A. Cramer, A. J. Brown, and G. D. Brown. 2013. "Differential adaptation of Candida albicans in vivo modulates immune recognition by dectin-1." *PLoS Pathog* 9 (4):e1003315. doi: 10.1371/journal.ppat.1003315.

Miya, A., P. Albert, T. Shinya, Y. Desaki, K. Ichimura, K. Shirasu, Y. Narusaka, N. Kawakami, H. Kaku, and N. Shibuya. 2007. "CERK1, a LysM receptor kinase, is essential for chitin elicitor signaling in Arabidopsis." *Proc Natl Acad Sci U S A* 104 (49):19613-8. doi: 10.1073/pnas.0705147104.

Monlish, D. A., S. T. Bhatt, and L. G. Schuettpelz. 2016. "The Role of Toll-Like Receptors in Hematopoietic Malignancies." *Front Immunol* 7:390. doi: 10.3389/fimmu.2016.00390.

Montesinos-Rongen, M., E. Godlewska, A. Brunn, O. D. Wiestler, R. Siebert, and M. Deckert. 2011. "Activating L265P mutations of the MYD88 gene are common in primary central nervous system lymphoma." *Acta Neuropathol* 122 (6):791-2. doi: 10.1007/s00401-011-0891-2.

Mora-Montes, H. M., M. G. Netea, G. Ferwerda, M. D. Lenardon, G. D. Brown, A. R. Mistry, B. J. Kullberg, C. A. O'Callaghan, C. C. Sheth, F. C. Odds, A. J. Brown, C. A. Munro, and N. A. Gow. 2011. "Recognition and blocking of innate immunity cells by Candida albicans chitin." *Infect Immun* 79 (5):1961-70. doi: 10.1128/IAI.01282-10.

Morales, D. K., and D. A. Hogan. 2010. "Candida albicans interactions with bacteria in the context of human health and disease." *PLoS Pathog* 6 (4):e1000886. doi: 10.1371/journal.ppat.1000886.

Mudaliar, M. A., R. D. Haggart, G. Miele, G. Sellar, K. A. Tan, J. R. Goodlad, E. Milne, D. M. Vail, I. Kurzman, D. Crowther, and D. J. Argyle. 2013. "Comparative gene expression profiling identifies common molecular signatures of NF-kappaB activation in canine and human diffuse large B cell lymphoma (DLBCL)." *PLoS One* 8 (9):e72591. doi: 10.1371/journal.pone.0072591.

Munro, C. A., and N. A. Gow. 2001. "Chitin synthesis in human pathogenic fungi." *Med Mycol* 39 Suppl 1:41-53.

Murray, P. J., and T. A. Wynn. 2011. "Protective and pathogenic functions of macrophage subsets." *Nat Rev Immunol* 11 (11):723-37. doi: 10.1038/nri3073.

Muzio, M., C. Scielzo, M. T. Bertilaccio, M. Frenquelli, P. Ghia, and F. Caligaris-Cappio. 2009. "Expression and function of toll like receptors in chronic lymphocytic leukaemia cells." *Br J Haematol* 144 (4):507-16. doi: 10.1111/j.1365-2141.2008.07475.x.

Newman, M. A., T. Sundelin, J. T. Nielsen, and G. Erbs. 2013. "MAMP (microbe-associated molecular pattern) triggered immunity in plants." *Front Plant Sci* 4:139. doi: 10.3389/fpls.2013.00139.

Ngo, V. N., R. M. Young, R. Schmitz, S. Jhavar, W. Xiao, K. H. Lim, H. Kohlhammer, W. Xu, Y. Yang, H. Zhao, A. L. Shaffer, P. Romesser, G. Wright, J. Powell, A. Rosenwald, H. K. Muller-Hermelink, G. Ott, R. D. Gascoyne, J. M. Connors, L. M. Rimsza, E. Campo, E. S. Jaffe, J. Delabie, E. B. Smeland, R. I. Fisher, R. M. Braziel, R. R. Tubbs, J. R. Cook, D. D. Weisenburger, W. C. Chan, and L. M. Staudt. 2011. "Oncogenically active MYD88 mutations in human lymphoma." *Nature* 470 (7332):115-9. doi: 10.1038/nature09671.

Ni, M., A. W. th MacFarlane, M. Toft, C. A. Lowell, K. S. Campbell, and J. A. Hamerman. 2012. "B-cell adaptor for PI3K (BCAP) negatively regulates Toll-like receptor signaling through activation of PI3K." *Proc Natl Acad Sci U S A* 109 (1):267-72. doi: 10.1073/pnas.1111957108.

Nilsen, N. J., G. I. Vladimer, J. Stenvik, M. P. Orning, M. V. Zeid-Kilani, M. Bugge, B. Bergstroem, J. Conlon, H. Husebye, A. G. Hise, K. A. Fitzgerald, T. Espevik, and E. Lien. 2015. "A role for the adaptor proteins TRAM and TRIF in toll-like receptor 2 signaling." *J Biol Chem* 290 (6):3209-22. doi: 10.1074/jbc.M114.593426.

O'Neill, L. A., A. Dunne, M. Edjeback, P. Gray, C. Jefferies, and C. Wietek. 2003. "Mal and MyD88: adapter proteins involved in signal transduction by Toll-like receptors." *J Endotoxin Res* 9 (1):55-9. doi: 10.1179/096805103125001351.

O'Neill, L. A., D. Golenbock, and A. G. Bowie. 2013. "The history of Toll-like receptors - redefining innate immunity." *Nat Rev Immunol* 13 (6):453-60. doi: 10.1038/nri3446.

Obeng, E. A., R. J. Chappell, M. Seiler, M. C. Chen, D. R. Campagna, P. J. Schmidt, R. K. Schneider, A. M. Lord, L. Wang, R. G. Gambe, M. E. McConkey, A. M. Ali, A. Raza, L. Yu, S. Buonamici, P. G. Smith, A. Mullally, C. J. Wu, M. D. Fleming, and B. L. Ebert. 2016. "Physiologic Expression of Sf3b1(K700E) Causes Impaired Erythropoiesis, Aberrant Splicing, and Sensitivity to Therapeutic Spliceosome Modulation." *Cancer Cell* 30 (3):404-417. doi: 10.1016/j.ccell.2016.08.006.

Okada, T., A. Maeda, A. Iwamatsu, K. Gotoh, and T. Kurosaki. 2000. "BCAP: the tyrosine kinase substrate that connects B cell receptor to phosphoinositide 3-kinase activation." *Immunity* 13 (6):817-27.

Oliveira-Nascimento, L., P. Massari, and L. M. Wetzler. 2012. "The Role of TLR2 in Infection and Immunity." *Front Immunol* 3:79. doi: 10.3389/fimmu.2012.00079.

Oosting, M., S. C. Cheng, J. M. Bolscher, R. Vestering-Stenger, T. S. Plantinga, I. C. Verschueren, P. Arts, A. Garritsen, H. van Eenennaam, P. Sturm, B. J. Kullberg, A. Hoischen, G. J. Adema, J. W. van der Meer, M. G. Netea, and L. A. Joosten. 2014. "Human TLR10 is an anti-inflammatory pattern-recognition receptor." *Proc Natl Acad Sci U S A* 111 (42):E4478-84. doi: 10.1073/pnas.1410293111.

Opal, S. M., and C. E. Huber. 2002. "Bench-to-bedside review: Toll-like receptors and their role in septic shock." *Crit Care* 6 (2):125-36.

Ozinsky, A., D. M. Underhill, J. D. Fontenot, A. M. Hajjar, K. D. Smith, C. B. Wilson, L. Schroeder, and A. Aderem. 2000. "The repertoire for pattern recognition of pathogens by the innate immune system is defined by cooperation between toll-like receptors." *Proc Natl Acad Sci U S A* 97 (25):13766-71. doi: 10.1073/pnas.250476497.

Pacheco-Arjona, J. R., and J. H. Ramirez-Prado. 2014. "Large-scale phylogenetic classification of fungal chitin synthases and identification of a putative cell-wall metabolism gene cluster in Aspergillus genomes." *PLoS One* 9 (8):e104920. doi: 10.1371/journal.pone.0104920.

Pasqualucci, L., V. Trifonov, G. Fabbri, J. Ma, D. Rossi, A. Chiarenza, V. A. Wells, A. Grunn, M. Messina, O. Elliot, J. Chan, G. Bhagat, A. Chadburn, G. Gaidano, C. G. Mullighan, R. Rabadan, and R. Dalla-Favera. 2011. "Analysis of the coding genome of diffuse large B-cell lymphoma." *Nat Genet* 43 (9):830-7. doi: 10.1038/ng.892.

Pauwels, A. M., M. Trost, R. Beyaert, and E. Hoffmann. 2017. "Patterns, Receptors, and Signals: Regulation of Phagosome Maturation." *Trends Immunol* 38 (6):407-422. doi: 10.1016/j.it.2017.03.006.

Pennini, M. E., D. J. Perkins, A. M. Salazar, M. Lipsky, and S. N. Vogel. 2013. "Complete dependence on IRAK4 kinase activity in TLR2, but not TLR4, signaling pathways underlies decreased cytokine production and increased susceptibility to Streptococcus pneumoniae infection in IRAK4 kinase-inactive mice." *J Immunol* 190 (1):307-16. doi: 10.4049/jimmunol.1201644.

Pham-Ledard, A., M. Prochazkova-Carlotti, L. Andrique, D. Cappellen, B. Vergier, F. Martinez, F. Grange, T. Petrella, M. Beylot-Barry, and J. P. Merlio. 2014. "Multiple

genetic alterations in primary cutaneous large B-cell lymphoma, leg type support a common lymphomagenesis with activated B-cell-like diffuse large B-cell lymphoma." *Mod Pathol* 27 (3):402-11. doi: 10.1038/modpathol.2013.156.

Picard, C., A. Puel, M. Bonnet, C. L. Ku, J. Bustamante, K. Yang, C. Soudais, S. Dupuis, J. Feinberg, C. Fieschi, C. Elbim, R. Hitchcock, D. Lammas, G. Davies, A. Al-Ghonaium, H. Al-Rayes, S. Al-Jumaah, S. Al-Hajjar, I. Z. Al-Mohsen, H. H. Frayha, R. Rucker, T. R. Hawn, A. Aderem, H. Tufenkeji, S. Haraguchi, N. K. Day, R. A. Good, M. A. Gougerot-Pocidalo, A. Ozinsky, and J. L. Casanova. 2003. "Pyogenic bacterial infections in humans with IRAK-4 deficiency." *Science* 299 (5615):2076-9. doi: 10.1126/science.1081902.

Picard, C., H. von Bernuth, P. Ghandil, M. Chrabieh, O. Levy, P. D. Arkwright, D. McDonald, R. S. Geha, H. Takada, J. C. Krause, C. B. Creech, C. L. Ku, S. Ehl, L. Marodi, S. Al-Muhsen, S. Al-Hajjar, A. Al-Ghonaium, N. K. Day-Good, S. M. Holland, J. I. Gallin, H. Chapel, D. P. Speert, C. Rodriguez-Gallego, E. Colino, B. Z. Garty, C. Roifman, T. Hara, H. Yoshikawa, S. Nonoyama, J. Domachowske, A. C. Issekutz, M. Tang, J. Smart, S. E. Zitnik, C. Hoarau, D. S. Kumararatne, A. J. Thrasher, E. G. Davies, C. Bethune, N. Sirvent, D. de Ricaud, Y. Camcioglu, J. Vasconcelos, M. Guedes, A. B. Vitor, C. Rodrigo, F. Almazan, M. Mendez, J. I. Arostegui, L. Alsina, C. Fortuny, J. Reichenbach, J. W. Verbsky, X. Bossuyt, R. Doffinger, L. Abel, A. Puel, and J. L. Casanova. 2010. "Clinical features and outcome of patients with IRAK-4 and MyD88 deficiency." *Medicine (Baltimore)* 89 (6):403-25. doi: 10.1097/MD.0b013e3181fd8ec3.

Puente, X. S., M. Pinyol, V. Quesada, L. Conde, G. R. Ordonez, N. Villamor, G. Escaramis, P. Jares, S. Bea, M. Gonzalez-Diaz, L. Bassaganyas, T. Baumann, M. Juan, M. Lopez-Guerra, D. Colomer, J. M. Tubio, C. Lopez, A. Navarro, C. Tornador, M. Aymerich, M. Rozman, J. M. Hernandez, D. A. Puente, J. M. Freije, G. Velasco, A. Gutierrez-Fernandez, D. Costa, A. Carrio, S. Guijarro, A. Enjuanes, L. Hernandez, J. Yague, P. Nicolas, C. M. Romeo-Casabona, H. Himmelbauer, E. Castillo, J. C. Dohm, S. de Sanjose, M. A. Piris, E. de Alava, J. San Miguel, R. Royo, J. L. Gelpi, D. Torrents, M. Orozco, D. G. Pisano, A. Valencia, R. Guigo, M. Bayes, S. Heath, M. Gut, P. Klatt, J. Marshall, K. Raine, L. A. Stebbings, P. A. Futreal, M. R. Stratton, P. J. Campbell, I. Gut, A. Lopez-Guillermo, X. Estivill, E. Montserrat, C. Lopez-Otin, and E. Campo. 2011. "Whole-genome sequencing identifies recurrent mutations in chronic lymphocytic leukaemia." *Nature* 475 (7354):101-5. doi: 10.1038/nature10113.

Purdue, M. P., Q. Lan, S. S. Wang, A. Kricker, I. Menashe, T. Z. Zheng, P. Hartge, A. E. Grulich, Y. Zhang, L. M. Morton, C. M. Vajdic, T. R. Holford, R. K. Severson, B. P. Leaderer, J. R. Cerhan, M. Yeager, W. Cozen, K. Jacobs, S. Davis, N. Rothman, S. J. Chanock, N. Chatterjee, and B. K. Armstrong. 2009. "A pooled investigation of Toll-like receptor gene variants and risk of non-Hodgkin lymphoma." *Carcinogenesis* 30 (2):275-81. doi: 10.1093/carcin/bgn262.

Raetz, M., A. Kibardin, C. R. Sturge, R. Pifer, H. Li, E. Burstein, K. Ozato, S. Larin, and F. Yarovinsky. 2013. "Cooperation of TLR12 and TLR11 in the IRF8-dependent IL-12 response to Toxoplasma gondii profilin." *J Immunol* 191 (9):4818-27. doi: 10.4049/jimmunol.1301301.

Rawlings, D. J., M. A. Schwartz, S. W. Jackson, and A. Meyer-Bahlburg. 2012. "Integration of B cell responses through Toll-like receptors and antigen receptors." *Nat Rev Immunol* 12 (4):282-94. doi: 10.1038/nri3190.

Reddy, A., J. Zhang, N. S. Davis, A. B. Moffitt, C. L. Love, A. Waldrop, S. Leppa, A. Pasanen, L. Meriranta, M. L. Karjalainen-Lindsberg, P. Norgaard, M. Pedersen, A. O. Gang, E. Hogdall, T. B. Heavican, W. Lone, J. Iqbal, Q. Qin, G. Li, S. Y. Kim, J. Healy, K. L. Richards, Y. Fedoriw, L. Bernal-Mizrachi, J. L. Koff, A. D. Staton, C. R. Flowers, O. Paltiel, N. Goldschmidt, M. Calaminici, A. Clear, J. Gribben, E. Nguyen, M. B. Czader, S. L. Ondrejka, A. Collie, E. D. Hsi, E. Tse, R. K. H. Au-Yeung, Y. L. Kwong, G. Srivastava, W. W. L. Choi, A. M. Evens, M. Pilichowska, M. Sengar, N. Reddy, S. Li, A. Chadburn, L. I. Gordon, E. S. Jaffe, S. Levy, R. Rempel, T. Tzeng, L. E. Happ, T. Dave, D. Rajagopalan, J. Datta, D. B. Dunson, and S. S. Dave. 2017. "Genetic and Functional Drivers of Diffuse Large B Cell Lymphoma." *Cell* 171 (2):481-494 e15. doi: 10.1016/j.cell.2017.09.027.

Reese, T. A., H. E. Liang, A. M. Tager, A. D. Luster, N. Van Rooijen, D. Voehringer, and R. M. Locksley. 2007. "Chitin induces accumulation in tissue of innate immune cells associated with allergy." *Nature* 447 (7140):92-6. doi: 10.1038/nature05746.

Regan, T., K. Nally, R. Carmody, A. Houston, F. Shanahan, J. Macsharry, and E. Brint. 2013. "Identification of TLR10 as a key mediator of the inflammatory response to Listeria monocytogenes in intestinal epithelial cells and macrophages." *Journal of immunology* 191 (12):6084-92. doi: 10.4049/jimmunol.1203245.

Rhyasen, G. W., L. Bolanos, J. Fang, A. Jerez, M. Wunderlich, C. Rigolino, L. Mathews, M. Ferrer, N. Southall, R. Guha, J. Keller, C. Thomas, L. J. Beverly, A. Cortelezzi, E. N. Oliva, M. Cuzzola, J. P. Maciejewski, J. C. Mulloy, and D. T. Starczynowski. 2013. "Targeting IRAK1 as a therapeutic approach for myelodysplastic syndrome." *Cancer Cell* 24 (1):90-104. doi: 10.1016/j.ccr.2013.05.006.

Richter, J., M. Schlesner, S. Hoffmann, M. Kreuz, E. Leich, B. Burkhardt, M. Rosolowski, O. Ammerpohl, R. Wagener, S. H. Bernhart, D. Lenze, M. Szczepanowski, M. Paulsen, S. Lipinski, R. B. Russell, S. Adam-Klages, G. Apic, A. Claviez, D. Hasenclever, V. Hovestadt, N. Hornig, J. O. Korbel, D. Kube, D. Langenberger, C. Lawerenz, J. Lisfeld, K. Meyer, S. Picelli, J. Pischimarov, B. Radlwimmer, T. Rausch, M. Rohde, M. Schilhabel, R. Scholtysik, R. Spang, H. Trautmann, T. Zenz, A. Borkhardt, H. G. Drexler, P. Moller, R. A. MacLeod, C. Pott, S. Schreiber, L. Trumper, M. Loeffler, P. F. Stadler, P. Lichter, R. Eils, R. Kuppers, M. Hummel, W. Klapper, P. Rosenstiel, A. Rosenwald, B. Brors, R. Siebert, and Icgc Mmml- Seq Project. 2012. "Recurrent mutation of the ID3 gene in Burkitt lymphoma identified by integrated genome, exome and transcriptome sequencing." *Nat Genet* 44 (12):1316-20. doi: 10.1038/ng.2469.

Rivera, A., M. C. Siracusa, G. S. Yap, and W. C. Gause. 2016. "Innate cell communication kick-starts pathogen-specific immunity." *Nat Immunol* 17 (4):356-63. doi: 10.1038/ni.3375.

Romero, M. M., J. I. Basile, L. Corra Feo, B. Lopez, V. Ritacco, and M. Aleman. 2016. "Reactive oxygen species production by human dendritic cells involves TLR2 and dectin-1 and is essential for efficient immune response against Mycobacteria." *Cell Microbiol* 18 (6):875-86. doi: 10.1111/cmi.12562.

Rosas, M., K. Liddiard, M. Kimberg, I. Faro-Trindade, J. U. McDonald, D. L. Williams, G. D. Brown, and P. R. Taylor. 2008. "The induction of inflammation by dectin-1 in vivo is dependent on myeloid cell programming and the progression of phagocytosis." *J Immunol* 181 (5):3549-57. doi: 181/5/3549 [pii].

Ryu, J. H., J. Y. Yoo, M. J. Kim, S. G. Hwang, K. C. Ahn, J. C. Ryu, M. K. Choi, J. H. Joo, C. H. Kim, S. N. Lee, W. J. Lee, J. Kim, D. M. Shin, M. N. Kweon, Y. S. Bae, and J. H. Yoon. 2013. "Distinct TLR-mediated pathways regulate house dust mite-induced allergic disease in the upper and lower airways." *J Allergy Clin Immunol* 131 (2):549-61. doi: 10.1016/j.jaci.2012.07.050.

Sandoval-Sus, J. D., J. Chavez, and S. Dalia. 2016. "A New Therapeutic Era in GCB and ABC Diffuse Large B-cell Lymphoma Molecular Subtypes: A Cell of Origin-Driven Review." *Curr Cancer Drug Targets* 16 (4):305-22.

Sato, M., H. Sano, D. Iwaki, K. Kudo, M. Konishi, H. Takahashi, T. Takahashi, H. Imaizumi, Y. Asai, and Y. Kuroki. 2003. "Direct binding of Toll-like receptor 2 to zymosan, and zymosan-induced NF-kappa B activation and TNF-alpha secretion are down-regulated by lung collectin surfactant protein A." *J Immunol* 171 (1):417-25.

Schauvliege, R., S. Janssens, and R. Beyaert. 2007. "Pellino proteins: novel players in TLR and IL-1R signalling." *J Cell Mol Med* 11 (3):453-61. doi: 10.1111/j.1582-4934.2007.00040.x.

Schlosser, A., T. Thomsen, J. B. Moeller, O. Nielsen, I. Tornoe, J. Mollenhauer, S. K. Moestrup, and U. Holmskov. 2009. "Characterization of FIBCD1 as an acetyl group-binding receptor that binds chitin." *J Immunol* 183 (6):3800-9. doi: 10.4049/jimmunol.0901526.

Scott, J. S., S. L. Degorce, R. Anjum, J. Culshaw, R. D. M. Davies, N. L. Davies, K. S. Dillman, J. E. Dowling, L. Drew, A. D. Ferguson, S. D. Groombridge, C. T. Halsall, J. A. Hudson, S. Lamont, N. A. Lindsay, S. K. Marden, M. F. Mayo, J. E. Pease, D. R. Perkins, J. H. Pink, G. R. Robb, A. Rosen, M. Shen, C. McWhirter, and D. Wu. 2017. "Discovery and Optimization of Pyrrolopyrimidine Inhibitors of Interleukin-1 Receptor Associated Kinase 4 (IRAK4) for the Treatment of Mutant MYD88(L265P) Diffuse Large B-Cell Lymphoma." *J Med Chem* 60 (24):10071-10091. doi: 10.1021/acs.jmedchem.7b01290.

Shan, S., D. Liu, R. Liu, Y. Zhu, T. Li, F. Zhang, L. An, G. Yang, and H. Li. 2017. "Non-mammalian Toll-like receptor 18 (Tlr18) recognizes bacterial pathogens in common carp (Cyprinus carpio L.): Indications for a role of participation in the NF-kappaB signaling pathway." *Fish Shellfish Immunol*. doi: 10.1016/j.fsi.2017.09.081.

Shibata, K., A. Hasebe, T. Into, M. Yamada, and T. Watanabe. 2000. "The N-terminal lipopeptide of a 44-kDa membrane-bound lipoprotein of Mycoplasma salivarium is responsible for the expression of intercellular adhesion molecule-1 on the cell surface of normal human gingival fibroblasts." *J Immunol* 165 (11):6538-44.

Shibata, Y., W. J. Metzger, and Q. N. Myrvik. 1997. "Chitin particle-induced cell-mediated immunity is inhibited by soluble mannan: mannose receptor-mediated phagocytosis initiates IL-12 production." *J Immunol* 159 (5):2462-7.

Shiratori, E., M. Itoh, and S. Tohda. 2017. "MYD88 Inhibitor ST2825 Suppresses the Growth of Lymphoma and Leukaemia Cells." *Anticancer Res* 37 (11):6203-6209. doi: 10.21873/anticanres.12070.

Singh, B., and E. Eyras. 2017. "The role of alternative splicing in cancer." *Transcription* 8 (2):91-98. doi: 10.1080/21541264.2016.1268245.

Smigiel, K. S., and W. C. Parks. 2018. "Macrophages, Wound Healing, and Fibrosis: Recent Insights." *Curr Rheumatol Rep* 20 (4):17. doi: 10.1007/s11926-018-0725-5.

Smith, Molly A, Kwangmin Choi, Nathan Salomonis, Matthew J. Walter, Kakajan Komurov, and Daniel T Starczynowski. 2016. "Alternative Splice Variants of IRAK4 That

Activate Innate Immune Signaling Are Associated with U2AF1 Mutations in Myelodysplastic Syndrome and Acute Myeloid Leukemia." *Blood* 128 (22):1531-1531.

Stack, J., S. L. Doyle, D. J. Connolly, L. S. Reinert, K. M. O'Keeffe, R. M. McLoughlin, S. R. Paludan, and A. G. Bowie. 2014. "TRAM is required for TLR2 endosomal signaling to type I IFN induction." *J Immunol* 193 (12):6090-102. doi: 10.4049/jimmunol.1401605.

Starczynowski, D. T., F. Kuchenbauer, B. Argiropoulos, S. Sung, R. Morin, A. Muranyi, M. Hirst, D. Hogge, M. Marra, R. A. Wells, R. Buckstein, W. Lam, R. K. Humphries, and A. Karsan. 2010. "Identification of miR-145 and miR-146a as mediators of the 5q- syndrome phenotype." *Nat Med* 16 (1):49-58. doi: 10.1038/nm.2054.

Suzuki, N., S. Suzuki, G. S. Duncan, D. G. Millar, T. Wada, C. Mirtsos, H. Takada, A. Wakeham, A. Itie, S. Li, J. M. Penninger, H. Wesche, P. S. Ohashi, T. W. Mak, and W. C. Yeh. 2002. "Severe impairment of interleukin-1 and Toll-like receptor signalling in mice lacking IRAK-4." *Nature* 416 (6882):750-6. doi: 10.1038/nature736.

Suzuki, Y., T. Yoshida, R. Horie, T. Tsuruta, T. Togano, M. Ohsaka, K. Miyazaki, M. Danbara, S. Ohtani, I. Okayasu, and M. Higashihara. 2010. "Constitutive activity of nuclear transcription factor kappaB is observed in follicular lymphoma." *J Clin Exp Hematop* 50 (1):45-50.

Sveen, A., S. Kilpinen, A. Ruusulehto, R. A. Lothe, and R. I. Skotheim. 2016. "Aberrant RNA splicing in cancer; expression changes and driver mutations of splicing factor genes." *Oncogene* 35 (19):2413-27. doi: 10.1038/onc.2015.318.

Swann, J. B., M. D. Vesely, A. Silva, J. Sharkey, S. Akira, R. D. Schreiber, and M. J. Smyth. 2008. "Demonstration of inflammation-induced cancer and cancer immunoediting during primary tumorigenesis." *Proc Natl Acad Sci U S A* 105 (2):652-6. doi: 10.1073/pnas.0708594105.

Takahara, K., S. Tokieda, K. Nagaoka, and K. Inaba. 2012. "Efficient capture of Candida albicans and zymosan by SIGNR1 augments TLR2-dependent TNF-alpha production." *Int Immunol* 24 (2):89-96. doi: 10.1093/intimm/dxr103.

Takeuchi, O., and S. Akira. 2010. "Pattern recognition receptors and inflammation." *Cell* 140 (6):805-20. doi: 10.1016/j.cell.2010.01.022.

Takeuchi, O., T. Kawai, P. F. Muhlradt, M. Morr, J. D. Radolf, A. Zychlinsky, K. Takeda, and S. Akira. 2001. "Discrimination of bacterial lipoproteins by Toll-like receptor 6." *Int Immunol* 13 (7):933-40.

Tan, R. S., B. Ho, B. P. Leung, and J. L. Ding. 2014. "TLR Cross-talk Confers Specificity to Innate Immunity." *International reviews of immunology*. doi: 10.3109/08830185.2014.921164.

Taylor, R. C., P. Richmond, and J. W. Upham. 2006. "Toll-like receptor 2 ligands inhibit TH2 responses to mite allergen." *J Allergy Clin Immunol* 117 (5):1148-54. doi: 10.1016/j.jaci.2006.02.014.

Tazi, J., N. Bakkour, and S. Stamm. 2009. "Alternative splicing and disease." *Biochim Biophys Acta* 1792 (1):14-26. doi: 10.1016/j.bbadis.2008.09.017.

Thomas, G. P., K. Hemmrich, K. M. Abberton, D. McCombe, A. J. Penington, E. W. Thompson, and W. A. Morrison. 2008. "Zymosan-induced inflammation stimulates neo-adipogenesis." *Int J Obes (Lond)* 32 (2):239-48. doi: 10.1038/sj.ijo.0803702.

Tian, N., J. Li, J. Shi, and G. Sui. 2017. "From General Aberrant Alternative Splicing in Cancers and Its Therapeutic Application to the Discovery of an Oncogenic DMTF1 Isoform." *Int J Mol Sci* 18 (3). doi: 10.3390/ijms18030191.

To, T., S. Stanojevic, G. Moores, A. S. Gershon, E. D. Bateman, A. A. Cruz, and L. P. Boulet. 2012. "Global asthma prevalence in adults: findings from the cross-sectional world health survey." *BMC Public Health* 12:204. doi: 10.1186/1471-2458-12-204.

Traverse-Glehen, A., E. Bachy, L. Baseggio, E. Callet-Bauchu, S. Gazzo, A. Verney, S. Hayette, L. Jallades, M. Ffrench, G. Salles, B. Coiffier, P. Felman, and F. Berger. 2013. "Immunoarchitectural patterns in splenic marginal zone lymphoma: correlations with chromosomal aberrations, IGHV mutations, and survival. A study of 76 cases." *Histopathology* 62 (6):876-93. doi: 10.1111/his.12092.

Turvey, Stuart E., and David H. Broide. 2010. "Innate immunity." *Journal of Allergy and Clinical Immunology* 125 (2):S24-S32. doi: 10.1016/j.jaci.2009.07.016.

Ullah, M. O., M. J. Sweet, A. Mansell, S. Kellie, and B. Kobe. 2016. "TRIF-dependent TLR signaling, its functions in host defense and inflammation, and its potential as a therapeutic target." *J Leukoc Biol* 100 (1):27-45. doi: 10.1189/jlb.2RI1115-531R.

van de Veerdonk, F. L., R. J. Marijnissen, B. J. Kullberg, H. J. Koenen, S. C. Cheng, I. Joosten, W. B. van den Berg, D. L. Williams, J. W. van der Meer, L. A. Joosten, and M. G. Netea. 2009. "The macrophage mannose receptor induces IL-17 in response to Candida albicans." *Cell Host Microbe* 5 (4):329-40. doi: 10.1016/j.chom.2009.02.006.

Varettoni, M., L. Arcaini, S. Zibellini, E. Boveri, S. Rattotti, R. Riboni, A. Corso, E. Orlandi, M. Bonfichi, M. Gotti, C. Pascutto, S. Mangiacavalli, G. Croci, V. Fiaccadori, L. Morello, M. L. Guerrera, M. Paulli, and M. Cazzola. 2013. "Prevalence and clinical significance of the MYD88 (L265P) somatic mutation in Waldenstrom's macroglobulinemia and related lymphoid neoplasms." *Blood* 121 (13):2522-8. doi: 10.1182/blood-2012-09-457101.

Vollmer, S., S. Strickson, T. Zhang, N. Gray, K. L. Lee, V. R. Rao, and P. Cohen. 2017. "The mechanism of activation of IRAK1 and IRAK4 by interleukin-1 and Toll-like receptor agonists." *Biochem J* 474 (12):2027-2038. doi: 10.1042/BCJ20170097.

von Bernuth, H., C. Picard, A. Puel, and J. L. Casanova. 2012. "Experimental and natural infections in MyD88- and IRAK-4-deficient mice and humans." *Eur J Immunol* 42 (12):3126-35. doi: 10.1002/eji.201242683.

Wagener, J., R. K. Malireddi, M. D. Lenardon, M. Koberle, S. Vautier, D. M. MacCallum, T. Biedermann, M. Schaller, M. G. Netea, T. D. Kanneganti, G. D. Brown, A. J. Brown, and N. A. Gow. 2014. "Fungal chitin dampens inflammation through IL-10 induction mediated by NOD2 and TLR9 activation." *PLoS Pathog* 10 (4):e1004050. doi: 10.1371/journal.ppat.1004050.

Wagner, E. J., M. L. Curtis, N. D. Robson, A. P. Baraniak, P. S. Eis, and M. A. Garcia-Blanco. 2003. "Quantification of alternatively spliced FGFR2 RNAs using the RNA invasive cleavage assay." *RNA* 9 (12):1552-61.

Wahl, M. C., C. L. Will, and R. Luhrmann. 2009. "The spliceosome: design principles of a dynamic RNP machine." *Cell* 136 (4):701-18. doi: 10.1016/j.cell.2009.02.009.

Walachowski, S., G. Tabouret, and G. Foucras. 2016. "Triggering Dectin-1-Pathway Alone Is Not Sufficient to Induce Cytokine Production by Murine Macrophages." *PLoS One* 11 (2):e0148464. doi: 10.1371/journal.pone.0148464.

Wan, Y., and C. J. Wu. 2013. "SF3B1 mutations in chronic lymphocytic leukemia." *Blood* 121 (23):4627-34. doi: 10.1182/blood-2013-02-427641.

Wang, J., J. Chai, and H. Wang. 2016. "Structure of the mouse Toll-like receptor 13 ectodomain in complex with a conserved sequence from bacterial 23S ribosomal RNA." *FEBS J* 283 (9):1631-5. doi: 10.1111/febs.13628.

Wang, J. Q., Y. S. Jeelall, L. L. Ferguson, and K. Horikawa. 2014. "Toll-Like Receptors and Cancer: MYD88 Mutation and Inflammation." *Front Immunol* 5:367. doi: 10.3389/fimmu.2014.00367.

Wang, L., A. N. Brooks, J. Fan, Y. Wan, R. Gambe, S. Li, S. Hergert, S. Yin, S. S. Freeman, J. Z. Levin, L. Fan, M. Seiler, S. Buonamici, P. G. Smith, K. F. Chau, C. L. Cibulskis, W. Zhang, L. Z. Rassenti, E. M. Ghia, T. J. Kipps, S. Fernandes, D. B. Bloch, D. Kotliar, D. A. Landau, S. A. Shukla, J. C. Aster, R. Reed, D. S. DeLuca, J. R. Brown, D. Neuberg, G. Getz, K. J. Livak, M. M. Meyerson, P. V. Kharchenko, and C. J. Wu. 2016. "Transcriptomic Characterization of SF3B1 Mutation Reveals Its Pleiotropic Effects in Chronic Lymphocytic Leukemia." *Cancer Cell* 30 (5):750-763. doi: 10.1016/j.ccell.2016.10.005.

Wang, L., Y. Zhao, J. Qian, L. Sun, Y. Lu, H. Li, Y. Li, J. Yang, Z. Cai, and Q. Yi. 2013. "Toll-like receptor-4 signaling in mantle cell lymphoma: effects on tumor growth and immune evasion." *Cancer* 119 (4):782-91. doi: 10.1002/cncr.27792.

Wang, Y., J. Liu, B. O. Huang, Y. M. Xu, J. Li, L. F. Huang, J. Lin, J. Zhang, Q. H. Min, W. M. Yang, and X. Z. Wang. 2015. "Mechanism of alternative splicing and its regulation." *Biomed Rep* 3 (2):152-158. doi: 10.3892/br.2014.407.

Ward, A. J., and T. A. Cooper. 2010. "The pathobiology of splicing." *J Pathol* 220 (2):152-63. doi: 10.1002/path.2649.

Wei, Y., S. Dimicoli, C. Bueso-Ramos, R. Chen, H. Yang, D. Neuberg, S. Pierce, Y. Jia, H. Zheng, H. Wang, X. Wang, M. Nguyen, S. A. Wang, B. Ebert, R. Bejar, R. Levine, O. Abdel-Wahab, M. Kleppe, I. Ganan-Gomez, H. Kantarjian, and G. Garcia-Manero. 2013. "Toll-like receptor alterations in myelodysplastic syndrome." *Leukemia* 27 (9):1832-40. doi: 10.1038/leu.2013.180.

Wells, C. A., J. A. Salvage-Jones, X. Li, K. Hitchens, S. Butcher, R. Z. Murray, A. G. Beckhouse, Y. L. Lo, S. Manzanero, C. Cobbold, K. Schroder, B. Ma, S. Orr, L. Stewart, D. Lebus, P. Sobieszczuk, D. A. Hume, J. Stow, H. Blanchard, and R. B. Ashman. 2008. "The macrophage-inducible C-type lectin, mincle, is an essential component of the innate immune response to Candida albicans." *J Immunol* 180 (11):7404-13.

Wilson, W. H., R. M. Young, R. Schmitz, Y. Yang, S. Pittaluga, G. Wright, C. J. Lih, P. M. Williams, A. L. Shaffer, J. Gerecitano, S. de Vos, A. Goy, V. P. Kenkre, P. M. Barr, K. A. Blum, A. Shustov, R. Advani, N. H. Fowler, J. M. Vose, R. L. Elstrom, T. M. Habermann, J. C. Barrientos, J. McGreivy, M. Fardis, B. Y. Chang, F. Clow, B. Munneke, D. Moussa, D. M. Beaupre, and L. M. Staudt. 2015. "Targeting B cell receptor signaling with ibrutinib in diffuse large B cell lymphoma." *Nat Med* 21 (8):922-6. doi: 10.1038/nm.3884.

Wu, X., R. C. Tschumper, and D. F. Jelinek. 2013. "Genetic characterization of SF3B1 mutations in single chronic lymphocytic leukemia cells." *Leukemia* 27 (11):2264-7. doi: 10.1038/leu.2013.155.

Xu, L., Z. R. Hunter, G. Yang, Y. Zhou, Y. Cao, X. Liu, E. Morra, A. Trojani, A. Greco, L. Arcaini, M. Varettoni, J. R. Brown, Y. T. Tai, K. C. Anderson, N. C. Munshi, C. J.

Patterson, R. J. Manning, C. K. Tripsas, N. I. Lindeman, and S. P. Treon. 2013. "MYD88 L265P in Waldenstrom macroglobulinemia, immunoglobulin M monoclonal gammopathy, and other B-cell lymphoproliferative disorders using conventional and quantitative allele-specific polymerase chain reaction." *Blood* 121 (11):2051-8. doi: 10.1182/blood-2012-09-454355.

Yang, G., Y. Zhou, X. Liu, L. Xu, Y. Cao, R. J. Manning, C. J. Patterson, S. J. Buhrlage, N. Gray, Y. T. Tai, K. C. Anderson, Z. R. Hunter, and S. P. Treon. 2013. "A mutation in MYD88 (L265P) supports the survival of lymphoplasmacytic cells by activation of Bruton tyrosine kinase in Waldenstrom macroglobulinemia." *Blood* 122 (7):1222-32. doi: 10.1182/blood-2012-12-475111.

Yarovinsky, F., S. Hieny, and A. Sher. 2008. "Recognition of Toxoplasma gondii by TLR11 prevents parasite-induced immunopathology." *J Immunol* 181 (12):8478-84.

Younes, I., and M. Rinaudo. 2015. "Chitin and chitosan preparation from marine sources. Structure, properties and applications." *Mar Drugs* 13 (3):1133-74. doi: 10.3390/md13031133.

Zhang, J. M., and J. An. 2007. "Cytokines, inflammation, and pain." *Int Anesthesiol Clin* 45 (2):27-37. doi: 10.1097/AIA.0b013e318034194e.

Zhu, J., R. L. Wei, Y. L. Pi, and Q. Guo. 2013. "Significance of Bcl10 gene mutations in the clinical diagnosis of MALT-type ocular adnexal lymphoma in the Chinese population." *Genet Mol Res* 12 (2):1194-204. doi: 10.4238/2013.April.12.6.